

ESSAYS IN INVESTMENTS AND ASSET ALLOCATION

by

Xianzhe Chen

A dissertation submitted to the faculty of
The University of North Carolina at Charlotte
in partial fulfillment of the requirements
for the degree of Doctor of Philosophy in
Business Administration

Charlotte

2016

Approved by:

Dr. Weidong Tian

Dr. Steven Clark

Dr. Chris Kirby

Dr. Jiancheng Jiang

ABSTRACT

XIANZHE CHEN. Essays in investments and asset allocation. (Under the direction of DR. WEIDONG TIAN)

This dissertation consists of three topics in investments and asset allocation. The first chapter studies the dynamics of macro factors and their application in asset allocation. Five meaningful economic factors are extracted from hundreds of economic series and dynamic structural models are constructed and estimated by using Bayesian techniques in conjunction with MCMC sampler. We find that these macro factors are able to capture important economic trends and systematic components of equity return variation and shed a light on the evolution of macro economy. Furthermore, the dynamic asset allocation based on macro factors could produce significant systematically out-of-sample economic gains. In addition, these macro factors could serve as the transmission channels of monetary policy so that investors could incorporate their views into portfolio construction and test the effects on various scenarios from a forward-looking perspective. Moreover, the impulse response analysis reveals appealing indications of the trajectories of asset future returns under monetary policy shocks, which could be informative and valuable for both central bankers and practical investors.

Consistent financial performance is the key element to success in asset management. In chapter 2, we construct a dynamic wealth constraint to represent the consistent performance, which takes into account the entire historical records as a benchmark. A general optimal policy is characterized so that the wealth could always stay at or

above this benchmark and a closed-form solution is obtained for a special case. Several implications are also discussed and it is recommended that this consistent performance constraint could be an appealing tool to be implemented in a volatile market. We further investigate its practical implications in chapter 3 and demonstrate that the portfolio wealth under this consistent performance strategy could exhibit an upward trend over time and has several remarkable features, such as capital-protection and low volatility which could make it valuable to practical investors.

ACKNOWLEDGMENTS

I want to thank dissertation chair, Dr. Weidong Tian, for his support, Dr. Steven Clark, Dr. Chris Kirby and Dr. Jiancheng Jiang for serving my committee. Additionally, I am very grateful to Dr. Tao-Hsien (Dolly) King and Dr. David Mauer for their encouragement during my study. Last, but not least, I would like to express my utmost gratitude and thanks to my wonderful parents for their unconditional love.

TABLE OF CONTENTS

LIST OF FIGURES	vii
LIST OF TABLES	xviii
CHAPTER 1: MACRO FACTORS, DYNAMIC ASSET ALLOCATION AND MONETARY POLICY	1
CHAPTER 2: OPTIMAL PORTFOLIO CHOICE AND CONSISTENT PERFORMANCE	78
CHAPTER 3: WHAT MATTERS MOST? IT'S THE CONSISTENCY!	98
REFERENCES	120
APPENDIX A: SIMULATION SMOOTHER	126
APPENDIX B: AUXILIARY PARTICLE FILTER	128
APPENDIX C: ESTIMATION PROCEDURES	131
APPENDIX D: SIMULATION STUDY	139
APPENDIX E: DATA DESCRIPTION	142
APPENDIX F: A HYBRID MODEL	151
APPENDIX G: CHAPTER 2 PROOFS	158
APPENDIX H: MODEL DESCRIPTION	168
APPENDIX I: PARAMETER CALIBRATION	172

LIST OF FIGURES

- FIGURE 1: The figure in Panel A depicts the simulated series and stochastic volatility. The figure in Panel B depicts the sample autocorrelation function, sample draws and posterior densities for simulated data. 38
- FIGURE 2: This figure shows the estimation results of α_{1t} , α_{2t} and h_t for the simulated data. The gray area represents the 99% confidence interval. The solid line denotes the true value of the state variable and the dashes line denotes the posterior mean. 39
- FIGURE 3: The figure depicts the posterior mean of stochastic volatility for macroeconomic factors under model DFVAR (2) with dynamic loadings and stochastic volatility. 40
- FIGURE 4: The figure depicts the time-varying correlation among macroeconomic factors under model DFVAR (2) with dynamic loadings and stochastic volatility. 41
- FIGURE 5: This figure shows the annualized return for three types of monthly rebalancing strategies under model FVAR1 for 10-sector data set. SP500 denotes the S&P 500 index. GMV0 is the global minimum volatility model without constraints, GMV1 is the global minimum volatility model with no-shorting constraint, and GMV2 is the global minimum volatility model with leverage constraint. MVOL0 denotes the minimum volatility model with target return of 0.5%, MVOL1 denotes the minimum volatility model with target return of 1%, MVOL2 denotes the minimum volatility model with target return of 4%. MR0 denotes the maximum return model with target volatility of 1%, MR1 denotes the maximum return model with target volatility of 2%, MR2 denotes the maximum return model with target volatility of 4%. 42

FIGURE 6: This figure shows the annualized volatility for three types of monthly rebalancing strategies under model FVAR1 for 10-sector data set. SP500 denotes the S&P 500 index. GMV0 is the global minimum volatility model without constraints, GMV1 is the global minimum volatility model with no-shorting constraint, and GMV2 is the global minimum volatility model with leverage constraint. MVOL0 denotes the minimum volatility model with target return of 0.5%, MVOL1 denotes the minimum volatility model with target return of 1%, MVOL2 denotes the minimum volatility model with target return of 4%. MR0 denotes the maximum return model with target volatility of 1%, MR1 denotes the maximum return model with target volatility of 2%, MR2 denotes the maximum return model with target volatility of 4%. 43

FIGURE 7: This figure shows the annualized return for three types of quarterly rebalancing strategies under model FVAR1 for 10-sector data set. SP500 denotes the S&P 500 index. GMV0 is the global minimum volatility model without constraints, GMV1 is the global minimum volatility model with no-shorting constraint, and GMV2 is the global minimum volatility model with leverage constraint. MVOL0 denotes the minimum volatility model with target return of 0.5%, MVOL1 denotes the minimum volatility model with target return of 1%, MVOL2 denotes the minimum volatility model with target return of 4%. MR0 denotes the maximum return model with target volatility of 1%, MR1 denotes the maximum return model with target volatility of 2%, MR2 denotes the maximum return model with target volatility of 4%. 44

FIGURE 8: This figure shows the annualized volatility for three types of quarterly rebalancing strategies under model FVAR1 for 10-sector data set. SP500 denotes the S&P 500 index. GMV0 is the global minimum volatility model without constraints, GMV1 is the global minimum volatility model with no-shorting constraint, and GMV2 is the global minimum volatility model with leverage constraint. MVOL0 denotes the minimum volatility model with target return of 0.5%, MVOL1 denotes the minimum volatility model with target return of 1%, MVOL2 denotes the minimum volatility model with target return of 4%. MR0 denotes the maximum return model with target volatility of 1%, MR1 denotes the maximum return model with target volatility of 2%, MR2 denotes the maximum return model with target volatility of 4%. 45

- FIGURE 9: This figure shows the portfolio weights under model FVAR2 for monthly rebalancing global minimum volatility strategy based on 10-sector data set. GMV0 denotes the global minimum volatility strategy without any constraints, GMV1 denotes the global minimum volatility strategy with no-shorting constraint, and GMV2 denotes the global minimum volatility strategy with leverage constraints. Note that there is no risk-free asset available for global minimum volatility strategy so that the cash position should be close to zero. 46
- FIGURE 10: This figure shows the portfolio weights under model FVAR2 for monthly rebalancing minimum volatility with target return strategy based on 10-sector data set. MVOL0 denotes the minimum volatility model with target return of 0.5%, MVOL1 denotes the minimum volatility model with target return of 1%, MVOL2 denotes the minimum volatility model with target return of 4%. 47
- FIGURE 11: This figure shows the portfolio weights under model FVAR2 for monthly rebalancing maximum expected return with target volatility strategy based on 10-sector data set. MR0 denotes the maximum return model with target volatility of 1%, MR1 denotes the maximum return model with target volatility of 2%, MR2 denotes the maximum return model with target volatility of 4%. 48
- FIGURE 12: This figure shows the annualized return for three types of monthly rebalancing strategies under model FVAR2 based on 10-sector data set. SP500 denotes the S&P 500 index. GMV0 is the global minimum volatility model without constraints, GMV1 is the global minimum volatility model with no-shorting constraint, and GMV2 is the global minimum volatility model with leverage constraint. MVOL0 denotes the minimum volatility model with target return of 0.5%, MVOL1 denotes the minimum volatility model with target return of 1%, MVOL2 denotes the minimum volatility model with target return of 4%. MR0 denotes the maximum return model with target volatility of 1%, MR1 denotes the maximum return model with target volatility of 2%, MR2 denotes the maximum return model with target volatility of 4%. 49

FIGURE 13: This figure shows the annualized volatility for three types of monthly rebalancing strategies under model FVAR2 based on 10-sector data set. SP500 denotes the S&P 500 index. GMV0 is the global minimum volatility model without constraints, GMV1 is the global minimum volatility model with no-shorting constraint, and GMV2 is the global minimum volatility model with leverage constraint. MVOL0 denotes the minimum volatility model with target return of 0.5%, MVOL1 denotes the minimum volatility model with target return of 1%, MVOL2 denotes the minimum volatility model with target return of 4%. MR0 denotes the maximum return model with target volatility of 1%, MR1 denotes the maximum return model with target volatility of 2%, MR2 denotes the maximum return model with target volatility of 4%. 50

FIGURE 14: This figure shows the portfolio weights under model FVAR2 for quarterly rebalancing global minimum volatility strategy based on 10-sector data set. GMV0 denotes the global minimum volatility strategy without any constraints, GMV1 denotes the global minimum volatility strategy with no-shorting constraint, and GMV2 denotes the global minimum volatility strategy with leverage constraints. Note that there is no risk-free asset available for global minimum volatility strategy so that the cash position should be close to zero. 51

FIGURE 15: This figure shows the portfolio weights under model FVAR2 for quarterly rebalancing minimum volatility with target return strategy based on 10-sector data set. MVOL0 denotes the minimum volatility model with target return of 0.5%, MVOL1 denotes the minimum volatility model with target return of 1%, MVOL2 denotes the minimum volatility model with target return of 4%. 52

FIGURE 16: This figure shows the portfolio weights under model FVAR2 for quarterly rebalancing maximum expected return with target volatility strategy based on 10-sector data set. MR0 denotes the maximum return model with target volatility of 1%, MR1 denotes the maximum return model with target volatility of 2%, MR2 denotes the maximum return model with target volatility of 4%. 53

FIGURE 17: This figure shows the annualized return for three types of quarterly rebalancing strategies under model FVAR2 based on 10-sector data set. SP500 denotes the S&P 500 index. GMV0 is the global minimum volatility model without constraints, GMV1 is the global minimum volatility model with no-shorting constraint, and GMV2 is the global minimum volatility model with leverage constraint. MVOL0 denotes the minimum volatility model with target return of 0.5%, MVOL1 denotes the minimum volatility model with target return of 1%, MVOL2 denotes the minimum volatility model with target return of 4%. MR0 denotes the maximum return model with target volatility of 1%, MR1 denotes the maximum return model with target volatility of 2%, MR2 denotes the maximum return model with target volatility of 4%. 54

FIGURE 18: This figure shows the annualized volatility for three types of quarterly rebalancing strategies under model FVAR2 based on 10-sector data set. SP500 denotes the S&P 500 index. GMV0 is the global minimum volatility model without constraints, GMV1 is the global minimum volatility model with no-shorting constraint, and GMV2 is the global minimum volatility model with leverage constraint. MVOL0 denotes the minimum volatility model with target return of 0.5%, MVOL1 denotes the minimum volatility model with target return of 1%, MVOL2 denotes the minimum volatility model with target return of 4%. MR0 denotes the maximum return model with target volatility of 1%, MR1 denotes the maximum return model with target volatility of 2%, MR2 denotes the maximum return model with target volatility of 4%. 55

FIGURE 19: This figure shows the annualized return for three types of monthly rebalancing strategies under model FVAR1 for 22-industry data set. SP500 denotes the S&P 500 index. GMV0 is the global minimum volatility model without constraints, GMV1 is the global minimum volatility model with no-shorting constraint, and GMV2 is the global minimum volatility model with leverage constraint. MVOL0 denotes the minimum volatility model with target return of 0.5%, MVOL1 denotes the minimum volatility model with target return of 1%, MVOL2 denotes the minimum volatility model with target return of 4%. MR0 denotes the maximum return model with target volatility of 1%, MR1 denotes the maximum return model with target volatility of 2%, MR2 denotes the maximum return model with target volatility of 4%. 56

FIGURE 20: This figure shows the annualized volatility for three types of monthly rebalancing strategies under model FVAR1 for 22-industry data set. SP500 denotes the S&P 500 index. GMV0 is the global minimum volatility model without constraints, GMV1 is the global minimum volatility model with no-shorting constraint, and GMV2 is the global minimum volatility model with leverage constraint. MVOL0 denotes the minimum volatility model with target return of 0.5%, MVOL1 denotes the minimum volatility model with target return of 1%, MVOL2 denotes the minimum volatility model with target return of 4%. MR0 denotes the maximum return model with target volatility of 1%, MR1 denotes the maximum return model with target volatility of 2%, MR2 denotes the maximum return model with target volatility of 4%. 57

FIGURE 21: This figure shows the annualized return for three types of quarterly rebalancing strategies under model FVAR1 for 22-industry data set. SP500 denotes the S&P 500 index. GMV0 is the global minimum volatility model without constraints, GMV1 is the global minimum volatility model with no-shorting constraint, and GMV2 is the global minimum volatility model with leverage constraint. MVOL0 denotes the minimum volatility model with target return of 0.5%, MVOL1 denotes the minimum volatility model with target return of 1%, MVOL2 denotes the minimum volatility model with target return of 4%. MR0 denotes the maximum return model with target volatility of 1%, MR1 denotes the maximum return model with target volatility of 2%, MR2 denotes the maximum return model with target volatility of 4%. 58

FIGURE 22: This figure shows the annualized volatility for three types of quarterly rebalancing strategies under model FVAR1 for 22-industry data set. SP500 denotes the S&P 500 index. GMV0 is the global minimum volatility model without constraints, GMV1 is the global minimum volatility model with no-shorting constraint, and GMV2 is the global minimum volatility model with leverage constraint. MVOL0 denotes the minimum volatility model with target return of 0.5%, MVOL1 denotes the minimum volatility model with target return of 1%, MVOL2 denotes the minimum volatility model with target return of 4%. MR0 denotes the maximum return model with target volatility of 1%, MR1 denotes the maximum return model with target volatility of 2%, MR2 denotes the maximum return model with target volatility of 4%. 59

FIGURE 23: This figure shows the annualized return for three types of monthly rebalancing strategies under model FVAR2 based on 22-industry data set. SP500 denotes the S&P 500 index. GMV0 is the global minimum volatility model without constraints, GMV1 is the global minimum volatility model with no-shorting constraint, and GMV2 is the global minimum volatility model with leverage constraint. MVOL0 denotes the minimum volatility model with target return of 0.5%, MVOL1 denotes the minimum volatility model with target return of 1%, MVOL2 denotes the minimum volatility model with target return of 4%. MR0 denotes the maximum return model with target volatility of 1%, MR1 denotes the maximum return model with target volatility of 2%, MR2 denotes the maximum return model with target volatility of 4%. 60

FIGURE 24: This figure shows the annualized volatility for three types of monthly rebalancing strategies under model FVAR2 based on 22-industry data set. SP500 denotes the S&P 500 index. GMV0 is the global minimum volatility model without constraints, GMV1 is the global minimum volatility model with no-shorting constraint, and GMV2 is the global minimum volatility model with leverage constraint. MVOL0 denotes the minimum volatility model with target return of 0.5%, MVOL1 denotes the minimum volatility model with target return of 1%, MVOL2 denotes the minimum volatility model with target return of 4%. MR0 denotes the maximum return model with target volatility of 1%, MR1 denotes the maximum return model with target volatility of 2%, MR2 denotes the maximum return model with target volatility of 4%. 61

FIGURE 25: This figure shows the annualized return for three types of quarterly rebalancing strategies under model FVAR2 based on 22-industry data set. SP500 denotes the S&P 500 index. GMV0 is the global minimum volatility model without constraints, GMV1 is the global minimum volatility model with no-shorting constraint, and GMV2 is the global minimum volatility model with leverage constraint. MVOL0 denotes the minimum volatility model with target return of 0.5%, MVOL1 denotes the minimum volatility model with target return of 1%, MVOL2 denotes the minimum volatility model with target return of 4%. MR0 denotes the maximum return model with target volatility of 1%, MR1 denotes the maximum return model with target volatility of 2%, MR2 denotes the maximum return model with target volatility of 4%. 62

- FIGURE 26: This figure shows the annualized volatility for three types of quarterly rebalancing strategies under model FVAR2 based on 22-industry data set. SP500 denotes the S&P 500 index. GMV0 is the global minimum volatility model without constraints, GMV1 is the global minimum volatility model with no-shorting constraint, and GMV2 is the global minimum volatility model with leverage constraint. MVOL0 denotes the minimum volatility model with target return of 0.5%, MVOL1 denotes the minimum volatility model with target return of 1%, MVOL2 denotes the minimum volatility model with target return of 4%. MR0 denotes the maximum return model with target volatility of 1%, MR1 denotes the maximum return model with target volatility of 2%, MR2 denotes the maximum return model with target volatility of 4%. 63
- FIGURE 27: This figure shows the next 12 months impulse response of constant loading with stochastic volatility model FVAR1 for ten sectors on 06/2004 as the Fed starts to increase interest rate by a quarter point. Note that the impulse response is recorded in percentage returns. 64
- FIGURE 28: This figure shows the next 12 months impulse response of constant loading with stochastic volatility model FVAR1 for ten sectors on 09/2007 as the Fed cut interest rate by half point since June 2003. Note that the impulse response is recorded in percentage returns. 65
- FIGURE 29: This figure shows the next 12 months impulse response of dynamic loading with stochastic volatility model DFVAR in (2) for ten sectors on 06/2004 as the Fed starts to increase interest rate by a quarter point. Note that the impulse response is recorded in percentage returns. 66
- FIGURE 30: This figure shows the next 12 months impulse response of dynamic loading with stochastic volatility model DFVAR in (2) for ten sectors on 09/2007 as the Fed cut interest rate by half point since June 2003. Note that the impulse response is recorded in percentage returns. 67

FIGURE 31: The figure in Panel A depicts wealth process and the consistent performance benchmark in Merton's model. Parameters are: $\mu = 0.07, \sigma = 0.2, r = 0.5\%, \rho = 0.25, \gamma = 0.8$, and $W_0 = 1$. The consistent performance benchmark parameters are chosen as $M_0 = 0.4, a = 0.01, b = r + a = 0.015$. Wealth $W(t)$ is characterized by equation (46) and the consistent performance benchmark $M(t)$ is calculated by equation (H-2). The figure in Panel B depicts the optimal wealth and the consistent performance benchmark. Both optimal wealth $W(t)$ and the consistent performance benchmark $M(t)$ are characterized by Proposition 4. The figures in Panel C and Panel D depict the Merton's wealth process and optimal wealth process with maximum drawdown benchmark $\alpha \max_{0 \leq s \leq t} W_t$, where $\alpha = 80\%$, respectively.

96

FIGURE 32: The figure in Panel A depicts the position in risky assets versus the ratio of wealth to the consistent performance benchmark for different values of parameter a . The parameters used in this example are chosen as $\mu = 0.08, \sigma^2 = 0.1, r = 0.5\%, \rho = 0.035, \gamma = 0.8, b = 0.03$, with $a = 0.03$ and 0.04 , respectively. The figure in Panel B depicts the position in risky assets versus the ratio of wealth to the consistent performance benchmark for different values of parameter r . The parameters used in this example are: $\mu = 0.08, \sigma^2 = 0.1, \rho = 0.035, \gamma = 0.8, a = 0.03, b = 0.03$, with $r = 0.5\%$ and 1% , respectively.

97

FIGURE 33: The figure in Panel A depicts the dynamics of portfolio wealth under traditional intertemporal policy. The parameters used in this example are chosen as $\mu = 6.46\%, \sigma = 18.35\%, r = 1.817\%, \rho = 0.05, \gamma = 0.3, a = 0.01$. The figure in Panel B depicts the optimal wealth dynamics under the consistent performance constraint with the same parameters.

109

FIGURE 34: The figure in Panel A depicts the composition of portfolio wealth under traditional intertemporal policy. The parameters used in this example are chosen as $\mu = 6.46\%, \sigma = 18.35\%, r = 1.817\%, \rho = 0.05, \gamma = 0.3, a = 0.01$. The figure in Panel B depicts the composition of portfolio under the consistent performance constraint with the same parameters.

110

- FIGURE 35: The figure in Panel A depicts the dynamics of portfolio wealth and consumption rule under traditional intertemporal policy. The parameters used in this example are chosen as $\mu = 6.46\%$, $\sigma = 18.35\%$, $r = 1.817\%$, $\rho = 0.05$, $\gamma = 0.3$, $a = 0.01$. The figure in Panel B depicts the dynamics of portfolio wealth and consumption under the consistent performance constraint with the same parameters. 111
- FIGURE 36: The figure in Panel A depicts the comparison of traditional consumption policy and the optimal consumption policy under consistent performance constraint. The parameters used in this example are chosen as $\mu = 6.46\%$, $\sigma = 18.35\%$, $r = 1.817\%$, $\rho = 0.05$, $\gamma = 0.3$, $a = 0.01$. The figure in Panel B depicts the comparison of traditional investment policy in the risky asset and the one under consistent performance constraint with the same parameters. 112
- FIGURE 37: The figure in Panel A depicts the capital cushion under the consistent performance constraint for different values of parameter a . Other parameters used in this example are chosen as $\mu = 6.46\%$, $\sigma = 18.35\%$, $r = 1.817\%$, $\rho = 0.05$, $\gamma = 0.3$. The figure in Panel B depicts the optimal consumption policy under the consistent performance constraint with the same parameters. 113
- FIGURE 38: The figure in Panel A depicts optimal risky asset investment policy under the consistent performance constraint for different values of parameter a . Other parameters used in this example are chosen as $\mu = 6.46\%$, $\sigma = 18.35\%$, $r = 1.817\%$, $\rho = 0.05$, $\gamma = 0.3$. The figure in Panel B depicts optimal riskless investment policy under the consistent performance constraint with the same parameters. 114
- FIGURE 39: The figure in Panel A depicts the capital cushion under the consistent performance constraint for different volatility values. Other parameters used in this example are chosen as $\mu = 6.46\%$, $r = 1.817\%$, $\rho = 0.05$, $\gamma = 0.3$, $a = 0.01$. The figure in Panel B depicts the optimal consumption policy under the consistent performance constraint with the same parameters. 115
- FIGURE 40: The figure in Panel A depicts optimal risky asset investment policy under the consistent performance constraint for different volatility values. Other parameters used in this example are chosen as $\mu = 6.46\%$, $r = 1.817\%$, $\rho = 0.05$, $\gamma = 0.3$, $a = 0.01$. The figure in Panel B depicts optimal riskless investment policy under the consistent performance constraint with the same parameters. 116

- FIGURE 41: The figure in Panel A depicts the capital cushion under the consistent performance constraint for different values of parameter γ . Other parameters used in this example are chosen as $\mu = 6.46\%$, $\sigma = 18.35\%$, $r = 1.817\%$, $\rho = 0.05$, $a = 0.01$. The figure in Panel B depicts the optimal consumption policy under the consistent performance constraint with the same parameters. 117
- FIGURE 42: The figure in Panel A depicts optimal risky asset investment policy under the consistent performance constraint for different values of parameter γ . Other parameters used in this example are chosen as $\mu = 6.46\%$, $\sigma = 18.35\%$, $r = 1.817\%$, $\rho = 0.05$, $a = 0.01$. The figure in Panel B depicts optimal riskless investment policy under the consistent performance constraint with the same parameters. 118
- FIGURE 43: The figure in Panel A depicts the simulated series and stochastic volatility. The figure in Panel B depicts the sample autocorrelation function, sample draws and posterior densities for simulated data 156
- FIGURE 44: This figure shows the estimation results of α_{1t} , α_{2t} and h_t for the simulated data. The gray area represents the 99% confidence interval. The solid line denotes the true value of the state variable and the dashes line denotes the posterior mean. 157

LIST OF TABLES

TABLE 1: Monthly rebalancing portfolio performance under model FVAR0	68
TABLE 2: Quarterly rebalancing portfolio performance under model FVAR0	69
TABLE 3: Monthly rebalancing portfolio performance under model FVAR1	70
TABLE 4: Quarterly rebalancing portfolio performance under model FVAR1	71
TABLE 5: Monthly rebalancing portfolio performance under model FVAR2	72
TABLE 6: Quarterly rebalancing portfolio performance under model FVAR2	73
TABLE 7: Monthly rebalancing portfolio performance under model FVAR1	74
TABLE 8: Quarterly rebalancing portfolio performance under model FVAR1	75
TABLE 9: Monthly rebalancing portfolio performance under model FVAR2	76
TABLE 10: Quarterly rebalancing portfolio performance under model FVAR2	77
TABLE 11: Measures of the portfolio performance under consistent performance constraint	119
TABLE 12: This table summarizes the estimation results for the simulated data.	141
TABLE 13: Estimation results summary for the simulated data including heavy tail and jump.	153

CHAPTER 1: MACRO FACTORS, DYNAMIC ASSET ALLOCATION AND MONETARY POLICY

I. Introduction

Macroeconomics has long featured two general views: it has weak predictive power for equity returns and little use for asset allocators (Chan, et al. 1998, Shanken and Weinstein 2006). Intuitively, it is natural to think the asset returns should vary with the changing economic environment. Such a disconnect between aggregate macroeconomic information and asset returns looks puzzled to both academic researchers and practical investors. However, to identify which variables could capture the systematic components of equity return variation and be the main drivers of equity movements is crucial to both academic scholars and practitioners. Therefore, in the past decades, numerous research attempts to identify the variables driving equity returns (Chen et al. 1986, Ferson and Harvey 1991, Chan, et al. 1998, Shanken and Weinstein 2006).

Given a number of papers claiming that the historical mean has done well at forecasting the equity premium, Welch and Goyal (2008) conduct a comprehensive empirical study on the equity premium prediction and show that most models with variables suggested by the academic literature to be good predictors actually predict poorly out-of-sample. They suggest that the forecasting ability is seriously impaired by model uncertainty and instability.¹ There are three possible reasons leading to

¹The original data time period covers up to 2005, and the time range is updated in 2013, as shown in the authors' website: <http://www.hec.unil.ch/agoyal/>. It seems that the conclusion still

their conclusions. One possible reason is that the base models tested in Welch and Goyal (2008) are linear and static. In other words, the models with predictors of good in-sample predictive ability may not perform well to predict out-of-sample in a linear and static framework. Lettau et al. (2008) find a strong relationship between the macroeconomic risk and stock market movements in a dynamic regime switching setting. Intuitively, the asset returns should vary with the changing environment, suggesting a time-varying relationship.² Recent research shows that fixed coefficient predictive models are almost dominated by time-varying coefficient models. These time-varying characteristics are found to be statistically and economically significant to improve return predictability and out-of-sample portfolio forecasting (Dangl and Halling 2012, Johannes et al. 2014).

The second possible reason is that the effect of parameter uncertainty is ignored in their analysis. Numerous research show that the estimation risk or uncertainty about the parameters has a profound effect on the return prediction (Avramov 2002, Cremers 2002) and portfolio construction in the sense that the regression coefficients may look weak by the usual statistical measures but could exert influential effects on portfolio decisions (Kandel and Stambaugh 1996, Barberis 2000, Xia 2001, Brandt et al. 2005).

holds up to 2013.

²The closely watched nonfarm job data on Friday, 04/03/2015 showed that the growth in nonfarm payrolls slowed in March to a seasonally adjusted 126,000, the weakest hiring in 15 months which was catching the rest of slumping indicators in recent months, such as consumer spending, capital investment, and manufacturing output. In normal circumstances, the sudden downturn in hiring should cause the stock to go south, that is, a positive relationship, as it may imply that the recovery was not robust. However, after a long weekend to digest it, the investors brushed off the disappointing jobs report and pushed the Dow Industrials higher ending back in positive territory for the year, suggesting a negative relationship instead.

The third reason could be that individual predictors may not contain sufficient information content to generate significant systematic economic values. In fact, a lot of variables that researchers scrutinize really don't matter that much. For example, the future of GDP growth almost has no correlation to the real stock returns over the subsequent decade. Or even we could predict the interest rate dynamics in the future, the market reaction could be another story. For instance, if the interest rate jumps due to the increasing inflation, then it might be a bad news for stocks; or if the interest rate jumps due to the real economic growth, then the stock market might welcome it. Also, if the profit margin falls due to the rising material costs, then it could send a bad signal to the market; or if the profit margin falls because of the increasing wages, then the market might like it as it leads to higher consumer spending and thereby more corporate revenue. Intuitively, markets seem too complex to reduce to one predictive metric, so relying on any single predictor is not going to work, which implies that we need take into account a wide range of information contents to understand the economy status and improve forecasting accuracy.

In order to enhance the forecasting ability, there are two common approaches to improve the accuracy of forecasts in the literature. One is to combine forecasting results from a number of individual predictive models (Rapach et al. 2010) and the other is to extract significant information from a large number of series into a small number of factors (Stock and Watson 2002, Bernanke and Boivin 2003, Bernanke et al. 2005). These two methods actually have similar implications, that is, we need a wide range of information set to be able to produce significant predictions. The rationale could be understood in two fold. On one hand, the textbook definitions

may not be clearly described by specific economic variables. For instance, a vague concept like economic activity could not be fully demonstrated by a couple of time series. On the other hand, a single indicator may not draw a complete picture and could send a misleading message.³ In fact, in the real world hundreds of economic variables are not only regularly monitored by central bankers in their policy-making processes (Bernanke and Boivin 2003, Greenspan 2004, Yellen 2014⁴), but also closely watched by practical investors.⁵

Therefore, to answer the question whether macro matters in asset allocation, we adopt a dynamic factor model with meaningful economic factors extracted from hun-

³The employment report on 05/02/2014 showed that the unemployment rate dropped to 6.3% which was a bit higher than that at the beginning of financial crisis in 2008. Textbooks indicate that the Fed should react ahead of time to raise interest rate. But the inflation has maintained below 2% for straight 23 months and the labor-force participation rate was only at a three-decade low of 62.8%. The reduced unemployment rate and participation rate actually implied a shrinking pool of American workers who were seeking for jobs. Therefore, the Dow Jones Industrial Average initially rose 61 points after the report was released, but eventually fell 45.98 points after the market figured out the real implications of the report. Additionally, there are many factors that could influence inflation and the Phillips curve, which implies the negative relationship between a falling unemployment rate and rising wages, forms the backbone of economic models. However, the fact is that the core inflation excluding food and energy prices was up 2% on April 2012 as the unemployment rate was 8.2%, and the core inflation has fallen to 1.2% since then but the unemployment has also fallen to 5.1%, implying a positive relationship. One possible reason could be the increasing globalization and meltdown of commodity market that could exert a downward pressure on the U.S. import price and thereby the domestic inflation.

⁴The Fed chairwomen Janet Yellen delivered a statement about the labor market at the 2014 Jackson Hole Economic Policy Symposium: "Our assessments of the degree of slack must be based on a wide range of variables and will require difficult judgements about the cyclical and structural influences in the labor market" (Wall Street Journal, 08/25/2014) and the Fed Vice Chairman Stanley Fischer answered the question of "What do you do if unemployment continues to fall, but inflation doesn't move or goes down because of what's happening in the rest of the world? Can you let things run a little bit longer in this abnormal state of very low interest rates?" in the interview at the WSJ CEO Council gathering: " We can do that, and if the inflation is really heading south, we will have to do that. We said we're data-driven and if that's where the data drives us, that's what we will do" (Wall Street Journal, 12/09/2014).

⁵On 06/02/2014, the Institute for Supply Management (ISM) initially reported the ISM Manufacturing Index as 53.2 in May and revised the index to 55.4 one hour and half later due to a software error. Accordingly, traders' reactions ranged from mild surprise to a relief, therefore the Dow Jones Industrial Average fell as much as 35 points following the release of the initial factory data, and then surged 30 points after the revision. The market sentiment soon settled down and Dow closed up 26.46 points.

dreds of series with Bayesian estimation which naturally takes into account parameter uncertainty problem in a time-varying environment in order to mitigate the effects of these three potential issues discussed above on our analysis. Intuitively, this time-varying framework could bring more flexibility to the model in order to closely capture fluctuations and dynamics of the driving forces, although less mathematically precise, and let the data tell us what the real world may look like instead of making hypothesis about how the world should work. Furthermore, this flexibility can connect portfolio theory, monetary policy and macroeconomics to answer many practical questions. Specifically, by incorporating model flexibility and harnessing a wide range of data, we could examine many aspects of portfolio choice, i.e., the economic forces driving asset returns, investors' slant on future economic trend, the effects of monetary policy on portfolio construction and so on.

Factor models are widely used in portfolio selection area to represent the latent forces that drives the asset price dynamics, such as Aguilar and West (2000), Chib et al. (2006) and Han (2006). One limitation of the latent factors is that it is not easy to understand the economic implications of the unobserved factors and the other limitation is that the ordering of the variables plays an important role in estimating the loading matrix due to the triangular identification restriction imposed in the latent factor models. In other words, different orderings of variables could yield different estimates and thus lead to different conclusions, and it is not clear about the exact effects of ordering on the estimation so far. By contrast, in this paper, we implement a two-step estimation procedure: in the first step, we extract significant information content from blocks of macroeconomic series with closely related variables

in one block and assign them with meaningful economic representations, and then use Bayesian techniques embedded in the MCMC sampler to estimate parameters in the second step. The explicit representation of factors could help us better understand the dynamics of the underlying driving forces that can move the asset prices and at the same time avoid the estimation issue involved in the latent factor models. Furthermore, the central bankers often continue to debate and search for clues from the trajectories of economic activity, labor market, and inflation on the rate-hike or rate-drop timing, sometimes the officials have to filter a range of conflicting signals before making a decision on the rate-hike or rate-drop timing⁶, and a time-varying correlation among the major drivers of economy is provided in this paper, which is absent in the previous literature and might shed a light on the timing of monetary policy for the regulators.

In comparison to Stock and Watson (2002) and Bernanke et al. (2005) in which several general principal components are extracted from a number of series, we further categorize a large number of series into several representative blocks assigned with meaningful economic implications and then estimate model parameters based on these economic factors. Ludvigson and Ng (2007) summarize a large number of economic information in three factors, i.e., volatility, risk premium and real factors, which could contain important information content that not included in commonly used predictor variables and their specifications can exhibit stable and statistically significant out-of-sample forecasting power. In this paper, we find that these five

⁶The academics seems not to provide a clear direction as well, i.e., Harvard professors Martin Feldstein and Lawrence Summers, who have been the economic advisers for republicans and democrats, respectively, argued for and against a rate-hike in September in the competing newspaper opinion columns (03/30/2015 Wall Street Journal and 02/08/2015 Washington Post).

fundamental factors are able to capture significant economic trends in a variety of aspects of economic activities and systematic components of equity return dynamics, and dynamic asset allocation based on these factors could generate systematically significant out-of-sample economic gains. Specifically, the global minimum volatility strategy looks appealing and could generate significant out-of-sample economic gains and higher Sharpe ratio than the buy-and-hold strategy for different model frameworks. Setting a reasonable target value plays an important role on the portfolio performance for minimum volatility strategy with target return and maximum return strategy with target volatility. In addition, the time horizon in general has a negative effect on the portfolio performance in the sense that the quarterly rebalancing portfolios underperform the monthly rebalancing portfolios, which is consistent with the conclusion of Ang and Bekaert (2007) and Boudoukh et al. (2008).

After the recent 2008 financial crisis, due to the fragile and unstable economic recovery, central banks around the world often intervene the real economy by adjusting their monetary policies, i.e., raising or reducing interest rate. This essentially create an "administrative" market in which asset prices are at least partly influenced by the central bank's policy, in addition to the normal market forces. From the perspective of investors, as they rebalance their portfolio positions, instead of just looking at past returns and risk, they should also look ahead of time and take into account the most significant future events that can dramatically influence their current strategies and positions, such as the rising interest rate. But the traditional studies in asset allocation literature are based on examining the past asset returns and volatility dynamics and then constructing portfolio weights, such as the classic mean-variance portfo-

lio selection by Markowitz (1952) and the intertemporal consumption and portfolio choice by Merton (1971). Few research takes into account investor's subjective judgement and conjecture about future possible events and investigates the corresponding effects. Black and Litterman (1991) incorporate investor's views with market equilibrium into their portfolio construction and the so-called Black-Litterman model has been widely used in practice (Goldman Sachs 1998). Hence, in this paper, we take into account the effect of monetary policy on our portfolio construction and conduct impulse response analysis for the effect of monetary policy on the equity returns. We find that the dynamic factor models with time-varying coefficients are able to reveal appealing indications about the future trajectories of equity returns, which could be informative and valuable for both policy makers and practical investors.

The remainder of the paper is organized as follows. Section 2 introduces the macro factors, presents their main characteristics and discusses their economic implications. We study the dynamic asset allocation based on macro factors for different trading strategies and investigate the monthly and quarterly rebalancing portfolio performance by using a variety of performance measures in Section 3. In Section 4, we examine the effects of monetary policy shocks on asset returns under different model specifications. Section 5 concludes.

II. Macroeconomic Factors

Factor model has tremendous intuitive appeal to model asset returns and been extensively studied in the literature including the famous arbitrage pricing theory (APT). The intuition is that the asset returns can be decomposed into some sys-

tematic components and an idiosyncratic component. The systematic components or factors cause the asset returns to be correlated and the idiosyncratic components are assumed to be uncorrelated across assets.

Let $r_{i,t}$ denote the asset returns observed at time t for asset $i = 1, \dots, n$ and $f_{j,t}$ denote the risk factor j observed at time t for $j = 1, \dots, k$, then we could represent the multi-factor asset pricing model as follows

$$r_{i,t} = \beta_{i0,t} + \sum_{j=1}^k \beta_{ij,t} f_{j,t} + \varepsilon_{i,t} \quad (1)$$

where the idiosyncratic risk $\varepsilon_{i,t} \sim (0, \sigma_{i,t}^2)$. However, the dynamics of $\beta_{ij,t}$ and $\sigma_{i,t}^2$ is, in general, unspecified in the asset pricing theory literature. A variety of static and linear models has been tested in the literature and shows poor out-of-sample performance (Chan et al. 1998, Shanken and Weinstein 2006, Welch and Goyal 2008). By allowing for dynamic loading and stochastic volatility, we wonder whether a time-varying environment could reveal the value of macro factors and produce economic gains in the asset allocation.

In addition, to incorporate the effects of investor's view about the monetary policy, we follow Bernanke et al. (2005) to adopt an augmented factor VAR model for asset returns within a dynamic framework. Another distinctive feature of our augmented factor model is that we allow a time-varying covariance structure instead of a constant covariance setting (Bollerslev 1990) in our model so that we could obtain a time-varying correlation among these economic factors in order to help us better understand the dynamic interactions among the driving forces, which is absent in many previous studies (Aguilar and West 2000, Bernanke et al. 2005, Chib et al. 2006, Han 2006).

Moreover, in comparison to the dynamic conditional correlation proposed by Engle (2002) in which the covariance matrix is set to follow a specified linear form, no assumption is made for the dynamics of covariance matrix in our case.

II.1 Description

There are two ways to treat the factors in the literature. One is to take the factors as latent variables (Aguilar and West 2000, Chib et al. 2006, Han 2006). One drawback of the latent factor models is that the factors are viewed as unobserved variables, implying that they are abstract and hard to understand in an intuitive and economic way. The other is to select various macro variables as proxy, but the out-of-sample performance is weak (Chan et al. 1998, Shanken and Weinstein 2006, Welch and Goyal 2008). Instead of choosing individual variables as predictors, we extract some significant economic factors from hundreds of time series which could explicitly represent various aspects of economic activities, and then study their time-varying interactive relationships. Specifically, we characterize five economic factors that could be used to represent different dimensions of the economy and viewed as the driving forces to cause various types of asset dynamics. Below we provide their economic explanations and the reality representations for these five factors. Data descriptions are shown in the Appendix.

1) Real economic factor: this factor aims to represent the state of real economic activity. Sixty three macroeconomic time series are selected in order to capture a wide range of aspects of economic activity, which includes information from industrial production across various industries, capacity utilization, a variety of indicators for

employment, wages, personal consumption, housing starts, imports and exports and so on.

2) Price factor: this factor aims to represent a wide range of inflation which includes various types of consumer price index (CPI), producer price index (PPI) and oil price. Twenty time series are chosen to represent this factor.

3) Interest rate factor: this factor aims to represent the effects of interest rate. Twenty one series are chosen in this group, which contains bond yields at different maturities and their spread with respect to the effective federal funds rate. It also incorporates the economic implications from exchange rates dynamics according to the interest rate parity theory (IRP).

4) Money and credit factor: this factor aims to represent various transmission channels of monetary policy that could have profound effects on every sectors of economy. Thirty two series are chosen in this block, which includes information from monetary base, reserves, demand deposits, savings deposits, consumer and commercial loans, outstanding credit, treasury and agency securities, and borrowing reserves of depository institutions.

5) Expectation factor: this factor aims to represent various types of expectations. Ten expectation series are chosen in this block, which includes production, employment, inventories, supplier deliveries, new orders and future inflations from NAPM and other surveys. Jones and Tuzel (2013) find significant implications of new orders and shipments to predict equity returns.

In this paper, we only consider one monetary instrument, that is, the effective federal funds rate. But our model setting and estimation procedures are feasible to

incorporate other types of monetary policies as well.

II.2 Econometric Framework

Let $r_t = (r_{1t}, \dots, r_{nt})'$ denote a vector of returns for n assets which follow the dynamic factor vector autoregressive model (DFVAR) as follows

$$\begin{aligned} r_t &= \Lambda_t^f f_t + \Lambda_t^z z_t + \varepsilon_t \\ &:= B_t Y_t + \varepsilon_t \end{aligned} \quad (2)$$

where $\Lambda_t^f \in \mathbb{R}^{n \times k}$ denotes the loading coefficient for factors f_t and $\Lambda_t^z \in \mathbb{R}^{n \times l}$ denotes the loading coefficient for monetary instrument z_t , and $B_t \in \mathbb{R}^{n \times m}$, $Y_t' = (f_t', z_t')$ with $f_t \in \mathbb{R}^k$ denoting the fundamental factors and $z_t \in \mathbb{R}^l$ denoting the monetary instruments, where $m = k + l$. Let $b_i \in \mathbb{R}^m$ denotes i -th the row elements of loading B_i , which follows a random walk process as follows

$$b_{i,t} = b_{i,t-1} + u_{i,bt} \quad (3)$$

The idiosyncratic noises follow a multivariate normal distribution with stochastic volatilities as $\varepsilon_t \sim N_n(0, H_t)$ with $H_t \sim \text{diag}(e^{h_{1t}}, \dots, e^{h_{nt}})$ and the log-volatilities follow a random walk process

$$h_{i,t} = h_{i,t-1} + u_{i,ht} \quad (4)$$

where $u_{i,ht} \sim N(0, \Sigma_{i,h})$ for $i = 1, \dots, n$. The factor equations of Y_t follow a time-varying VAR(p) model with time-varying covariance as follows

$$Y_t = C_{0t} + C_{1t}Y_{t-1} + C_{2t}Y_{t-2} + \dots + C_{pt}Y_{t-p} + v_t \quad (5)$$

where $p \geq 1; m \geq 2$, $Y_t, C_{0t} \in \mathbb{R}^m$ and $C_{it} \in \mathbb{R}^{m \times m}$ for $i = 1, 2, \dots, p$ and $t = 1, 2, \dots, T$. We could transfer equation (5) to the following vector notation

$$\begin{aligned} Y_t &= C_t \mathcal{Y}_{t-1} + v_t \\ &= (\mathcal{Y}'_{t-1} \otimes \mathbf{I}_m) \text{vec}(C_t) + v_t \\ &:= y'_{t-1} \beta_t + v_t \end{aligned} \quad (6)$$

where $C_t = (C_{0t}, C_{1t}, \dots, C_{pt}) \in \mathbb{R}^{m \times (mp+1)}$, $\mathcal{Y}_{t-1} = (1, Y'_{t-1}, Y'_{t-2}, \dots, Y'_{t-p})' \in \mathbb{R}^{mp+1}$, $y_{t-1} \in \mathbb{R}^{(m^2 p+m) \times m}$ and $\beta_t = \text{vec}(C_t) \in \mathbb{R}^{m^2 p+m}$. Here $\text{vec}(\cdot)$ denotes the column-stacking operator and \otimes denotes the Kronecker product.

In this paper, we assume that $v_t \sim N(0, \Omega_t)$ with a time-varying covariance matrix $\Omega_t \in \mathbb{R}^{m \times m}$. By following Cogley and Sargent (2005) and Primiceri (2005), we could decompose the covariance matrix into

$$A_t \Omega_t A_t' = \Sigma_t \Sigma_t' \quad (7)$$

or equivalently,

$$\Omega_t = A_t^{-1} \Sigma_t \Sigma_t' (A_t')^{-1} \quad (8)$$

where $\Sigma_t = \text{diag}(e^{\sigma_{1t}/2}, e^{\sigma_{2t}/2}, \dots, e^{\sigma_{mt}/2})$ is the diagonal matrix and A_t is a lower triangular matrix with units on the main diagonal shown as follows

$$A_t = \begin{pmatrix} 1 & 0 & \cdots & 0 \\ \alpha_{21,t} & 1 & \ddots & \vdots \\ \vdots & \ddots & \ddots & 0 \\ \alpha_{m1,t} & \cdots & \alpha_{m,m-1,t} & 1 \end{pmatrix} \quad (9)$$

Thus, the factor equation (6) can be rewritten as

$$Y_t = y'_{t-1}\beta_t + A_t^{-1}\Sigma_t u_{yt} \quad (10)$$

and the coefficients follow a random walk as follows

$$\beta_t = \beta_{t-1} + u_{\beta t} \quad (11)$$

$$\alpha_t = \alpha_{t-1} + u_{\alpha t} \quad (12)$$

$$\sigma_t = \sigma_{t-1} + u_{\sigma t} \quad (13)$$

and the noise in the random walk are assumed to be jointly normally distributed with variance as follows

$$V = \text{var} \begin{pmatrix} u_{yt} \\ u_{bt} \\ u_{\beta t} \\ u_{\alpha t} \\ u_{\sigma t} \\ u_{ht} \end{pmatrix} = \begin{pmatrix} \mathbf{I} & 0 & 0 & 0 & 0 & 0 \\ 0 & \Sigma_b & 0 & 0 & 0 & 0 \\ 0 & 0 & \Sigma_\beta & 0 & 0 & 0 \\ 0 & 0 & 0 & \Sigma_\alpha & 0 & 0 \\ 0 & 0 & 0 & 0 & \Sigma_\sigma & 0 \\ 0 & 0 & 0 & 0 & 0 & \Sigma_h \end{pmatrix}. \quad (14)$$

In order to keep our model parsimony and computation efficient, we adopt the random walk process for the volatility evolution process, but the random walk assumption could be extended to a standard three-parameter (μ, ϕ, σ) stochastic volatility process, i.e., $h_t - \mu = \phi(h_{t-1} - \mu) + \sigma\eta_t$.⁷ Although under the random walk pro-

⁷To estimate (μ, ϕ, σ) , a Metropolis-hastings algorithm (Chib and Greenberg 1995) is needed with a multivariate-t as the proposal distribution. The mode of the likelihood function is commonly chosen as the mean of multivariate-t and the inverse of the negative Hessian matrix of the likelihood function is selected as the covariance of the multivariate-t. This process is time-consuming as it involves in an optimization procedure and estimation of a Hessian matrix. The loading ϕ is highly persistent in our data, between 0.95 to 1.00, thus for simplicity, we adopt the random walk setting.

cess assumption, our model still includes a large number of parameters and latent variables. For example, for n assets with k macroeconomic factors and l monetary instruments, we have $n(k + l)$ parameters in loading matrix B and n parameters in Σ_h . For a p -lag VAR model, we have $m^2p + m$ parameters in Σ_β and $m(m - 1)/2$ parameters in Σ_α and m parameters in Σ_σ . On the other hand, we would have $(T - 1)[n + (m^2p + m) + m(m - 1)/2 + m]$ latent state variables. Therefore, for $n = 10$ assets with $k = 5$ factors augmented by $l = 1$ monetary policy under $T = 284$ and $p = 3$ lags, we would have 205 parameters and 41,035 unobserved state variables.

II.3 Data

Two data sets are investigated in this paper. We first study a monthly data set of 10 sectors from *S&P* 500 index. The 10 sectors that include 1) industrial, 2) Consumer discretionary, 3) Information technology, 4) Financial, 5) Materials, 6) Telecom, 7) Health care, 8) Consumer staple, 9) Energy, and 10) Utility are collected from Bloomberg ranging from 09/1989 to 05/2013. We collect 147 macroeconomic time series from Federal Reserve Bank of St. Louis during the same time period and transform these series according to the format described in the Appendix. A simulation study is present in the Appendix as well in order to show that our algorithm is efficient and fairly robust to capture the data dynamics.

We estimate the dynamic loading model with stochastic volatility in equation (2) with 3-lag and run 30,000 iterations after discarding the initial 3,000 burn-in samples.

The posterior estimates seem satisfactory.⁸ We also test 6-lag model, which presents

⁸The sample autocorrelations are quite low after five hundred draws and the sample draws look stable, which indicates that the proposed sampling approach seems efficient to draw samples with low autocorrelation. And the mean of inefficiency factors (IFs) for all hyperparameters in variance matrix

similar qualitative feature but need much more computational resources. Thus, the empirical analysis is based on 3-lag model in this section.

In addition, for the asset allocation study, we estimate both the 10-sector data set and a larger data set of 22 industry groups classified by Global Industry Classification Standard (GICS)⁹ from Bloomberg ranging from 09/1989 to 05/2013. The 22 industry groups consists of 1) Automobiles and Components, 2) Consumer Durables and Apparel, 3) Consumer Services, 4) Media, 5) Retailing, 6) Food and Staples Retailing, 7) Food Beverage and Tobacco, 8) Household and Personal Products, 9) Energy, 10) Banks, 11) Diversified Financials, 12) Insurance, 13) Health Care Equipment and Services, 14) Pharmaceuticals, Biotechnology and Life, 15) Capital Goods, 16) Commercial and Professional Services, 17) Transportation, 18) Software and Services, 19) Technology Hardware and Equipment, 20) Materials, 21) Telecommunication Services, 22) Utilities.

II.4 Stochastic Volatility of Macro Factors

We first study the stochastic volatility of macro factors. Figure 3 demonstrates the stochastic volatility for the five economic factors in equation (6). From February 1994 to February 1995, the Fed began to raise the federal funds rate in 7 steps from 3% to 6% since the economy started to expand in late 1993 and the zero real federal funds rate was not needed any more. On one hand, we could observe that there was

(14) is 13.08, the median of IFs is 16.43, and the minimum value of IFs is 0.91, the maximum value of IFs is 129.23, and the 10th percentile IFs is 1.06 and the 90th percentile IFs is 13.71. Considering the large number of parameters and to keep the draft concise, complete estimates results including sample autocorrelation function, sample draws, and posterior densities are not present in the draft and are available upon request.

⁹The GICS classification system consists of 24 industry groups, but the Real Estate industry data is discontinued after 08/2002 and the Semiconductors and Semiconductor Equipment industry level 2 data is not available, hence we conduct empirical study based on 22 industry groups.

an upward shock in the volatility of interest rate factor, on the other hand, there was little shock in the volatility of price factor, which was consistent with the fact that the inflation showed little tendency to accelerate and remained between 2.5% and 3% during the same time period.

Because of the advances in computer and information technology and the improved productivity growth from 1996 to 1999, this period was characterized with an optimism of future income prospects, we could see an upward shock in the volatility of real activity factor and expectation factor. The federal funds rate was held at 5.25% until 1997, so shock to interest rate factor quickly declined in that period, and it was cut by 75 basis points in the aftermath of the 1998 Russian debt default and then reversed the 75 basis points in 1999, thus there was an upward shock to the volatility of interest rate factor from 1998 to 1999. And the core CPI ranged between 2% and 2.5% during the entire period.

During the 2001 internet bubble, the Fed started to loosen the monetary policy and the federal funds rate was cut from 6.25% to 1.75% in 2001 and it was kept going down in 2002 and 2003 to 1% at a slower rate. There was a sharp spike in the volatility of the money and credit factor in the aftermath of the dotcom bubble. The Fed started to increase federal funds rate in June 2004 gradually until June 2006 when the rate reached the plateau of 5.25%, and the core CPI approached to 3% but with more volatile due to the rapid increase in energy prices. Then the fund rate was quickly cut to near zero during the 2008 housing bubble,¹⁰ thus we could clearly

¹⁰Taylor (2007) argued that since the period of low interest rate policy kept from 2003 to 2004 was too low and for too long, it fueled to the housing boom and bust, and eventually destabilized the U.S. economy.

observe that there was a drastic shock to interest rate factor, price factor and money and credit factor during that time period.

The stochastic volatility of real activity factor kept increasing from 2001 to 2009, and the volatility of expectation factor also kept rising from 2009 to 2011, one possible explanation about the expectation factor volatility could be that due to the increasing globalization and competition from abroad, the volatility of forecasting becomes larger. The fund rates has been kept to near zero since 2008 to stimulate business investment, encourage consumption and improve the job market, and we could observe an upward trend in the volatility of real activity factor and price factor after 2011, indicating the slow recovery of economy. Overall, these macro factors look reasonable and satisfactory to capture significant economic trends from a variety of aspects of real economy over time.

II.5 Dynamic Interactions Among Macro Factors

The magnitude of shock for each macro factor could be represented in the stochastic volatility measure. Furthermore, it's also interesting and informative to see the direction of the simultaneous movements among macro factors in order to better understand how the economy evolve over time. Therefore, the time-varying correlation among macroeconomic factors is shown in Figure 4. The first row presents the time-varying correlation between the real activity factor and other factors. In general, real factor has negative relationship with other factors. Specifically, the negative relationship between real activity factor and price factor was diminishing after 1999. In other words, this weak relationship indicates that the real activity shock has little effect on

inflation shock after 1999, which could be justified by the recent fact that the stock markets hit record highs with continuously growing firms' earnings but with lower than expected inflation target of 2%.

The correlation between real factor and interest rate factor was negative at most of time except the time period from 2004 to 2005, in which the Fed started to raise funds rate. The negative relationship implies that the inflation was not the big concern for the Fed so that a positive shock in real factor was accompanied with negative shock in interest rate factor, justifying that the Fed's credibility for low inflation. On the other hand, the positive correlation from 2004 and 2005 indicates that inflation was the concern for the Fed, which may reflect the Taylor's opinion that the funds rate was kept too low for too long from 2003 to 2004. An intuitive way to understand the dynamic relationship is that a negative correlation implies that the main task of interest rate factor is to stimulate economy and a positive relationship indicates attempts to control inflation. There was a downward trend for the correlation between real factor and money and credit factor from 1994 to 2006, indicating a strengthening relationship between them, and an upward trend for the correlation between real factor and expectation factor during the same time period, implying a weakening relationship between them. The negative correlation suggests that a positive shock to the real economy would be accompanied with a negative shock to money and credit factor and expectation factor.

The second row of Figure 4 describes the dynamic correlation between price factor and other factors. Interestingly, there was a positive correlation between price factor and interest rate factor before 2010, which indicates that the Fed's credibility of keep-

ing low inflation, however, this relationship has been broken since 2010, which implies that to stimulate the economy was the main concern of the Fed so that a positive shock to price factor was accompanied with a negative shock to interest rate factor. The negative correlation between price factor and money and credit factor implies that the money and credit factor could be used to offset the inflation pressure. There was also a downward trend for the correlation between price factor and expectation factor from 1994 to 2006, suggesting that the market was quite concerned about the future inflation pressure. The time-varying effects of macroeconomic factors on price factor could shed a light on the headache problem of weak inflation for central bankers, suggesting that we need look at a wide range of factors and investigate their dynamic strengthening or offsetting relationships in order to solve the low inflation problem.

Before 2008, the correlation between interest rate factor and money credit factor stays negative, which is consistent with the concept that to reduce the money and credit circulating in the market, we should increase interest rate. However, this rule has been broken since 2008 and this correlation is approaching to a positive zone because of the Fed's quantitative easing policy and zero interest rate policy, implying the relatively healthy economics of United States in comparison to other global markets so that a positive shock to the interest rate factor is accompanied with a positive shock to money and credit factor, which is consistent with the recent phenomenon that global capital flows into U.S. market because of the improved U.S. economy and anticipated higher interest rate.

There was a downward trend in the correlation between interest rate factor and expectation factor from 1994 to 2006, and a negative correlation from 1998 to 2011

indicates that a positive shock in the interest rate would lead to a negative market expectation about future economic activity, but the view reversed after 2011. It could be understood that on one hand, a negative shock to interest rate was to stimulate the economy from 1998 to 2011, leading to a positive shock to the market view, on the other hand, a positive shock in interest rate was to control the potential future inflation pressure after 2011, leading to a favorable shock to the market expectation. The correlation between money and credit factor and expectation factor was negative before 2004 and positive afterwards. There were two sharp spikes in the correlation, i.e., one negative spike occurred at 2002 and the other positive spike occurred at 2009, and the timing of the spikes were consistent with the stochastic volatility for money and credit factor shown in Figure 3. This relationship could be understood that before 2004, to keep low inflation was the main concern so that a positive shock to the money and credit factor would lead to a negative shock to the future market expectation, on the other hand, after 2004, to stimulate the economy was the main issue so that a positive shock to the money and credit would lead to a positive shock to the future market perspective.

III. Asset Allocation Based on Macro Factors

In this section, we investigate the out-of-sampling performance of asset allocation based on macroeconomic factors. We study three representative and intuitive models with constant loadings as follows.¹¹ The first model can be thought as the macro

¹¹Snyder (2008) show that it requires at least 10^{11} particles for a 200-dimensional state and Bengtsson et al. (2008) show that the maximum of weights associated with the sample approach to unity as the sample size and dimension go to infinity. The dynamic loading factor DFVAR model (2) contains 205 states and requires substantial computational resources, thus we adopt the models with constant loadings for our asset allocation study, although the model with dynamic loadings

factors follow a Gaussian distribution with stochastic volatility process which implies that the macro factors are generated from random shocks and uncorrelated over time. It's denoted as FVAR0 and shown as follows.

$$\begin{aligned} r_t &= Bf_t + \epsilon_t \\ f_t &= \Sigma_t u_{ft} \end{aligned} \tag{15}$$

The second model can be viewed as the macro factors follow a VAR(1) model with stochastic volatility process and denoted as FVAR1, indicating that macro factors are autocorrelated and the past status could affect their future dynamics, i.e.,

$$\begin{aligned} r_t &= Bf_t + \epsilon_t \\ f_t &= Cf_{t-1} + \Sigma_t u_{ft} \end{aligned} \tag{16}$$

Note that the above two settings assume that macro factors are uncorrelated with each other, but intuitively, these factors could affect each other, i.e., the interest rate factor can influence money and credit factor, and money and credit factor can affect real economic factor, and these simultaneous interactions among factors are fundamental and natural. Therefore, we investigate the third model by taking into account these simultaneous interactions among the underneath driving forces, which is new to the literature based on author's knowledge. It's denoted as FVAR2 and

reveals much better impulse response than the constant loading model.

shown as follows

$$\begin{aligned} r_t &= Bf_t + \epsilon_t \\ f_t &= Cf_{t-1} + A_t^{-1}\Sigma_t u_{ft} \end{aligned} \tag{17}$$

where C is the constant loading, A_t refers to the lower triangular matrix in equation (9), $\epsilon_t \sim N(0, H_t)$ and $H_t = \text{diag}(e^{h_{1t}}, \dots, e^{h_{nt}})$ with a random walk vector as following

$$h_t = h_{t-1} + u_{ht} \tag{18}$$

and u_{ft} is a standard multivariate Gaussian distribution and $\Sigma_t = \text{diag}(e^{\sigma_{1t}/2}, \dots, e^{\sigma_{kt}/2})$ with a random walk vector as following

$$\sigma_t = \sigma_{t-1} + u_{\sigma t} \tag{19}$$

III.1 Investor's Preferences

The investors could rebalance their asset allocations according to a variety of objective functions, i.e. maximum expected utility, minimum volatility, and maximum expected return by using the predictive expected returns and covariances. Let $\mu_{t+1|t} = E[r_{t+1}|\mathcal{F}_t]$ and $\Sigma_{t+1|t} = E[(r_{t+1} - \mu_{t+1|t})(r_{t+1} - \mu_{t+1|t})'|\mathcal{F}_t]$ denote the conditional mean and covariance of future asset returns r_{t+1} based on current information set \mathcal{F}_t . The conditional covariance for constant loading and stochastic volatility model

can be found according to conditional variance formula as follows

$$\begin{aligned}
\Sigma_{t+1|t} &= \text{var}(r_{t+1}|\mathcal{F}_t, \Gamma^*) \\
&= E[\text{var}(r_{t+1}|\mathcal{F}_{t+1})|\mathcal{F}_t, \Gamma^*] + \text{var}[E(r_{t+1}|\mathcal{F}_{t+1})|\mathcal{F}_t, \Gamma^*] \\
&= \int H(h_{t+1})d\pi(h_{t+1}|\mathcal{F}_t, \Gamma^*) + B\Sigma(f_{t+1}|\mathcal{F}_t, \Gamma^*)B' \\
&= \frac{1}{M} \sum_{i=1}^M H(h_{t+1}^{(i)}) + B\Sigma(f_{t+1}^{(i)})B' \tag{20}
\end{aligned}$$

where Γ^* denotes the estimated parameters and $\pi(h_{t+1}|\mathcal{F}_t, \Gamma^*)$ denotes the predictive distribution of h_{t+1} and $\Sigma_t(f_{t+1}|\mathcal{F}_t, \Gamma^*)$ denotes the covariance of predictive distribution f_{t+1} under estimated parameters. The integral can be estimated by Monte Carlo simulation, where $h_{t+1}^{(i)}$ and $f_{t+1}^{(i)}$ are the sample draws from the joint predictive distribution which is generated from the Chapman-Kolmogorov equation as follows

$$\pi(f_{t+1}, h_{t+1}|\mathcal{F}_t, \Gamma^*) = \int \pi(f_{t+1}, h_{t+1}|f_t, h_t, \mathcal{F}_t, \Gamma^*)\pi(f_t, h_t|\mathcal{F}_t, \Gamma^*)df_tdh_t$$

The filtering samples could be obtained by using auxiliary particle filter described in the Appendix and thus the predictive draws can be found by using their transition dynamics.

Accordingly, the conditional mean for the constant loading model can be calculated as follows

$$\begin{aligned}
\mu_{t+1|t} &= E[r_{t+1}|\mathcal{F}_t, \Gamma^*] \\
&= E[E[(r_{t+1}|\mathcal{F}_{t+1})]|\mathcal{F}_t, \Gamma^*] \\
&= \frac{1}{M} \sum_{i=1}^M Bf_{t+1}^{(i)} \tag{21}
\end{aligned}$$

We consider four types of preferences under asset allocation framework with different constraints: 1) mean-variance objective, i.e.,

$$\max_{\omega_t} \mu_{t+1} - \frac{\gamma}{2} \sigma_{t+1}^2 \quad (22)$$

where $\mu_{t+1} = \omega_t' \mu_{t+1|t} + (1 - \omega_t' \mathbf{1}) r_f$, $\sigma_{t+1}^2 = \omega_t' \Sigma_{t+1|t} \omega_t$, ω_t is a vector of weights in n risky assets, γ is the risk-aversion coefficient and r_f is the risk-free rate. So the optimal weights are

$$\omega_t^* = \frac{1}{\gamma} \Sigma_{t+1|t}^{-1} (\mu_{t+1|t} - \mathbf{1} r_f)$$

In addition, we also consider the no-shorting constraint, i.e., $\omega_t^* \geq 0$ and leverage constraints, i.e., $-1 \leq \omega_{i,t}^* \leq 2$, that is, there are boundaries on the short and leverage positions. We implement the genetic algorithm to solve the constrained optimization problem.¹²

2) global minimum volatility objective, i.e.,

$$\min_{\omega_t} \omega_t' \Sigma_{t+1|t} \omega_t \quad (23)$$

with $\omega_t' \mathbf{1} = 1$ and note that we assume no risk-free asset is available, thus we could obtain the optimal weights

$$\omega_t^* = \frac{\Sigma_{t+1|t}^{-1} \mathbf{1}}{\mathbf{1}' \Sigma_{t+1|t}^{-1} \mathbf{1}}$$

¹²The commonly used gradient type searching algorithm only produces suboptimal solutions, because it tends to get trapped in local optima instead of a global optimum when confronted with complex optimization problems. We use a random type search algorithm called genetic algorithm (GA) to search for the optimal portfolio weights under constraints. GA utilizes the idea from biology to mimic the evolution process of organisms that survive and flourish in a changing environment. Interested readers could refer to the book review of Goldberg (1989).

In addition, we also investigate the cases of no-shorting constraint and leverage constraints imposed on mean-variance framework. Note that for global optima, the sum of weights should be close to one, indicating a nearly zero cash position.

3) minimum volatility given certain level of conditional expected return (Fleming et al. 2001 and Fleming et al. 2003), i.e.,

$$\min_{\omega_t} \frac{1}{2} \omega_t' \Sigma_{t+1|t} \omega_t \quad (24)$$

s.t. $\omega_t' \mu_{t+1|t} + (1 - \omega_t' \mathbf{1}) r_f = \mu^*$, where μ^* is the target expected return. Thus we could have the following optimal weights

$$\omega_t^* = \frac{(\mu^* - r_f) \Sigma_{t+1|t}^{-1} (\mu_{t+1|t} - \mathbf{1} r_f)}{(\mu_{t+1|t} - \mathbf{1} r_f)' \Sigma_{t+1|t}^{-1} (\mu_{t+1|t} - \mathbf{1} r_f)}$$

4) maximum expected return given certain level of conditional volatility, i.e.,

$$\max_{\omega_t} \omega_t' \mu_{t+1|t} + (1 - \omega_t' \mathbf{1}) r_f \quad (25)$$

s.t. $\omega_t' \Sigma_{t+1|t} \omega_t = (\sigma^*)^2$ where σ^* is the target volatility. Hence we could obtain the following optimal weights

$$\omega_t^* = \frac{\Sigma_{t+1|t}^{-1} (\mu_{t+1|t} - \mathbf{1} r_f) \sigma^*}{\sqrt{(\mu_{t+1|t} - \mathbf{1} r_f)' \Sigma_{t+1|t}^{-1} (\mu_{t+1|t} - \mathbf{1} r_f)}}$$

III.2 Multi-period Forecasting

We could also conduct multi-period forecasting by using particle filtering. For example, for the s -day ahead return

$$r_{t+s}^s = \sum_{j=1}^s r_{t+j} | \mathcal{F}_t, \Gamma^* \quad (26)$$

Assuming the independence of the future returns, we could find the s -day ahead predictive conditional covariance as follows

$$\Psi_{t+s|t}^s = \sum_{j=1}^s \Psi_{t+j} | \mathcal{F}_t, \Gamma^* \quad (27)$$

where $\Psi_{t+j} = \frac{1}{M} \sum_{i=1}^M H_t(h_{t+j}^{(i)}) + B \Sigma_t(f_{t+j}^{(i)}) B'$ and $h_{t+j}^{(i)}, f_{t+j}^{(i)}$ are the sample draws from the predictive density that are propagated from the particles $h_t^{(i)}, f_t^{(i)}$. Also, we could find the s -day ahead expected return as follows

$$\mu_{t+s|t}^s = \sum_{j=1}^s E[r_{t+j} | \mathcal{F}_t, \Gamma^*] \quad (28)$$

where $E[r_{t+j} | \mathcal{F}_t, \Gamma^*] = \frac{1}{M} \sum_{i=1}^M B f_{t+j}^{(i)}$.

III.3 Portfolio Performance Measures

In order to measure the portfolio performance, we use Sharpe ratio, worst draw-down, risk-adjusted abnormal return, performance fee and beat rate to investigate the out-of-sample performance of various strategies from a variety of perspectives. Sharpe ratio is the most commonly used measure and defined as $SR = (\mu_p - r_f) / \sigma_p$, where μ_p is the realized portfolio return, σ_p is the standard deviation of the realized portfolio returns and r_f is the constant risk-free rate. Moreover, to quantify the economic gains related to the Sharpe ratio, we use the $M2$ measure defined by Modigliani and Modigliani (1997) to compute the risk-adjusted abnormal return ($M2$) in the sense that the abnormal return obtained by the dynamic strategy as if it has the same risk

as the buy-and-hold strategy. Specifically, it is defined as follows

$$\begin{aligned} M2 &= \frac{\sigma_{bh}}{\sigma_p}(\mu_p - r_f) - (\mu_{bh} - r_f) \\ &= \sigma_{bh}(SR_p - SR_{bh}) \end{aligned} \quad (29)$$

From the perspective of an allocator, he may want to know how much performance fee he has to pay in order to switch from a buy-and-hold strategy, i.e., holding a passive index, to a dynamic strategy. By following Fleming et al. (2001), we need to find a constant Φ so that the average utility of a dynamic strategy should be equal to that of the buy-and-hold strategy, i.e.,

$$\frac{1}{T} \sum_{t=0}^{T-1} \left[(R_{dp,t+1} - \Phi) - \frac{\gamma}{2(1+\gamma)} (R_{dp,t+1} - \Phi)^2 \right] = \frac{1}{T} \sum_{t=0}^{T-1} \left[R_{bh,t+1} - \frac{\gamma}{2(1+\gamma)} R_{bh,t+1}^2 \right]$$

where $R_{dp,t+1}$ represents the realized gross returns of a dynamic strategy and $R_{bh,t+1}$ denotes the gross return of the buy-and-hold strategy, and γ is the investor's relative risk aversion coefficient and set to be 6 in the paper.

In addition to use the standard deviation of the portfolio returns to measure the variation of portfolio returns, the worst drawdown is also used to measure the largest loss of the dynamic strategy could occur. Furthermore, instead of one extreme performance measure, we also consider the beat rate to check how often the dynamic strategies could beat the buy-and-hold strategy. The beat rate (BR) measure is defined as the percentage of time periods in which the gross return of the dynamic strategy could beat that of the buy-and-hold strategy, i.e.

$$BR_{dp} = \frac{\sum_{t=1}^T I(GR_{dp,t} > GR_{bh,t})}{T}$$

where $GR_{dp,t}$ denotes the gross return of dynamic strategy at time t and $GR_{bh,t}$ denotes the gross return of buy-and-hold strategy at time t , and $I(\cdot)$ is the indicator function with value of 1 if the argument is true and 0 otherwise.

III.4 Out-of-sample Empirical Analysis

We first consider the model FVAR0 in equation (15) in which the macro factors are assumed to follow a Gaussian distribution. Table 1 shows the monthly rebalancing out-of-sample portfolio performance, which implies that except the global minimum volatility strategy, the other dynamic strategies do not perform well. Specifically, under mean-variance framework, the MV0 model with no constraints generate no excess returns, so do the MV2 model with leverage constraints. The MV1 model with no-shorting constraints could not outperform the buy-and-hold strategy, although the standard deviation is lower than that of the buy-and-hold strategy. The cause of low volatility is because MV1 tends to hold cash most of time and invest lightly in the risky assets. In addition, the mean-variance framework doesn't perform well in other settings, i.e., FVAR1 and FVAR2 as well, which is consistent with the consensus that the mean-variance strategy tends to generate extreme values and doesn't work well in the practice, thus we leave out the discussions of mean-variance strategy in this paper.

It is interesting to see that the global minimum strategies with or without constraints could generate better annualized return than the buy-and-hold strategy with less annualized volatility. Thus, the global minimum strategies are able to generate higher Sharpe ratio and positive abnormal returns and performance fees. On the

other hand, the minimum volatility with target return strategy does not work at all in the sense that the portfolio is completely wiped out. In addition, the maximum return strategy with target volatility do not work well as well.

Table 2 shows the quarterly rebalancing out-of-sample portfolio performance, implying similar results as monthly rebalancing outcomes. These results indicate that the setting in which the factors follow a Gaussian distribution probably is not a good fit to describe the dynamics of underneath driving factors for portfolio construction except global minimum volatility strategy. The reason that global minimum volatility strategy works is because to implement the model FVAR0 does not involve estimating predictive mean so that it can actually generate similar returns as FVAR1 and FVAR2 frameworks. In other words, the portfolio construction based on volatility strategy by using macro factors indeed could capture the asset dynamics and be able to generate significant out-of-sample economic gains.

We then investigate the FVAR1 model in equation (16) in which the macro factors follow VAR(1) process for the 10-sector data set. Table 3 reports the out-of-sample portfolio performance for monthly rebalancing strategies. In general, the global minimum strategy looks attractive with significant out-of-sample annualized return and lower volatility than the buy-and-hold strategy, thereby leading to higher Sharpe ratio and positive abnormal returns and performance fees. The minimum volatility strategy with target return seems to underperform the buy-and-hold strategy. Specifically, as the target return increases, the strategy generates more volatile outputs as shown in Figure 5 and Figure 6. Especially as the target return is equal to 4%, the portfolio generates extreme weights in order to reach the expected target so that it

turns out to obtain unfavorable realized return. As to the maximum return strategy with target volatility, the Sharpe ratio is higher than buy-and-hold strategy when the target volatility is equal to 1% or 2%. As the target volatility rises to 4%, the Sharpe ratio falls and annualized return becomes more volatile. Therefore, these outcomes imply that it's crucial to set a reasonable target range for either minimum volatility or maximum return strategies for portfolio construction.

To investigate the horizon effect on the portfolio choice, we also investigate the performance of quarterly rebalancing strategies. Table 4 summarizes the portfolio performance. It seems that the global minimum volatility strategy still works well under quarterly rebalancing frequency. Figure 7 and Figure 8 shows the annualized return and volatility, respectively. It shows that the performance of minimum volatility strategy with target return and maximum return strategy with target volatility significantly deteriorates and is almost dominated by the buy-and-hold strategy. Especially for minimum volatility strategy with target return, as the target return is equal to 4%, the portfolio is completely wiped out. These results indicate that asset allocators should pay attention to the rebalancing frequency since it could have a profound effect on the portfolio performance.

Then we investigate FVAR2 model in which the macro factors follow a VAR(1) with simultaneous interactions among factors based on 10-sector data set. Table 5 summarizes the monthly rebalancing portfolio outcomes. The global minimum volatility strategies in the FVAR2 model can generate better outcomes than the FVAR1 model. Specifically, the GMV0 model with no constraint tends to generate higher annualized return than the buy-and-hold strategy but with lower volatility and worst drawdown.

Figure 12 shows that the annualized return of GMV0 is quite close to that of the buy-and-hold strategy of S&P 500 index, but the annualized volatility is smaller than that of buy-and-hold strategy as shown in Figure 13, and both risk-adjusted return and performance fee are positive. To have a deeper understanding about how the strategy works, we look into the portfolio weights distribution in 10 sectors for global minimum strategy shown in Figure 9. It shows that the GMV0 is increasing the position in consumer staples and health care sectors and building short positions in consumer discretionary and energy sectors, implying a long-short strategy, that is, the long positions in some of the defensive sectors and short positions in some of the cyclic sectors. And the GMV1 strategy takes no-shorting positions with lower weight in cyclic sectors, while the GMV2 strategy with boundary shorting and leverage constraints tends to heavily invest in industrial sector and build short positions in consumer discretionary and energy sectors. Note that the cash position is close to zero, indicating that the global optima are obtained since there is no risk-free asset for global minimum strategy.

Figure 10 presents the weight distribution for minimum volatility strategy with target return. The low volatility for MVOL0 actually indicates that this strategy tends to hold a large amount of cash over time and invest a small position in risky assets so that the Sharpe ratio could be as high as 1.27. As the target return rises to 4%, it shows that this strategy tends to generate extreme weights and take high leverage positions, and thereby volatile annualized return and volatility shown in Figure 12 and Figure 13. From Figure 11, the maximum return model MR0 with target volatility of 1% also tends to hold cash over time in order to maintain low

level volatility. The MR1 model with target volatility of 2% starts to invest more in risky assets and keep modest level of cash, which demonstrates an appealing feature that it could generate close annualized return to buy-and-hold strategy but maintain a lower level of volatility than the buy-and-hold strategy shown from Figure 13. If the target volatility increases to 4% in MR2 model, the Sharpe ratio, risk-adjusted return, and performance fee all decline, suggesting that to set a reasonable volatility target and maintain certain level of cash could have a significant effect on the portfolio performance.

Then we study the horizon effect on FVAR2 model. Figure 14 shows the portfolio weights distribution for global minimum volatility strategy. In comparison to the monthly rebalancing global minimum strategy, the quarterly rebalancing strategy tends to become conservative in the sense that both long and short positions decrease in the magnitude. On the one hand, the quarterly rebalancing minimum volatility strategy with target return leads to more extreme weights shown in Figure 15 in comparison to the monthly rebalancing strategy, and on the other hand, the quarterly rebalancing maximum return strategy with target volatility generates less extreme weights shown in Figure 16 in comparison to the monthly rebalancing strategy. Intuitively, if the asset allocator looks at longer horizon, then he would confront with more uncertainties, therefore, to achieve the expected target return, the strategy tends to generate more aggressive weights, while to reach the expected target volatility, the strategy has more room to generate relatively less aggressive weights as shown in Figure 17 and Figure 18.

In addition, we also investigate a larger data set consisting of 22 industry groups.

Table 7 summarizes the monthly rebalancing. Similar to the 10-sector data set, the global minimum volatility strategy based on 22-industry data set could also generate higher annualized return with lower annualized volatility shown in Figure 19 and Figure 20 and thereby higher Shape ratio and positive abnormal returns and performance fees. Also, to set a reasonable target value is crucial for the performance of minimum volatility strategy with target return and maximum return strategy with target volatility. Table 8 demonstrates that the time horizon has a negative effect on the portfolio performance. Figure 21 and Figure 22 show that the quarterly rebalancing global minimum volatility strategy still works although the performance is inferior to the monthly rebalancing strategy, but the minimum volatility strategy with target return and maximum return strategy with target volatility underperform the buy-and-hold strategy.

We then study the monthly rebalancing portfolio performance for FVAR2 model based on 22-industry data set shown in Table 9. Similar to the outcomes of FVAR2 model based on 10-sector data set, the global minimum volatility strategy works as shown in Figure 23 and Figure 24, and target range is sensitive to the performance of minimum volatility strategy and maximum return strategy. Table 10 presents the quarterly rebalancing portfolio performance based on 22-industry data set. Figure 25 and Figure 26 show the annualized return and annualized volatility, respectively. Also, it indicates that in general, the portfolio performance deteriorates under quarterly rebalancing frequency.

Some existing studies claim that long-horizon return predictability is much better than the short-horizon predictability. However, Ang and Bekaert (2007) show that

dividend yield only has short-horizon predictive power and Boudoukh et al. (2008) argue that long-horizon return predictability is largely an illusion arises simply from the mechanical growth in a model's R^2 statistic with the estimated horizon length. In this paper, we find that in general the long-horizon out-of-sample portfolio performance is inferior to the short-horizon portfolio performance. Overall, based on the empirical studies of different data sets, the macro factors indeed could provide important meaningful information content which could shed a light on the systematic components of equity return dynamics, and the dynamic asset allocation based on these macro factors could generate systematically significant out-of-sample economic gains.

IV. Implications of Monetary Shocks

History might be not a perfect predictor, especially for the current era in which stocks are heavily dependent on the Fed support of holding the interest rates at a very low level for over last five years, which is unprecedented. Many believe that the Fed's efforts to inject money into the financial markets are the prime driver of the bull market. As the Fed wound down the quantitative easing program and started to raise interest rate last December and is heading into interest-rate-hike cycle in the next a couple of years. The crucial question is by how much and when will the Fed raises rates, and what the market's reaction will be. Thus, it would be informative and valuable to investigate how the financial market reacts under those monetary shocks. Therefore, we conduct an impulse response analysis in order to shed a light on the dynamics of the financial market reactions, which could be valuable to both policy

decision makers and practical investors, i.e., Maio (2014) implement some trading strategies to produce significant economic gains based on the Fed Funds Rate (FFR).

IV.1 Monetary Shocks on S&P 500 Sectors

Intuitively, these macro factors could be thought as the transmission channels of monetary policy to affect asset returns. We follow Bernanke, Boivin, and Eliasziw (2005) and standardize the monetary policy shock to correspond to 25-basis-point innovation in the federal funds rate. We specifically look at two time spots. One is as the Fed raises key short-term rate a quarter point on 06/30/2004 and the other is as the Fed cut the interest rate by half of a percentage point on 09/18/2007 to 4.75% in a bold acknowledgement that the central bank is concerned about the mortgage meltdown. We first look at the impulse response of FVAR1 model with constant loadings as the Fed starts to increase interest rate shown in Figure 27, the responses over next 12 months for ten financial sectors are almost flat and close to zero, implying that the constant loading model may not fit to reflect expected mean in the return variations. As the Fed cuts interest rate, the constant loading model demonstrates similar patterns shown in Figure 28.

We then test the dynamic loading model DFVAR in equation (2). Figure 29 shows the responses of ten financial sector returns over next 12 months as the Fed starts to increase interest rate. We could observe that the impulse responses seem to capture the long-term trend and curvature of sector realized returns. Interestingly, the response could reveal appealing indications of the future return trajectories of industrial, consumer discretionary, financial, consumer staples and utilities sectors. As the

Fed cuts the interest rate, the responses of cyclic sectors seem to follow the realized return trajectory and the responses of healthcare, utility, and telecom sectors in the defensive group also reveal appealing trajectories of future return trend.

V. Concluding Remarks

It is interesting and thought provoking for academics to produce empirical models that could capture the dynamics of equity returns and provide economic insights to help investors for their practical portfolio construction.¹³ In this paper, We attempt to provide a dynamic factor framework including meaningful economic information content to shed a light on the evolution of macro economy through a handful of factors. Five macro factors are extracted from hundreds of series and dynamic asset allocation constructed on these macro factors could produce systematically significant out-of-sample economic gains. Furthermore, these macro factors could serve as the transmission channels of monetary policy so that investors could incorporate their views in the portfolio construction and test the effects in various scenarios from a forward-looking perspective, which could be informative and valuable for both policy makers and practical investors.

¹³For example, financial data often contains heavy tail and jump. A recent algorithm has been developed to estimate a hybrid model including constant and dynamic loading, stochastic volatility, heavy tail and jump (see Appendix F). Such dynamic structural model could be tested in the future.

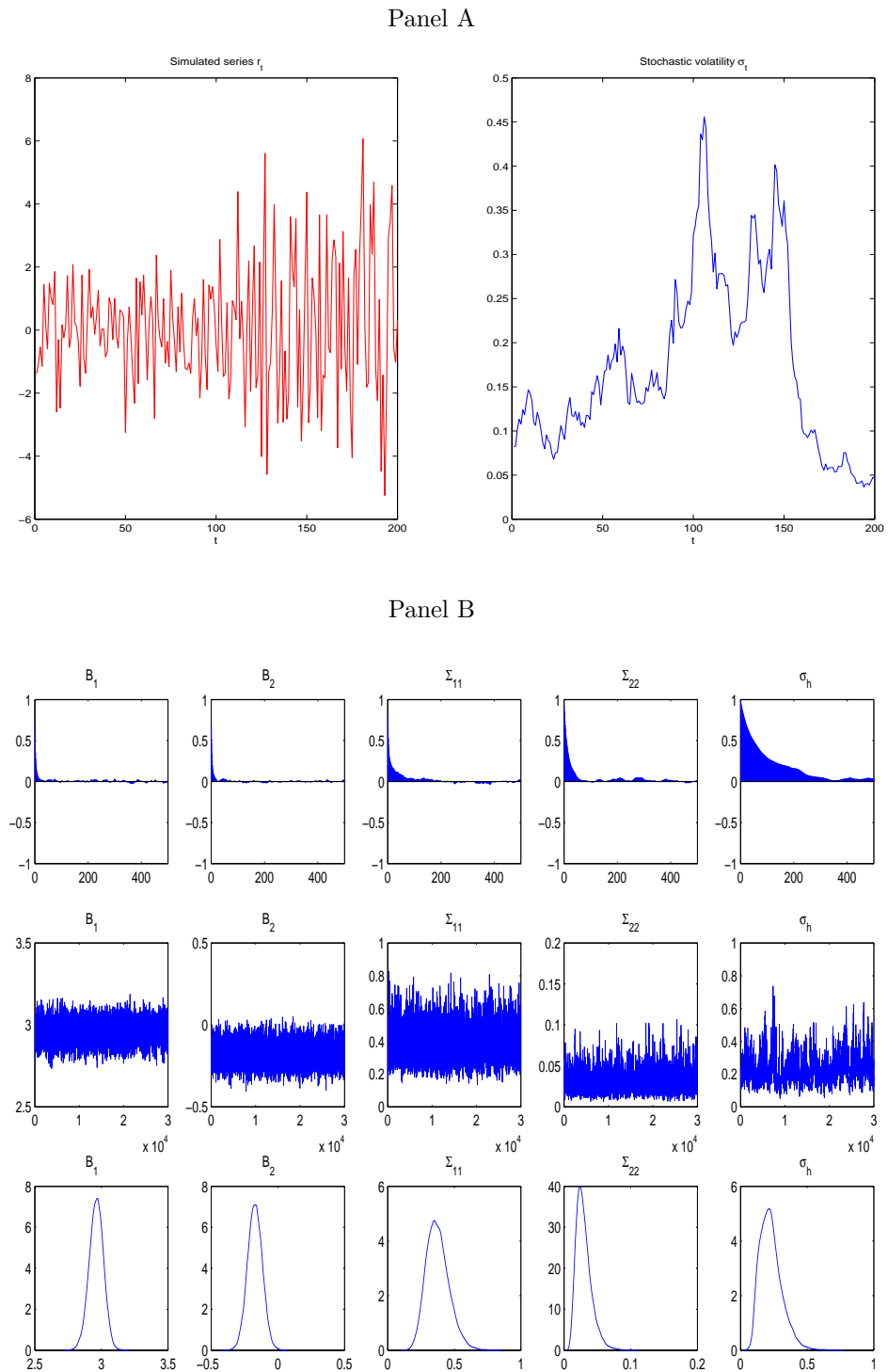


Figure 1: The figure in Panel A depicts the simulated series and stochastic volatility. The figure in Panel B depicts the sample autocorrelation function, sample draws and posterior densities for simulated data.

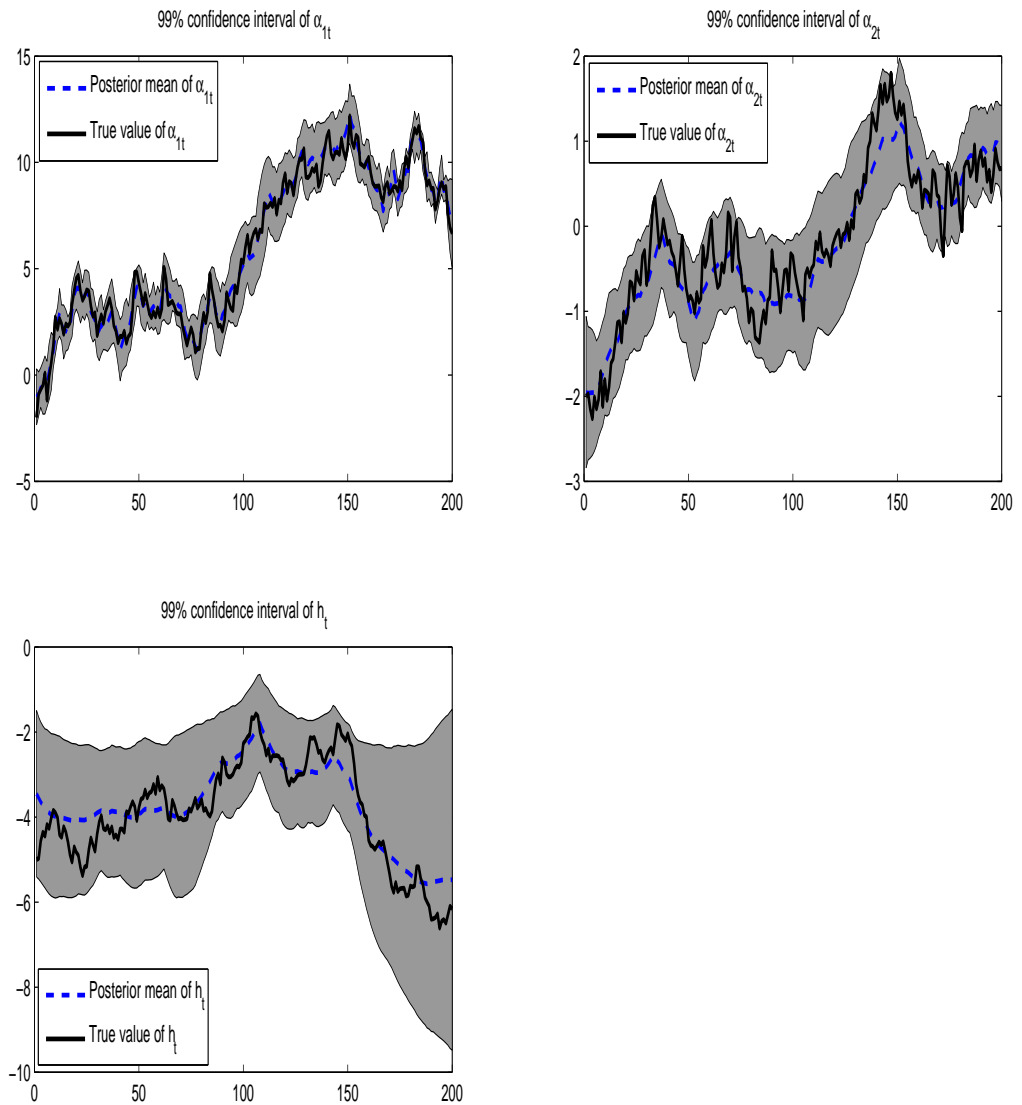


Figure 2: This figure shows the estimation results of α_{1t} , α_{2t} and h_t for the simulated data. The gray area represents the 99% confidence interval. The solid line denotes the true value of the state variable and the dashes line denotes the posterior mean.

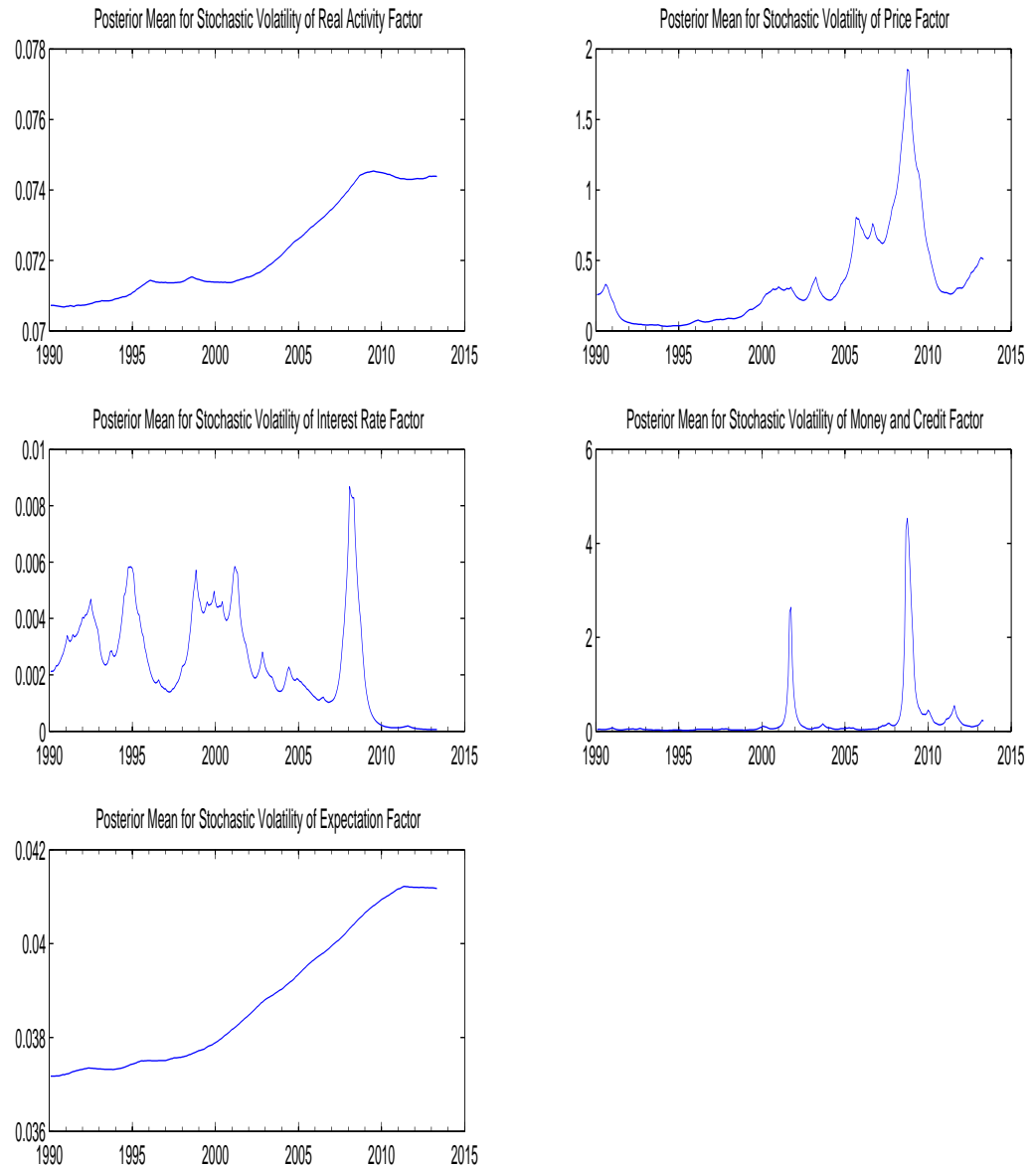


Figure 3: The figure depicts the posterior mean of stochastic volatility for macroeconomic factors under model DFVAR (2) with dynamic loadings and stochastic volatility.

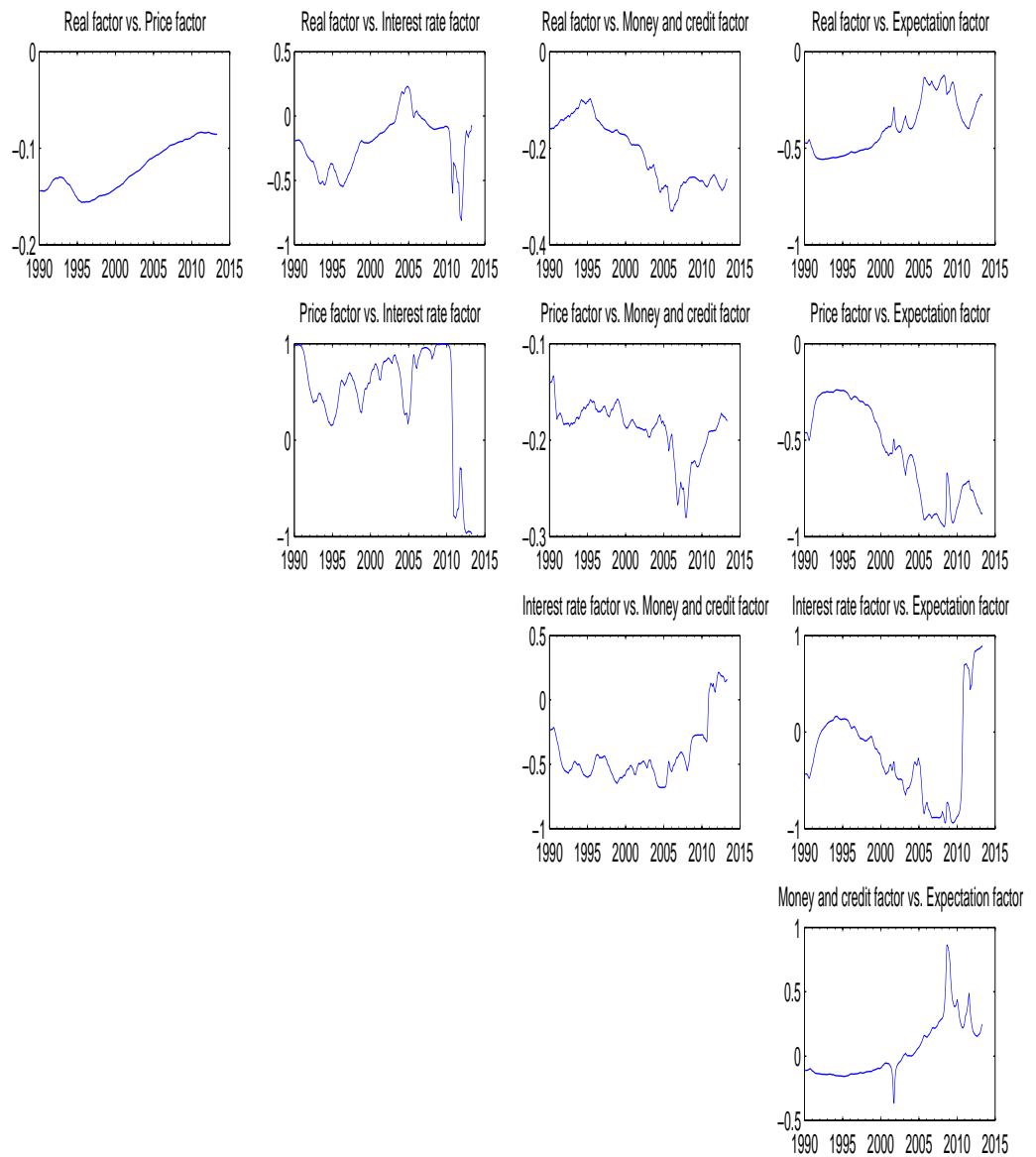


Figure 4: The figure depicts the time-varying correlation among macroeconomic factors under model DFVAR (2) with dynamic loadings and stochastic volatility.

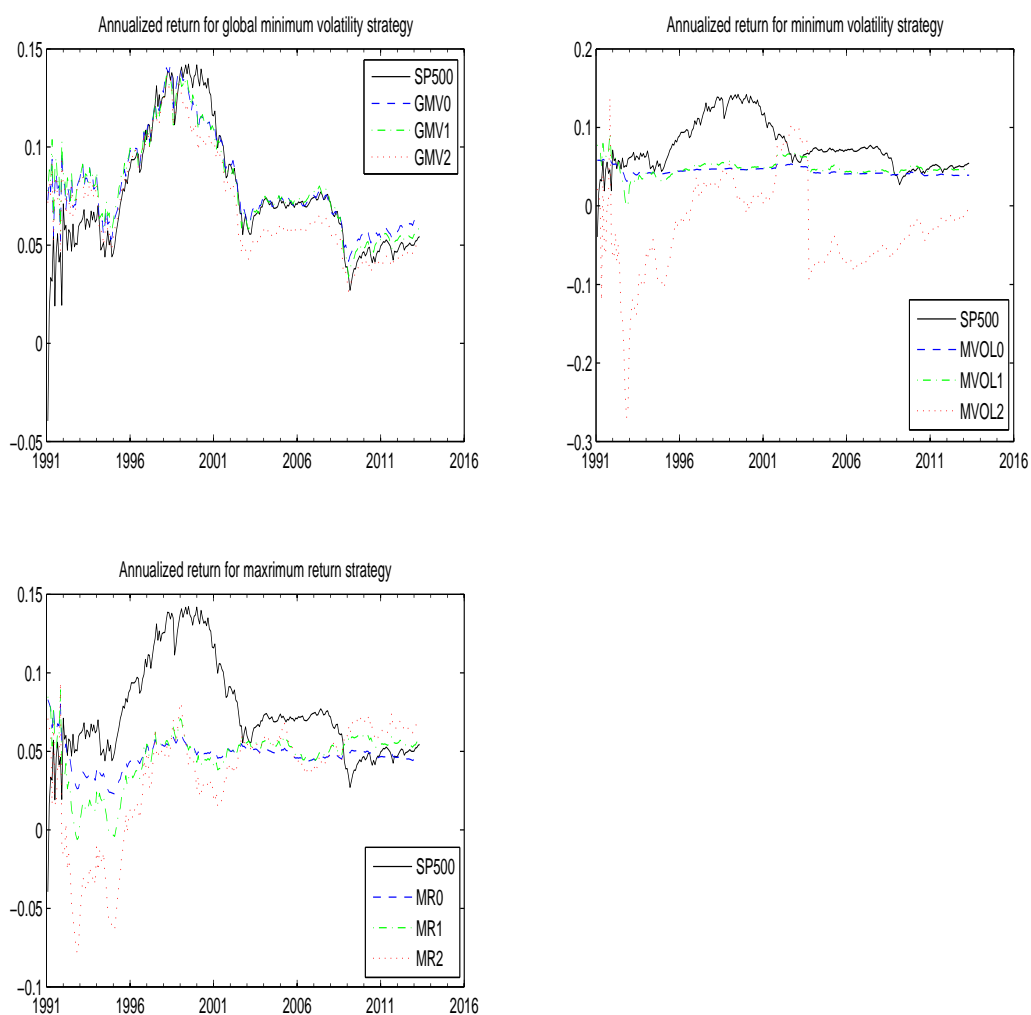


Figure 5: This figure shows the annualized return for three types of monthly rebalancing strategies under model FVAR1 for 10-sector data set. SP500 denotes the S&P 500 index. GMV0 is the global minimum volatility model without constraints, GMV1 is the global minimum volatility model with no-shorting constraint, and GMV2 is the global minimum volatility model with leverage constraint. MVOL0 denotes the minimum volatility model with target return of 0.5%, MVOL1 denotes the minimum volatility model with target return of 1%, MVOL2 denotes the minimum volatility model with target return of 4%. MR0 denotes the maximum return model with target volatility of 1%, MR1 denotes the maximum return model with target volatility of 2%, MR2 denotes the maximum return model with target volatility of 4%.

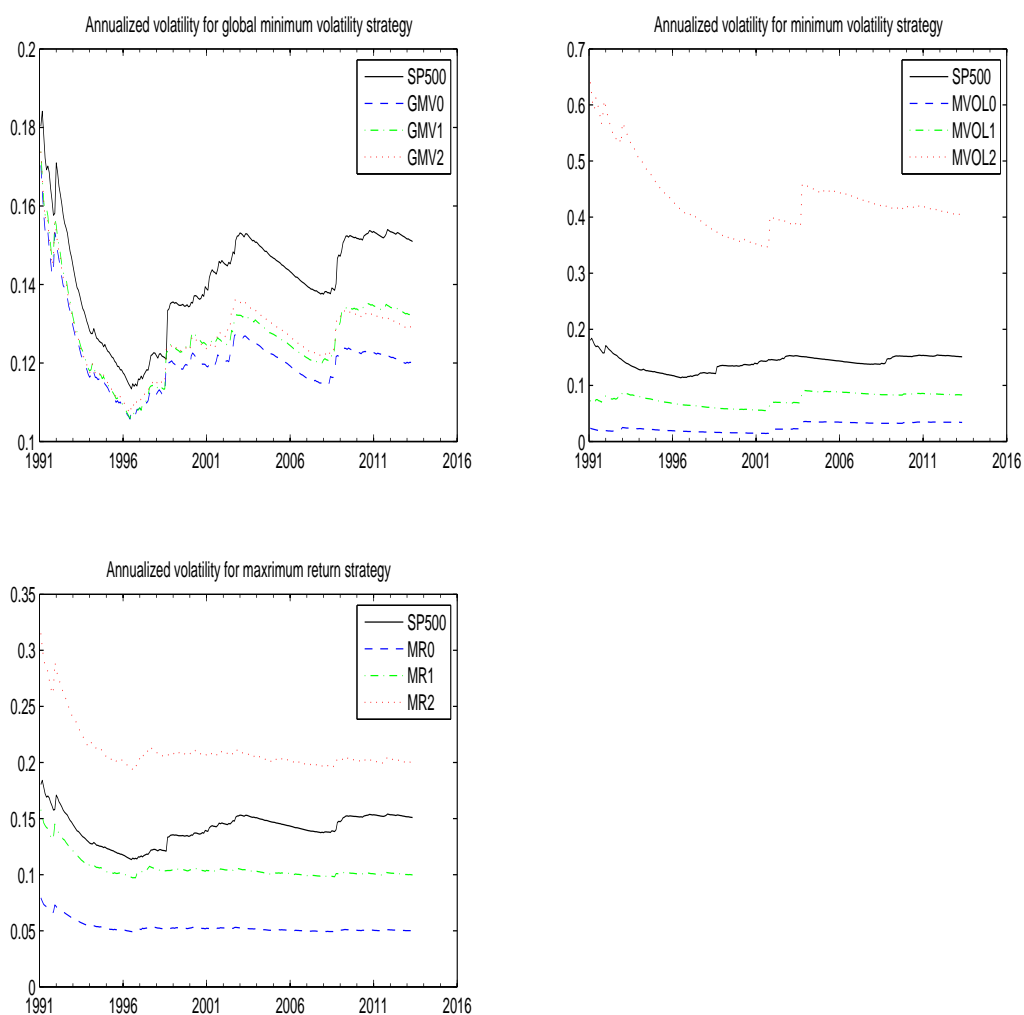


Figure 6: This figure shows the annualized volatility for three types of monthly rebalancing strategies under model FVAR1 for 10-sector data set. SP500 denotes the S&P 500 index. GMV0 is the global minimum volatility model without constraints, GMV1 is the global minimum volatility model with no-shorting constraint, and GMV2 is the global minimum volatility model with leverage constraint. MVOL0 denotes the minimum volatility model with target return of 0.5%, MVOL1 denotes the minimum volatility model with target return of 1%, MVOL2 denotes the minimum volatility model with target return of 4%. MR0 denotes the maximum return model with target volatility of 1%, MR1 denotes the maximum return model with target volatility of 2%, MR2 denotes the maximum return model with target volatility of 4%.

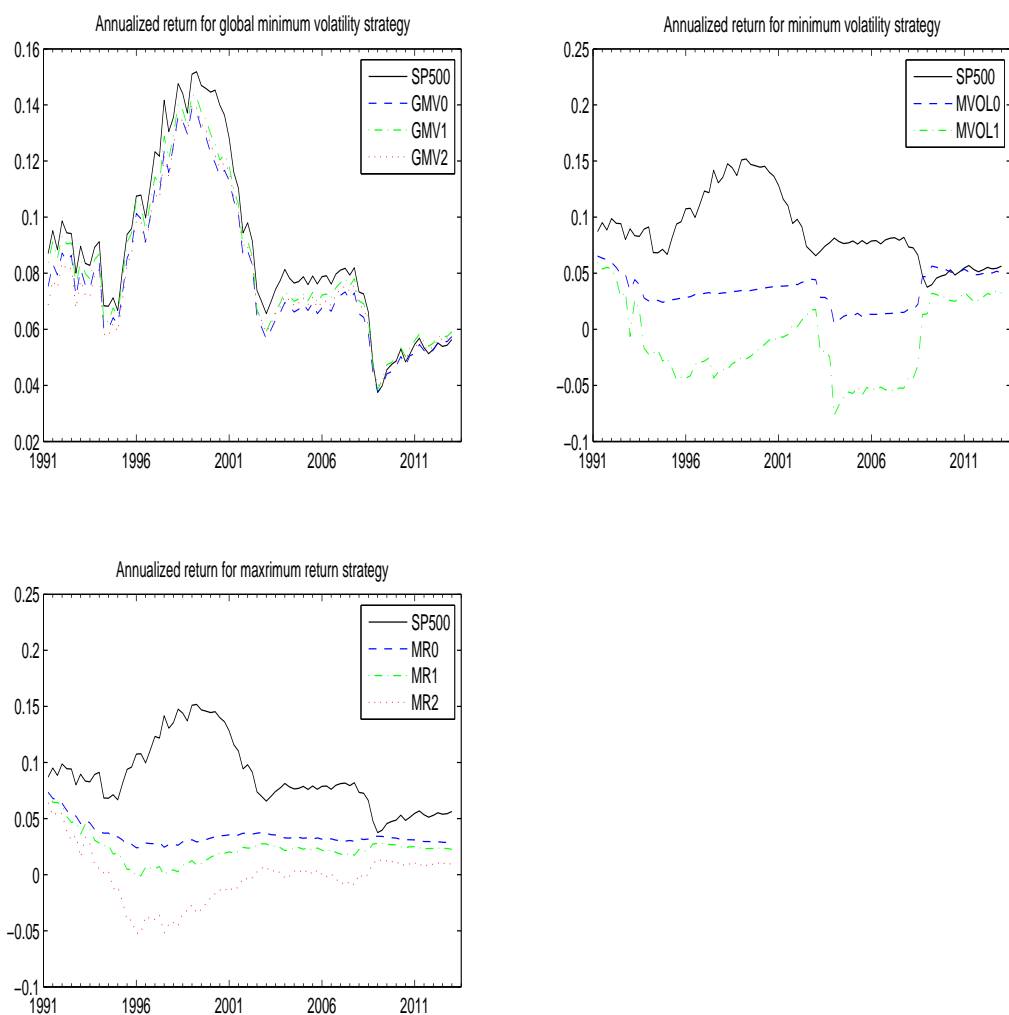


Figure 7: This figure shows the annualized return for three types of quarterly rebalancing strategies under model FVAR1 for 10-sector data set. SP500 denotes the S&P 500 index. GMV0 is the global minimum volatility model without constraints, GMV1 is the global minimum volatility model with no-shorting constraint, and GMV2 is the global minimum volatility model with leverage constraint. MVOL0 denotes the minimum volatility model with target return of 0.5%, MVOL1 denotes the minimum volatility model with target return of 1%, MVOL2 denotes the minimum volatility model with target return of 4%. MR0 denotes the maximum return model with target volatility of 1%, MR1 denotes the maximum return model with target volatility of 2%, MR2 denotes the maximum return model with target volatility of 4%.

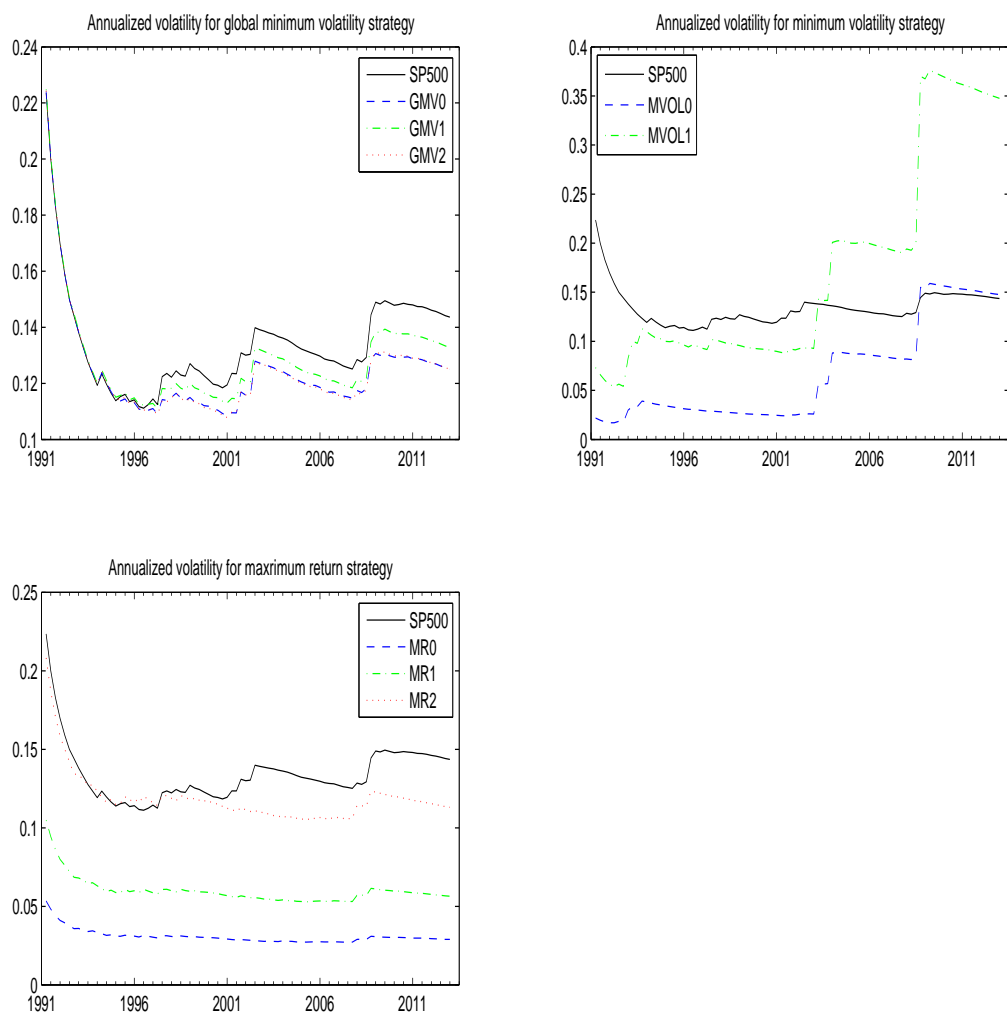


Figure 8: This figure shows the annualized volatility for three types of quarterly rebalancing strategies under model FVAR1 for 10-sector data set. SP500 denotes the S&P 500 index. GMV0 is the global minimum volatility model without constraints, GMV1 is the global minimum volatility model with no-shorting constraint, and GMV2 is the global minimum volatility model with leverage constraint. MVOL0 denotes the minimum volatility model with target return of 0.5%, MVOL1 denotes the minimum volatility model with target return of 1%, MVOL2 denotes the minimum volatility model with target return of 4%. MR0 denotes the maximum return model with target volatility of 1%, MR1 denotes the maximum return model with target volatility of 2%, MR2 denotes the maximum return model with target volatility of 4%.

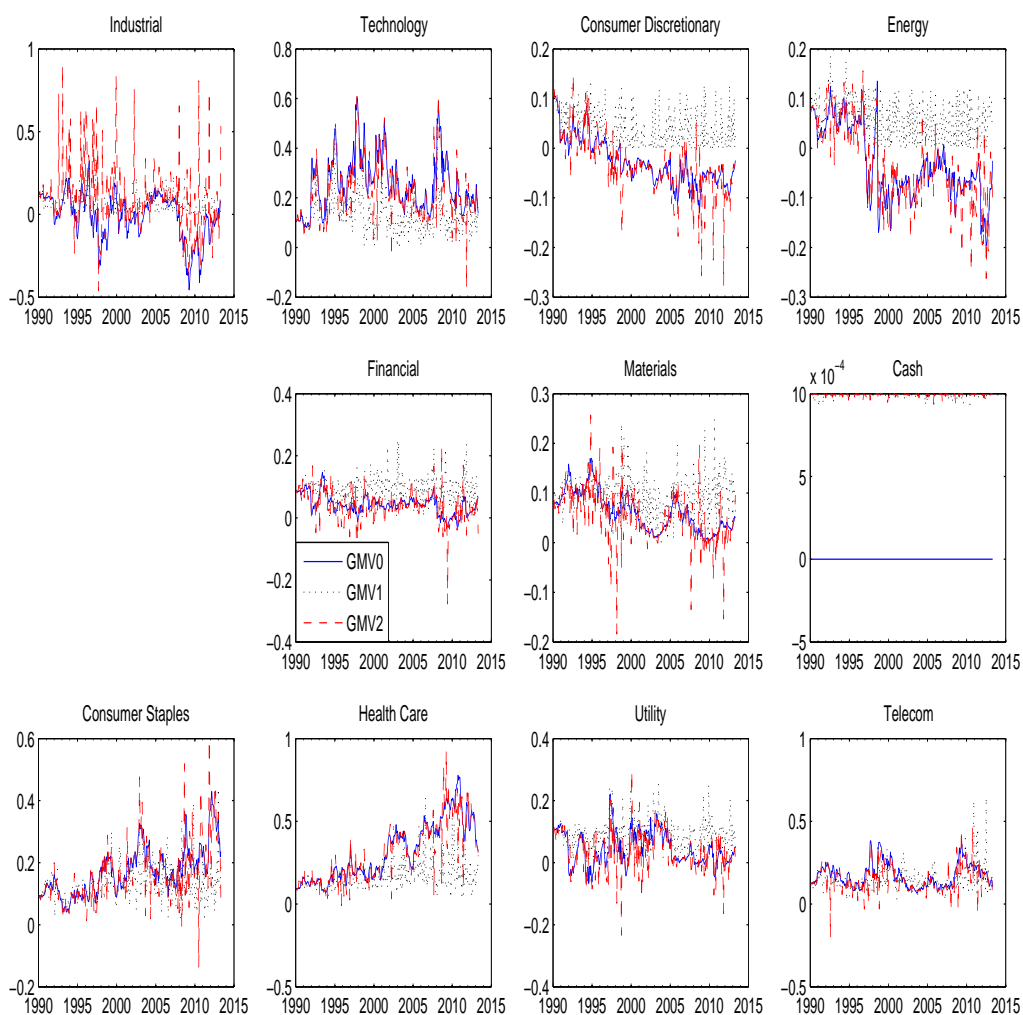


Figure 9: This figure shows the portfolio weights under model FVAR2 for monthly rebalancing global minimum volatility strategy based on 10-sector data set. GMV0 denotes the global minimum volatility strategy without any constraints, GMV1 denotes the global minimum volatility strategy with no-shorting constraint, and GMV2 denotes the global minimum volatility strategy with leverage constraints. Note that there is no risk-free asset available for global minimum volatility strategy so that the cash position should be close to zero.

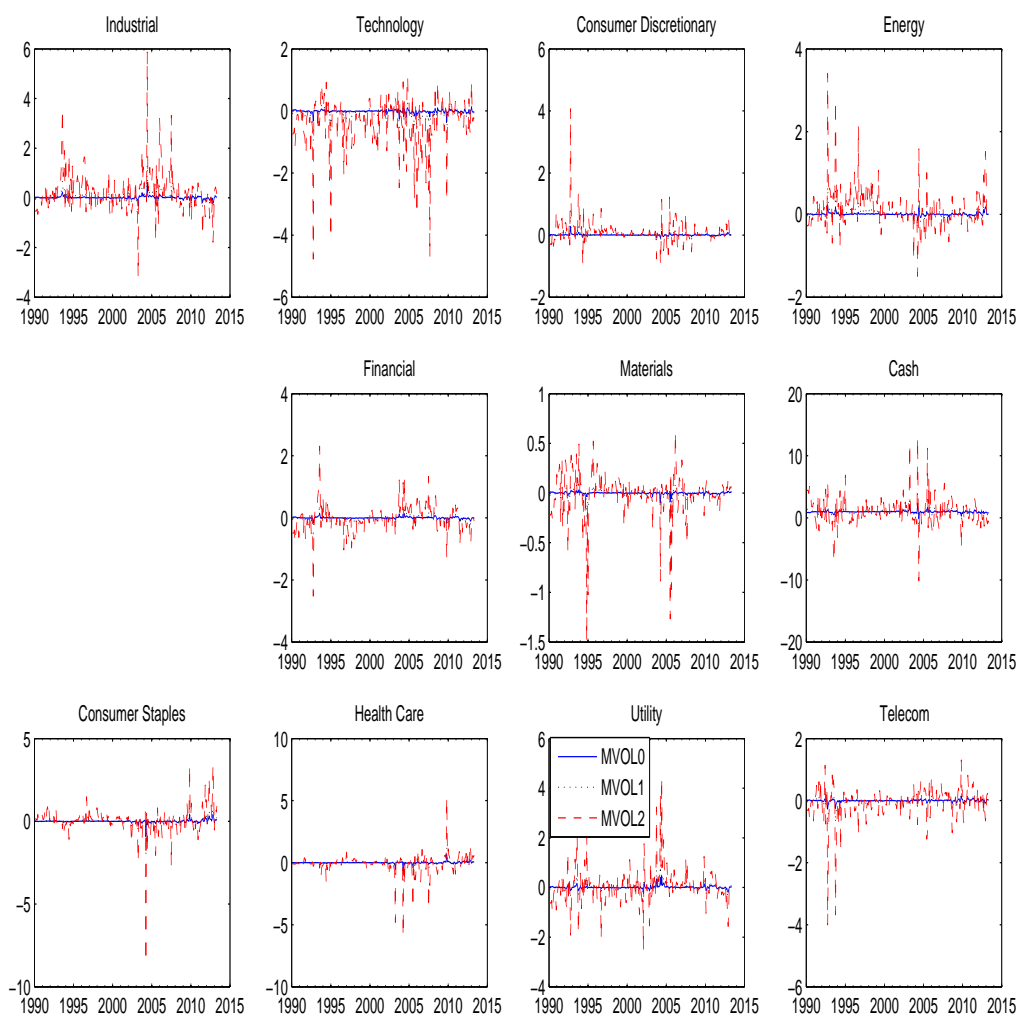


Figure 10: This figure shows the portfolio weights under model FVAR2 for monthly re-balancing minimum volatility with target return strategy based on 10-sector data set. MVOL0 denotes the minimum volatility model with target return of 0.5%, MVOL1 denotes the minimum volatility model with target return of 1%, MVOL2 denotes the minimum volatility model with target return of 4%.

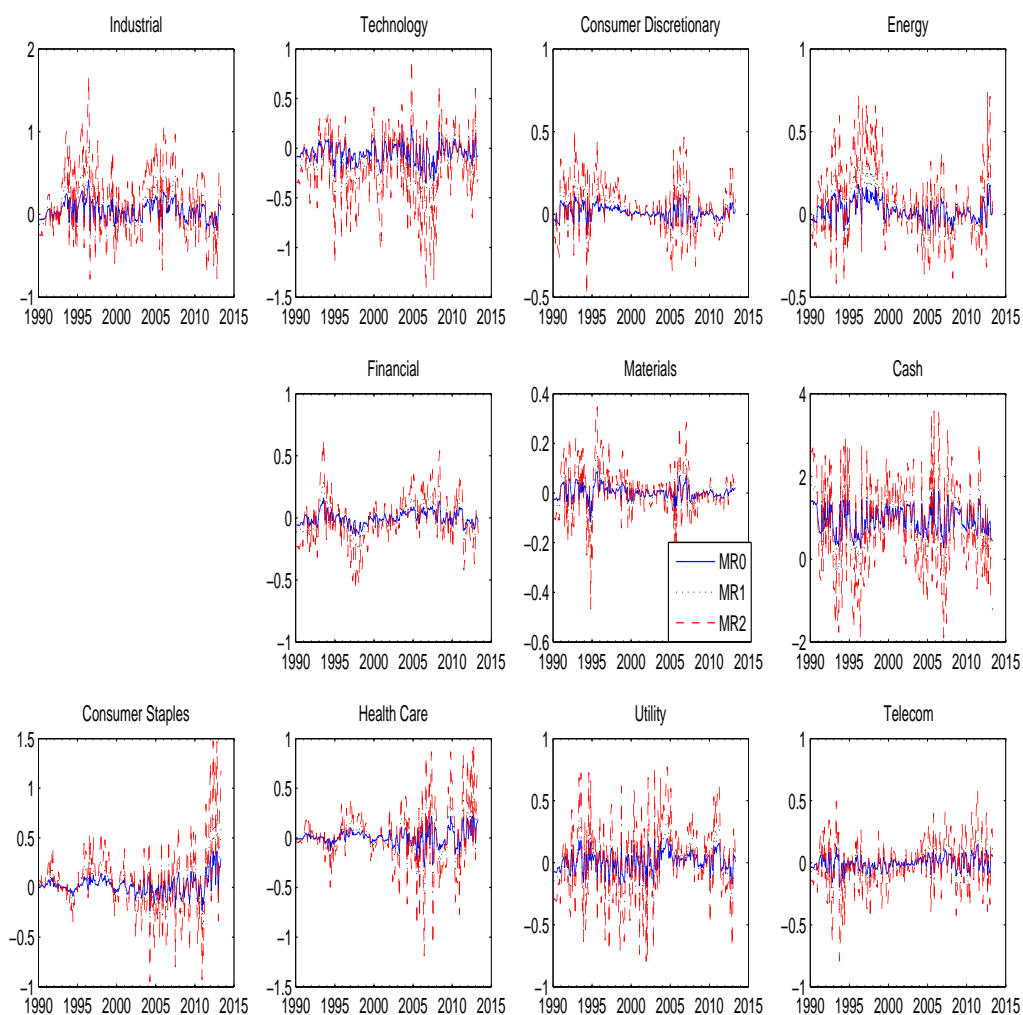


Figure 11: This figure shows the portfolio weights under model FVAR2 for monthly rebalancing maximum expected return with target volatility strategy based on 10-sector data set. MR0 denotes the maximum return model with target volatility of 1%, MR1 denotes the maximum return model with target volatility of 2%, MR2 denotes the maximum return model with target volatility of 4%.

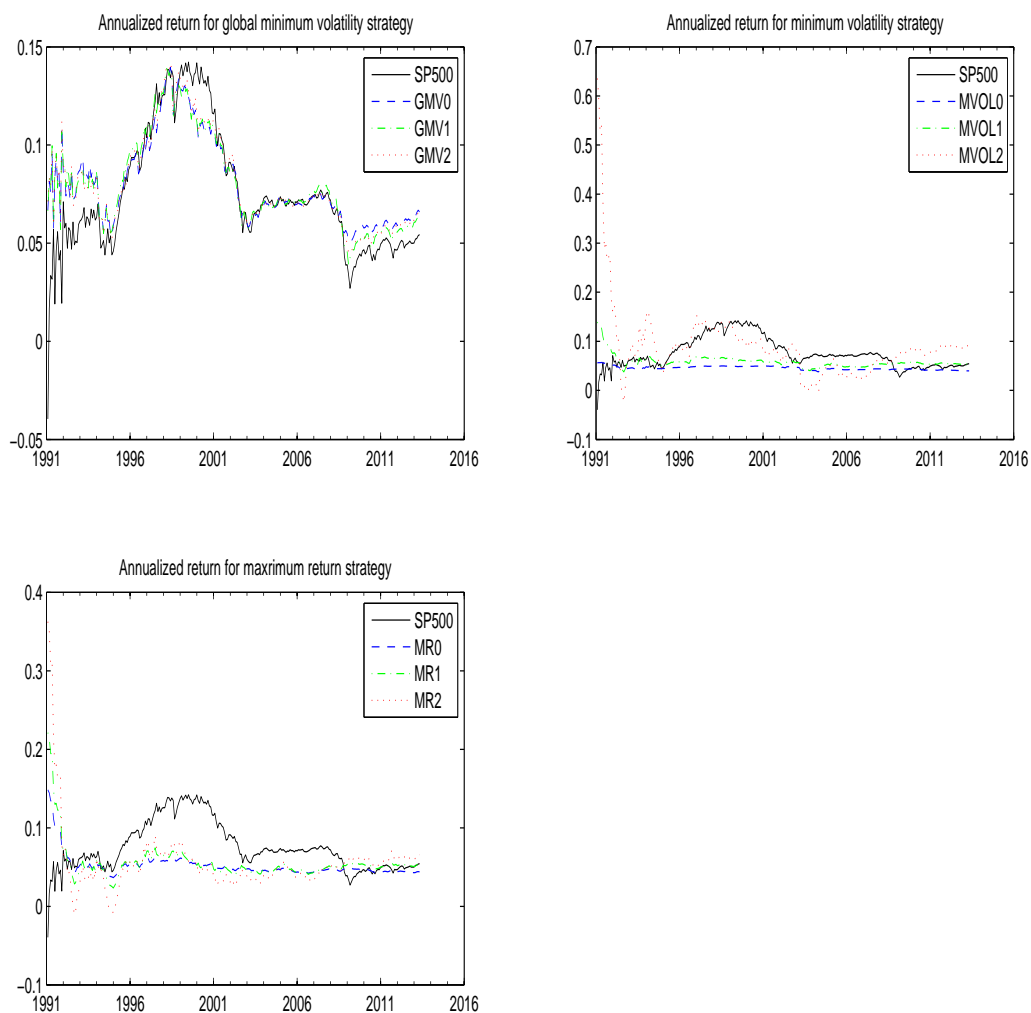


Figure 12: This figure shows the annualized return for three types of monthly rebalancing strategies under model FVAR2 based on 10-sector data set. SP500 denotes the S&P 500 index. GMV0 is the global minimum volatility model without constraints, GMV1 is the global minimum volatility model with no-shorting constraint, and GMV2 is the global minimum volatility model with leverage constraint. MVOL0 denotes the minimum volatility model with target return of 0.5%, MVOL1 denotes the minimum volatility model with target return of 1%, MVOL2 denotes the minimum volatility model with target return of 4%. MR0 denotes the maximum return model with target volatility of 1%, MR1 denotes the maximum return model with target volatility of 2%, MR2 denotes the maximum return model with target volatility of 4%.

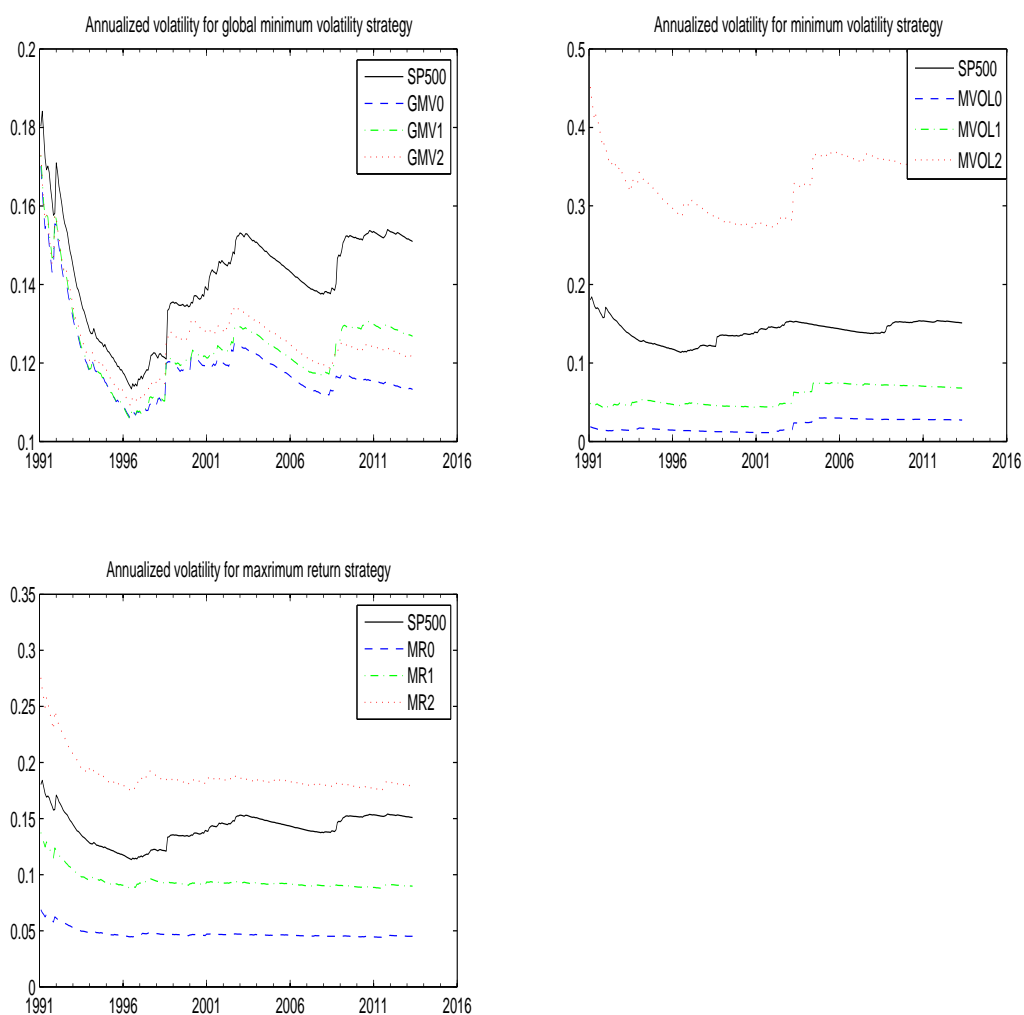


Figure 13: This figure shows the annualized volatility for three types of monthly rebalancing strategies under model FVAR2 based on 10-sector data set. SP500 denotes the S&P 500 index. GMV0 is the global minimum volatility model without constraints, GMV1 is the global minimum volatility model with no-shorting constraint, and GMV2 is the global minimum volatility model with leverage constraint. MVOL0 denotes the minimum volatility model with target return of 0.5%, MVOL1 denotes the minimum volatility model with target return of 1%, MVOL2 denotes the minimum volatility model with target return of 4%. MR0 denotes the maximum return model with target volatility of 1%, MR1 denotes the maximum return model with target volatility of 2%, MR2 denotes the maximum return model with target volatility of 4%.

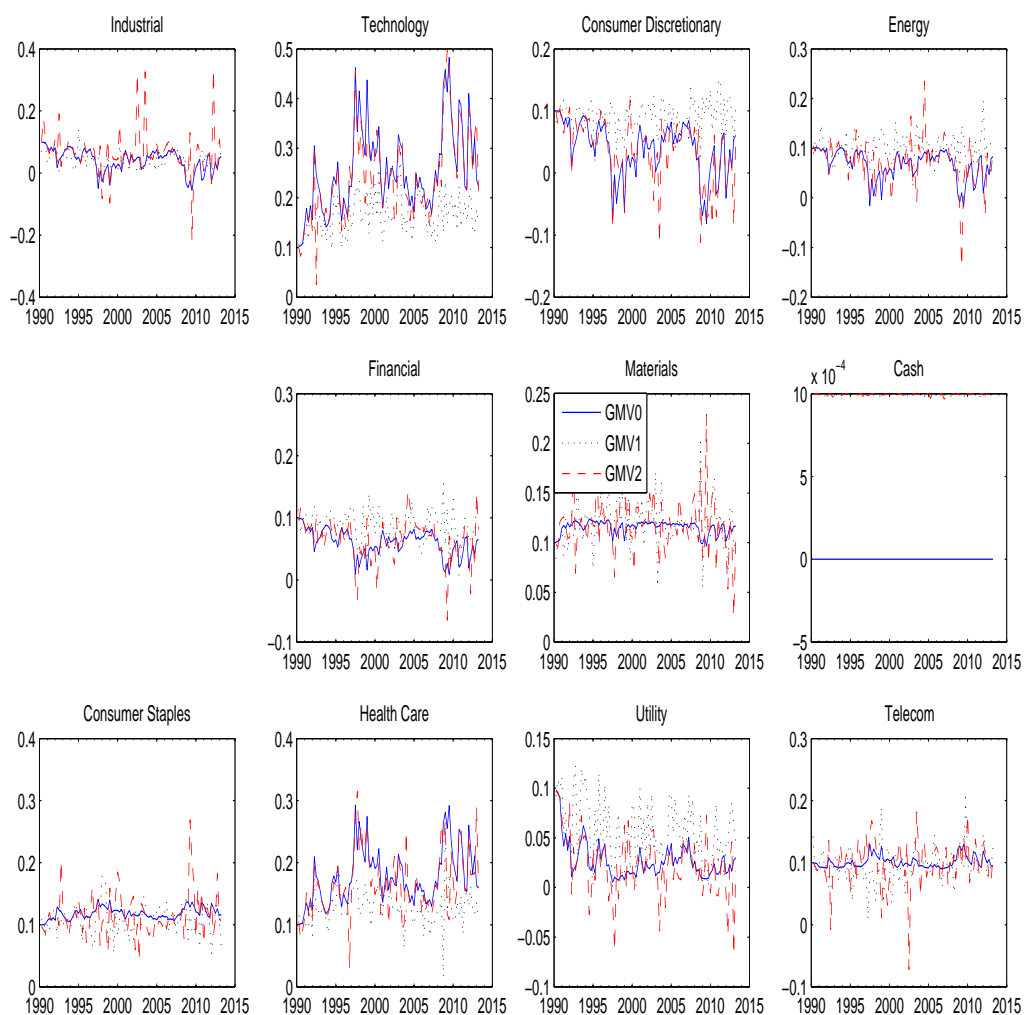


Figure 14: This figure shows the portfolio weights under model FVAR2 for quarterly rebalancing global minimum volatility strategy based on 10-sector data set. GMV0 denotes the global minimum volatility strategy without any constraints, GMV1 denotes the global minimum volatility strategy with no-shorting constraint, and GMV2 denotes the global minimum volatility strategy with leverage constraints. Note that there is no risk-free asset available for global minimum volatility strategy so that the cash position should be close to zero.

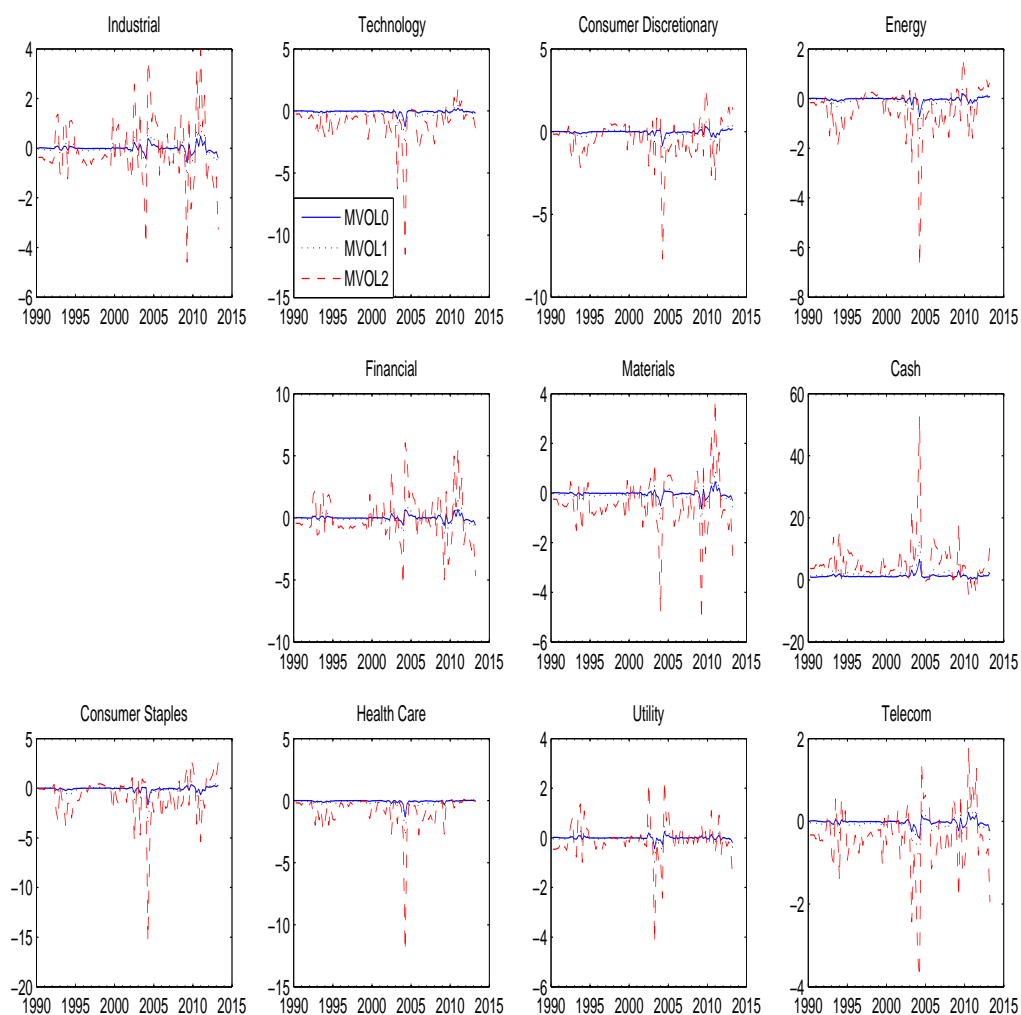


Figure 15: This figure shows the portfolio weights under model FVAR2 for quarterly rebalancing minimum volatility with target return strategy based on 10-sector data set. MVOL0 denotes the minimum volatility model with target return of 0.5%, MVOL1 denotes the minimum volatility model with target return of 1%, MVOL2 denotes the minimum volatility model with target return of 4%.

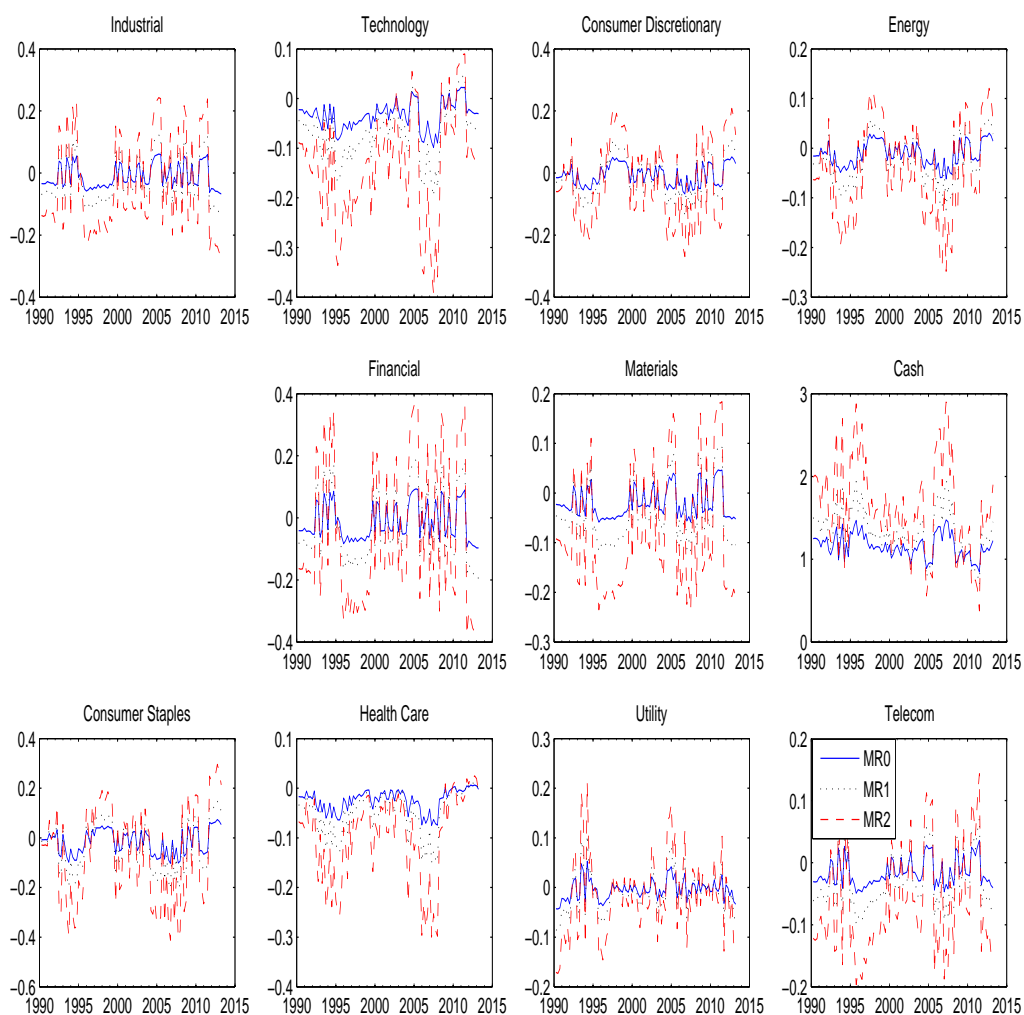


Figure 16: This figure shows the portfolio weights under model FVAR2 for quarterly rebalancing maximum expected return with target volatility strategy based on 10-sector data set. MR0 denotes the maximum return model with target volatility of 1%, MR1 denotes the maximum return model with target volatility of 2%, MR2 denotes the maximum return model with target volatility of 4%.

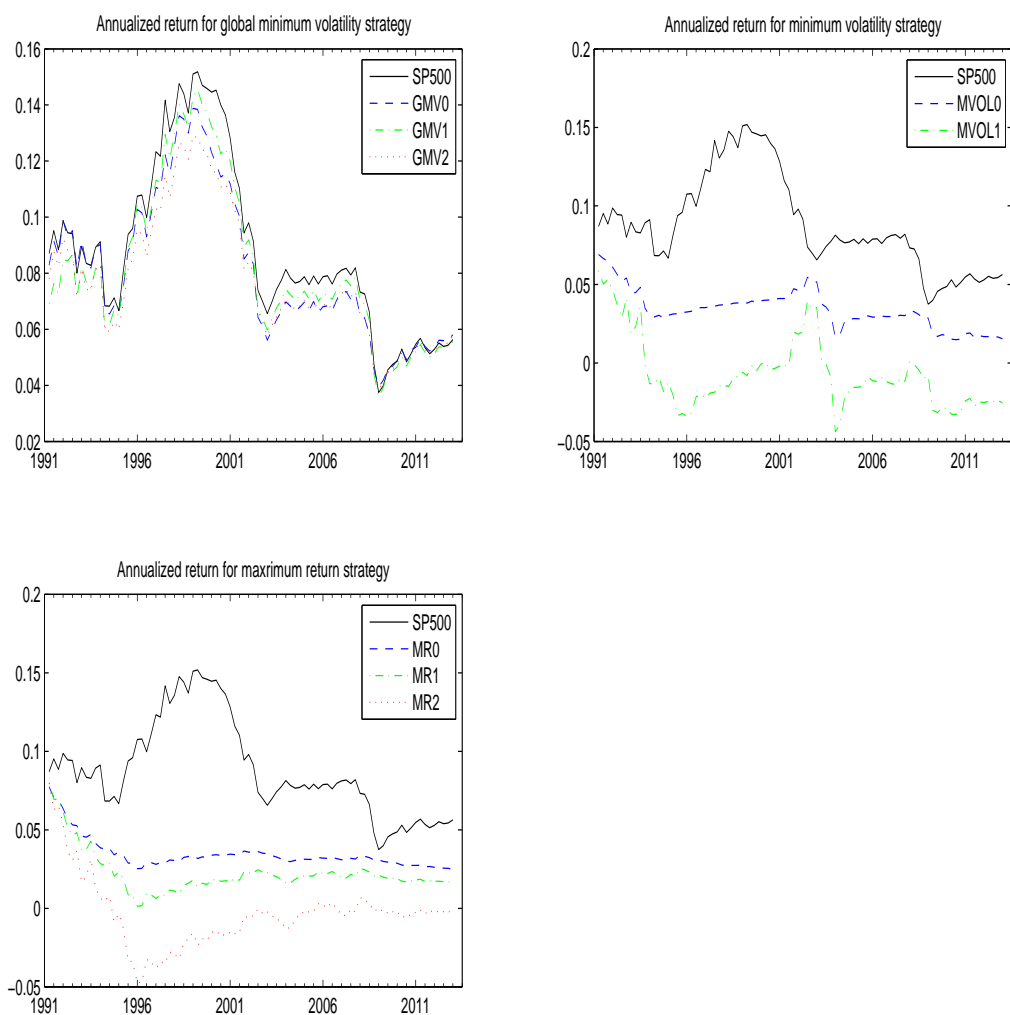


Figure 17: This figure shows the annualized return for three types of quarterly rebalancing strategies under model FVAR2 based on 10-sector data set. SP500 denotes the S&P 500 index. GMV0 is the global minimum volatility model without constraints, GMV1 is the global minimum volatility model with no-shorting constraint, and GMV2 is the global minimum volatility model with leverage constraint. MVOL0 denotes the minimum volatility model with target return of 0.5%, MVOL1 denotes the minimum volatility model with target return of 1%, MVOL2 denotes the minimum volatility model with target return of 4%. MR0 denotes the maximum return model with target volatility of 1%, MR1 denotes the maximum return model with target volatility of 2%, MR2 denotes the maximum return model with target volatility of 4%.

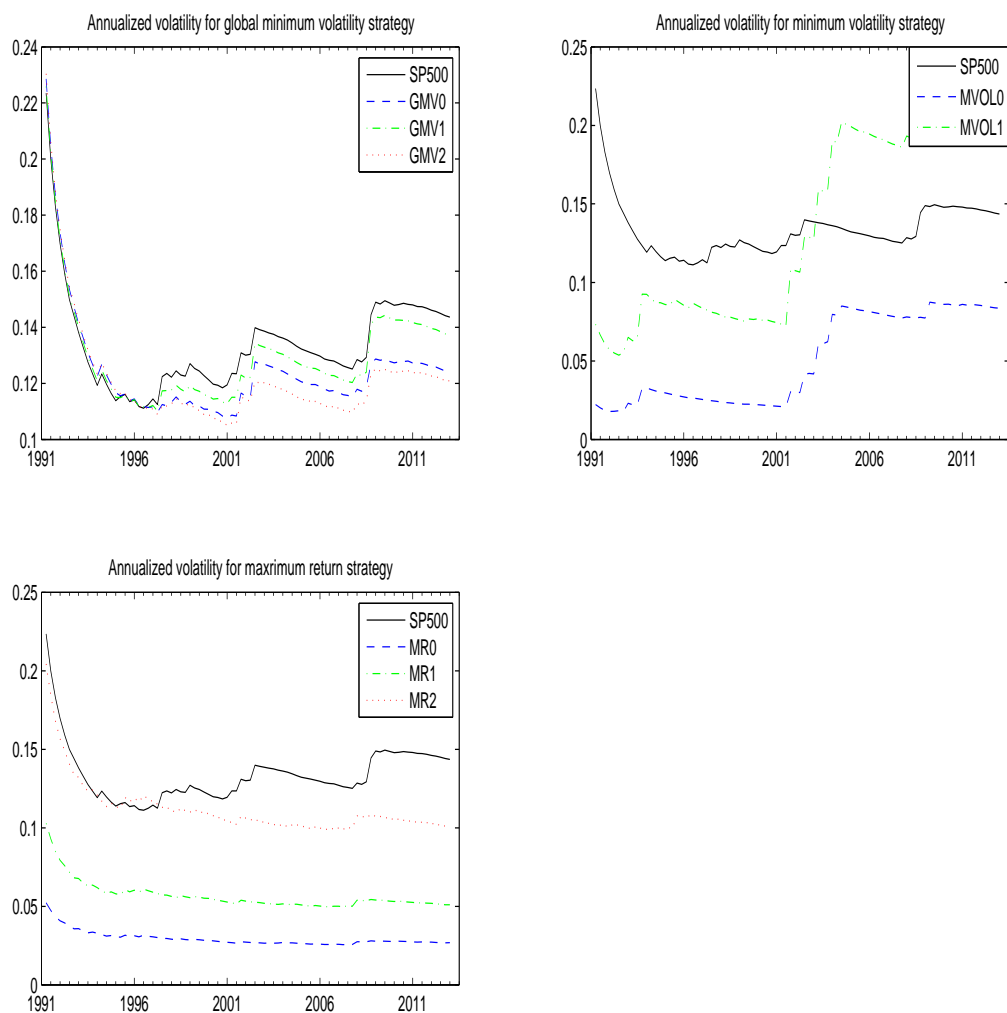


Figure 18: This figure shows the annualized volatility for three types of quarterly rebalancing strategies under model FVAR2 based on 10-sector data set. SP500 denotes the S&P 500 index. GMV0 is the global minimum volatility model without constraints, GMV1 is the global minimum volatility model with no-shorting constraint, and GMV2 is the global minimum volatility model with leverage constraint. MVOL0 denotes the minimum volatility model with target return of 0.5%, MVOL1 denotes the minimum volatility model with target return of 1%, MVOL2 denotes the minimum volatility model with target return of 4%. MR0 denotes the maximum return model with target volatility of 1%, MR1 denotes the maximum return model with target volatility of 2%, MR2 denotes the maximum return model with target volatility of 4%.

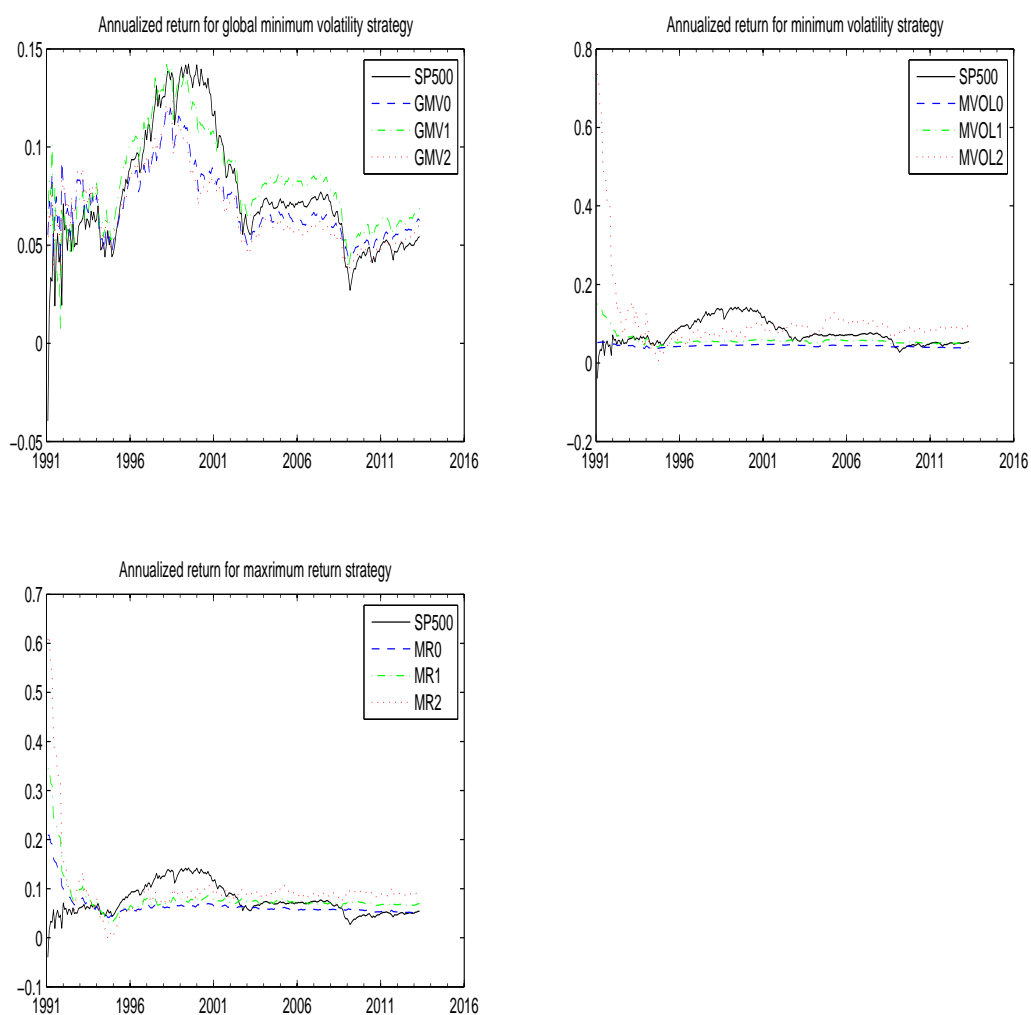


Figure 19: This figure shows the annualized return for three types of monthly rebalancing strategies under model FVAR1 for 22-industry data set. SP500 denotes the S&P 500 index. GMV0 is the global minimum volatility model without constraints, GMV1 is the global minimum volatility model with no-shorting constraint, and GMV2 is the global minimum volatility model with leverage constraint. MVOL0 denotes the minimum volatility model with target return of 0.5%, MVOL1 denotes the minimum volatility model with target return of 1%, MVOL2 denotes the minimum volatility model with target return of 4%. MR0 denotes the maximum return model with target volatility of 1%, MR1 denotes the maximum return model with target volatility of 2%, MR2 denotes the maximum return model with target volatility of 4%.

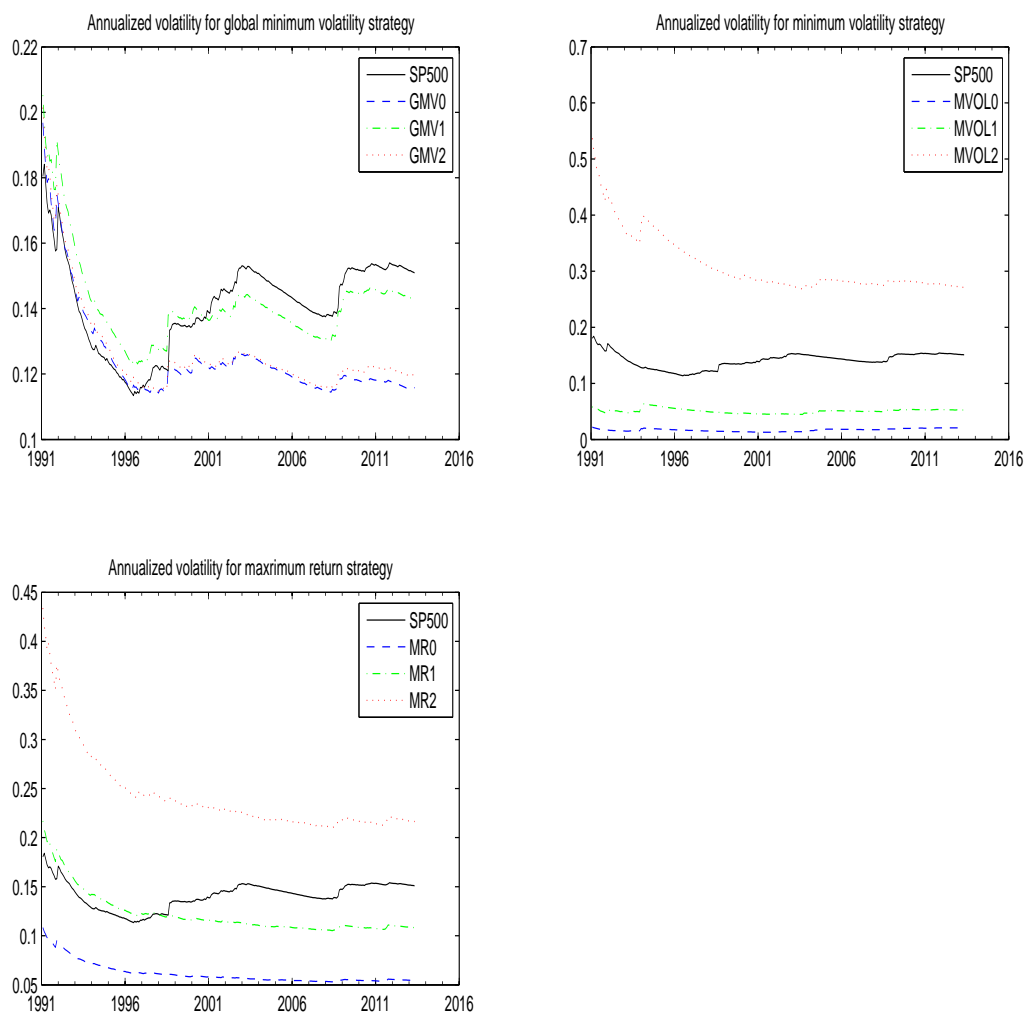


Figure 20: This figure shows the annualized volatility for three types of monthly rebalancing strategies under model FVAR1 for 22-industry data set. SP500 denotes the S&P 500 index. GMV0 is the global minimum volatility model without constraints, GMV1 is the global minimum volatility model with no-shorting constraint, and GMV2 is the global minimum volatility model with leverage constraint. MVOL0 denotes the minimum volatility model with target return of 0.5%, MVOL1 denotes the minimum volatility model with target return of 1%, MVOL2 denotes the minimum volatility model with target return of 4%. MR0 denotes the maximum return model with target volatility of 1%, MR1 denotes the maximum return model with target volatility of 2%, MR2 denotes the maximum return model with target volatility of 4%.

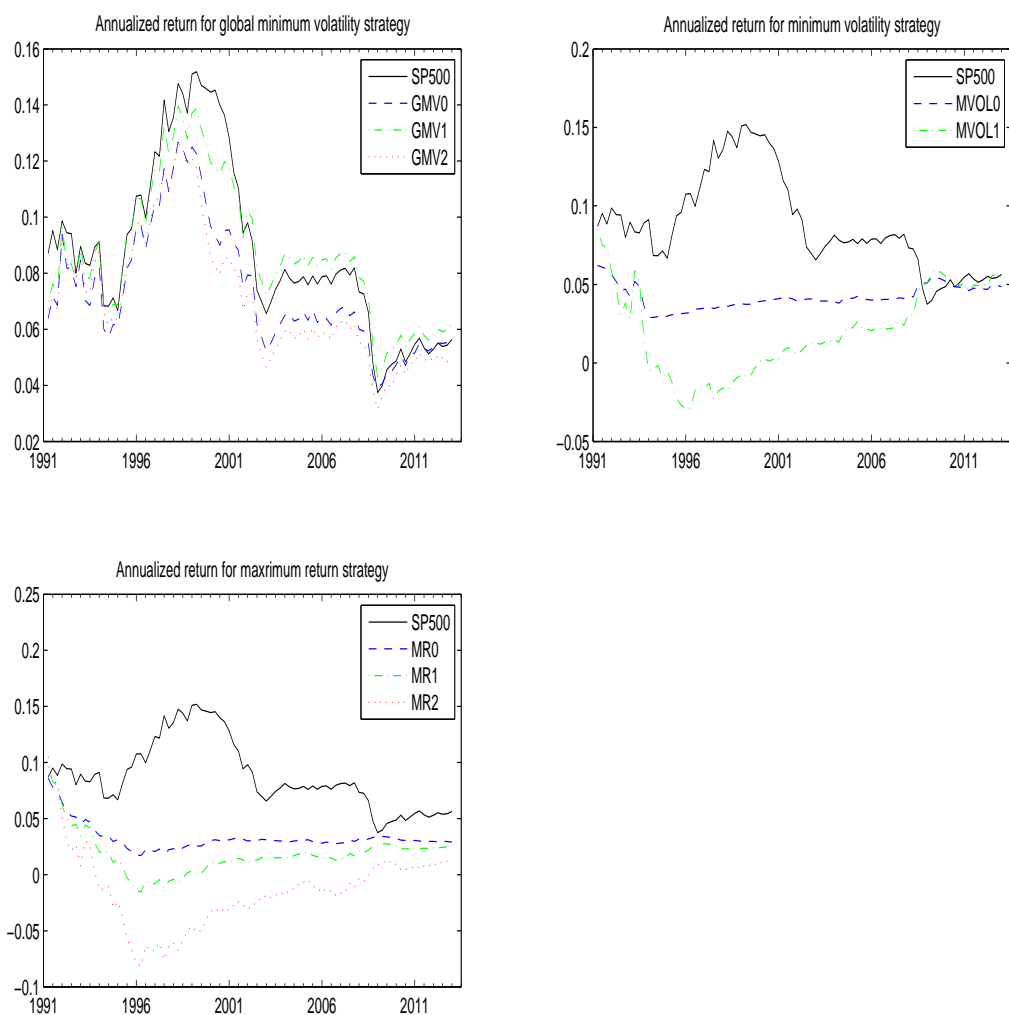


Figure 21: This figure shows the annualized return for three types of quarterly rebalancing strategies under model FVAR1 for 22-industry data set. SP500 denotes the S&P 500 index. GMV0 is the global minimum volatility model without constraints, GMV1 is the global minimum volatility model with no-shorting constraint, and GMV2 is the global minimum volatility model with leverage constraint. MVOL0 denotes the minimum volatility model with target return of 0.5%, MVOL1 denotes the minimum volatility model with target return of 1%, MVOL2 denotes the minimum volatility model with target return of 4%. MR0 denotes the maximum return model with target volatility of 1%, MR1 denotes the maximum return model with target volatility of 2%, MR2 denotes the maximum return model with target volatility of 4%.

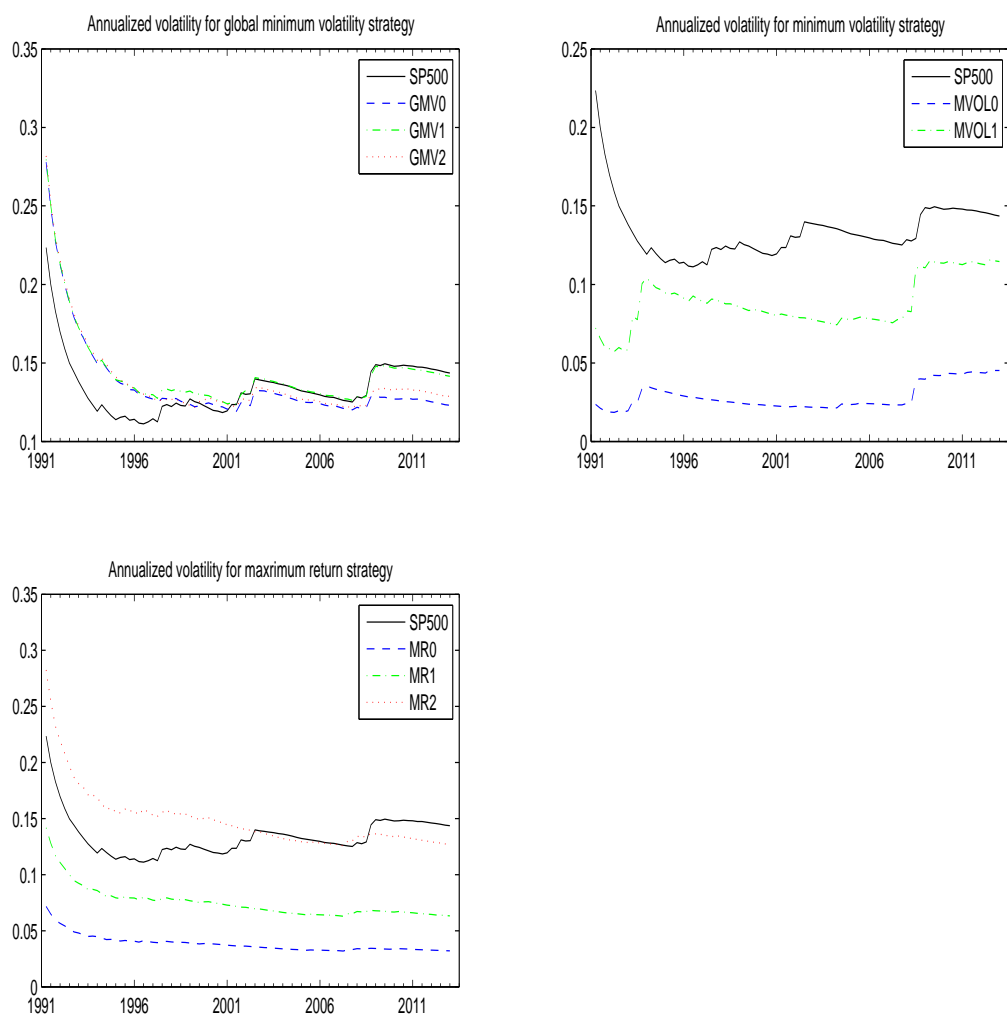


Figure 22: This figure shows the annualized volatility for three types of quarterly rebalancing strategies under model FVAR1 for 22-industry data set. SP500 denotes the S&P 500 index. GMV0 is the global minimum volatility model without constraints, GMV1 is the global minimum volatility model with no-shorting constraint, and GMV2 is the global minimum volatility model with leverage constraint. MVOL0 denotes the minimum volatility model with target return of 0.5%, MVOL1 denotes the minimum volatility model with target return of 1%, MVOL2 denotes the minimum volatility model with target return of 4%. MR0 denotes the maximum return model with target volatility of 1%, MR1 denotes the maximum return model with target volatility of 2%, MR2 denotes the maximum return model with target volatility of 4%.

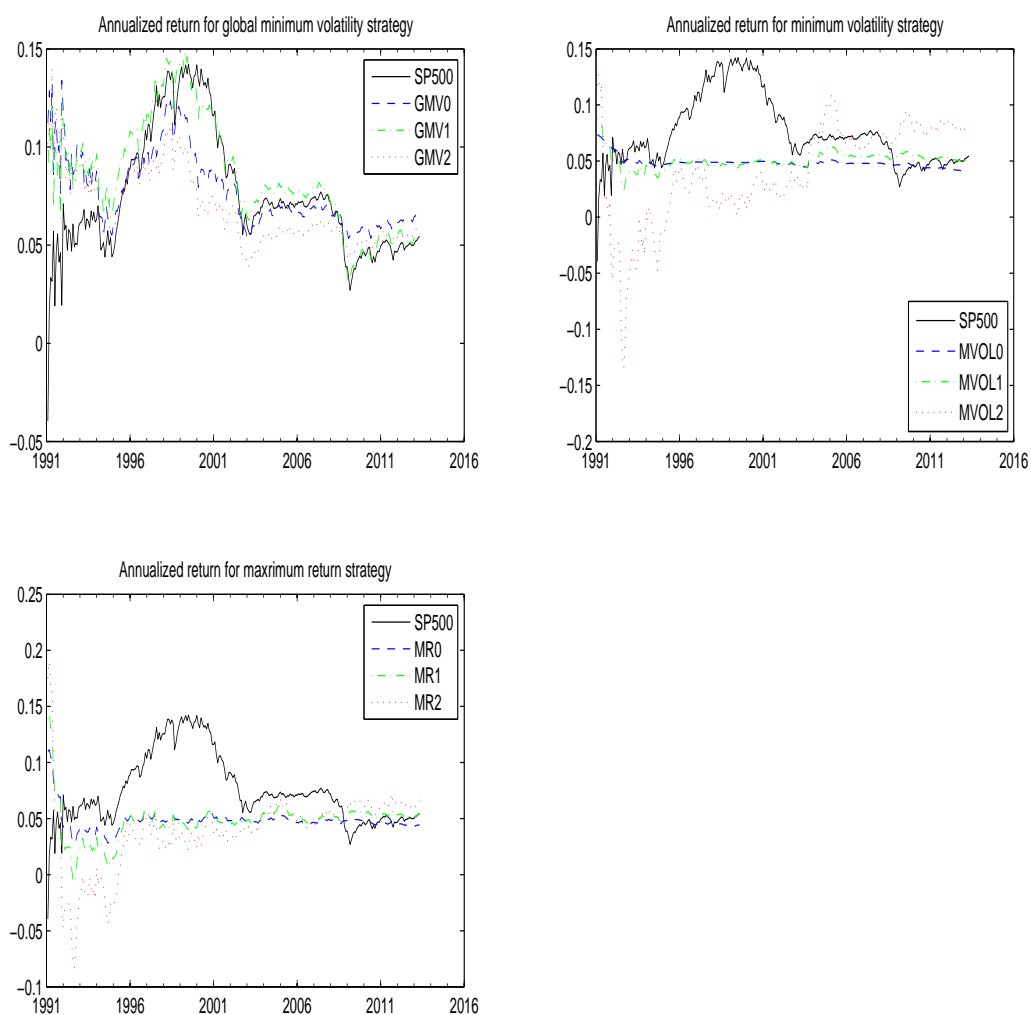


Figure 23: This figure shows the annualized return for three types of monthly rebalancing strategies under model FVAR2 based on 22-industry data set. SP500 denotes the S&P 500 index. GMV0 is the global minimum volatility model without constraints, GMV1 is the global minimum volatility model with no-shorting constraint, and GMV2 is the global minimum volatility model with leverage constraint. MVOL0 denotes the minimum volatility model with target return of 0.5%, MVOL1 denotes the minimum volatility model with target return of 1%, MVOL2 denotes the minimum volatility model with target return of 4%. MR0 denotes the maximum return model with target volatility of 1%, MR1 denotes the maximum return model with target volatility of 2%, MR2 denotes the maximum return model with target volatility of 4%.

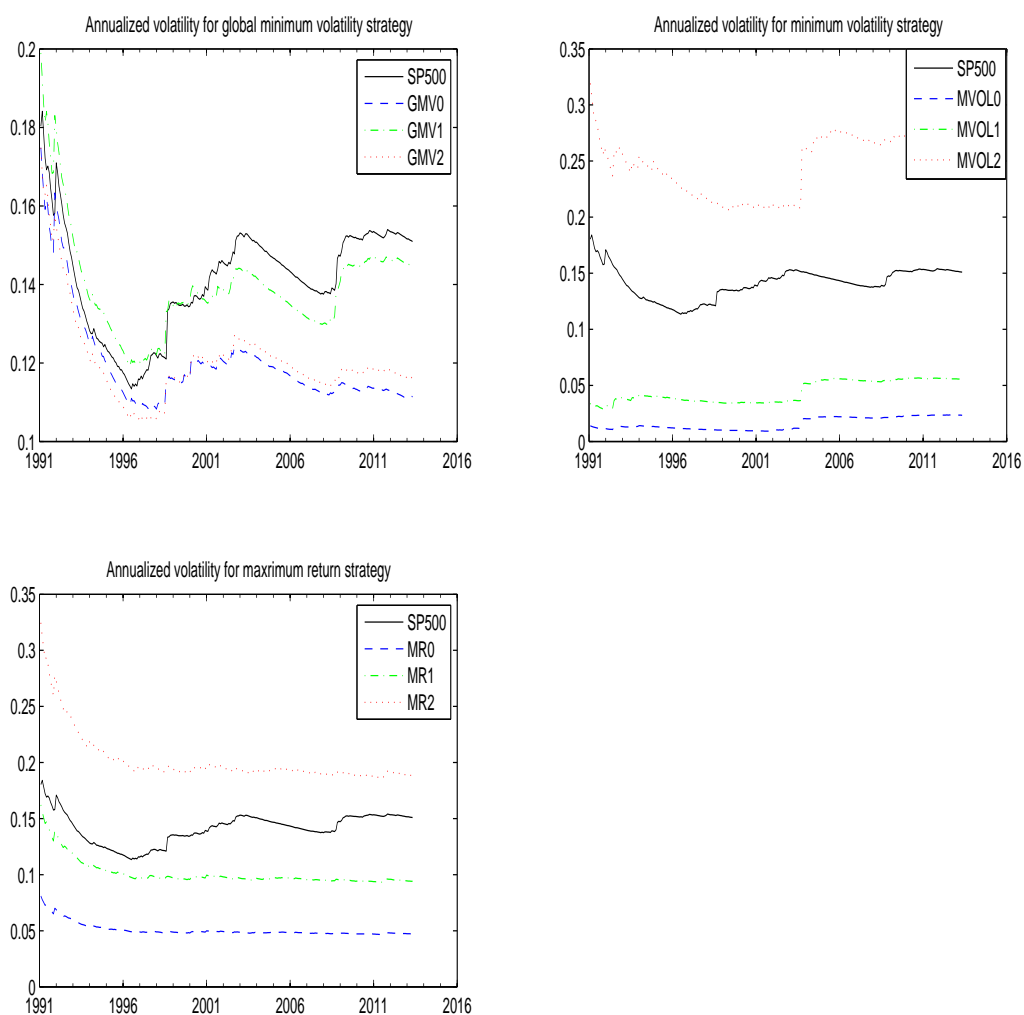


Figure 24: This figure shows the annualized volatility for three types of monthly rebalancing strategies under model FVAR2 based on 22-industry data set. SP500 denotes the S&P 500 index. GMV0 is the global minimum volatility model without constraints, GMV1 is the global minimum volatility model with no-shorting constraint, and GMV2 is the global minimum volatility model with leverage constraint. MVOL0 denotes the minimum volatility model with target return of 0.5%, MVOL1 denotes the minimum volatility model with target return of 1%, MVOL2 denotes the minimum volatility model with target return of 4%. MR0 denotes the maximum return model with target volatility of 1%, MR1 denotes the maximum return model with target volatility of 2%, MR2 denotes the maximum return model with target volatility of 4%.

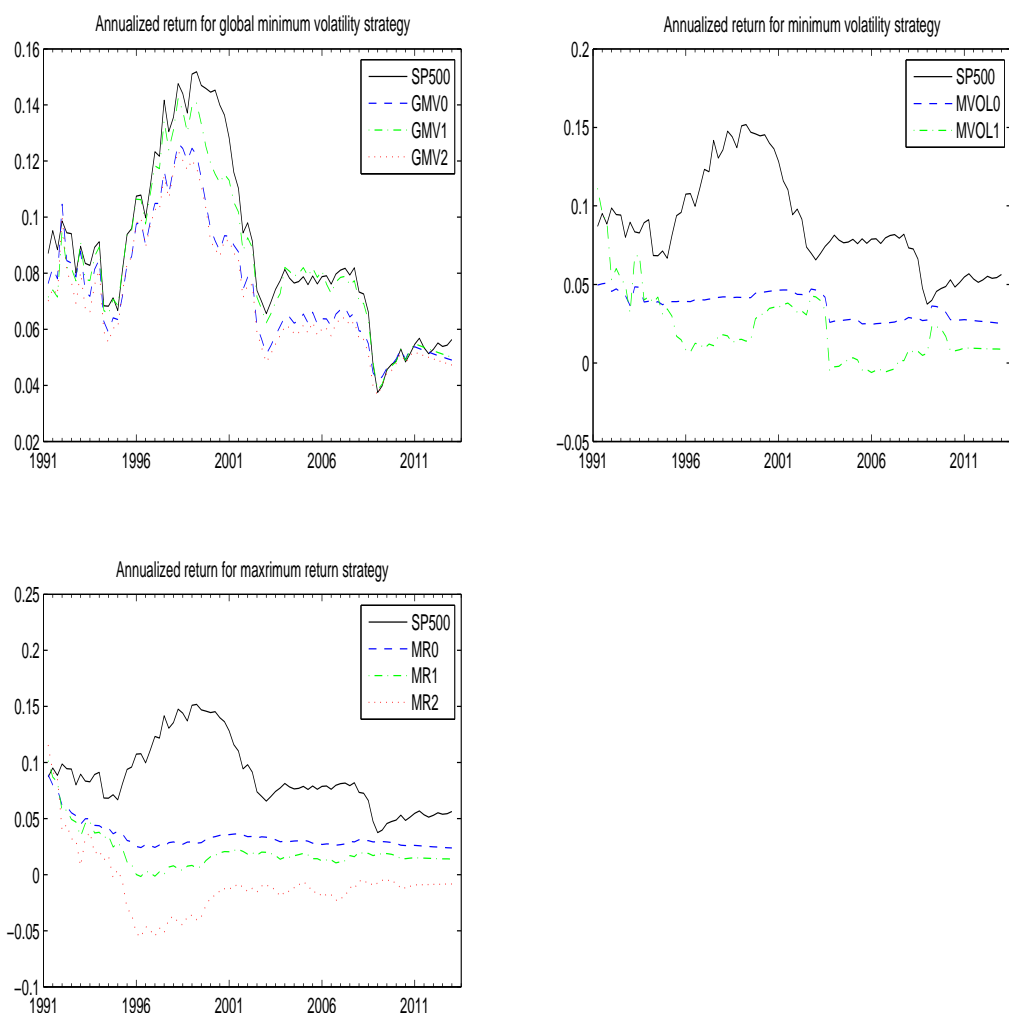


Figure 25: This figure shows the annualized return for three types of quarterly rebalancing strategies under model FVAR2 based on 22-industry data set. SP500 denotes the S&P 500 index. GMV0 is the global minimum volatility model without constraints, GMV1 is the global minimum volatility model with no-shorting constraint, and GMV2 is the global minimum volatility model with leverage constraint. MVOL0 denotes the minimum volatility model with target return of 0.5%, MVOL1 denotes the minimum volatility model with target return of 1%, MVOL2 denotes the minimum volatility model with target return of 4%. MR0 denotes the maximum return model with target volatility of 1%, MR1 denotes the maximum return model with target volatility of 2%, MR2 denotes the maximum return model with target volatility of 4%.

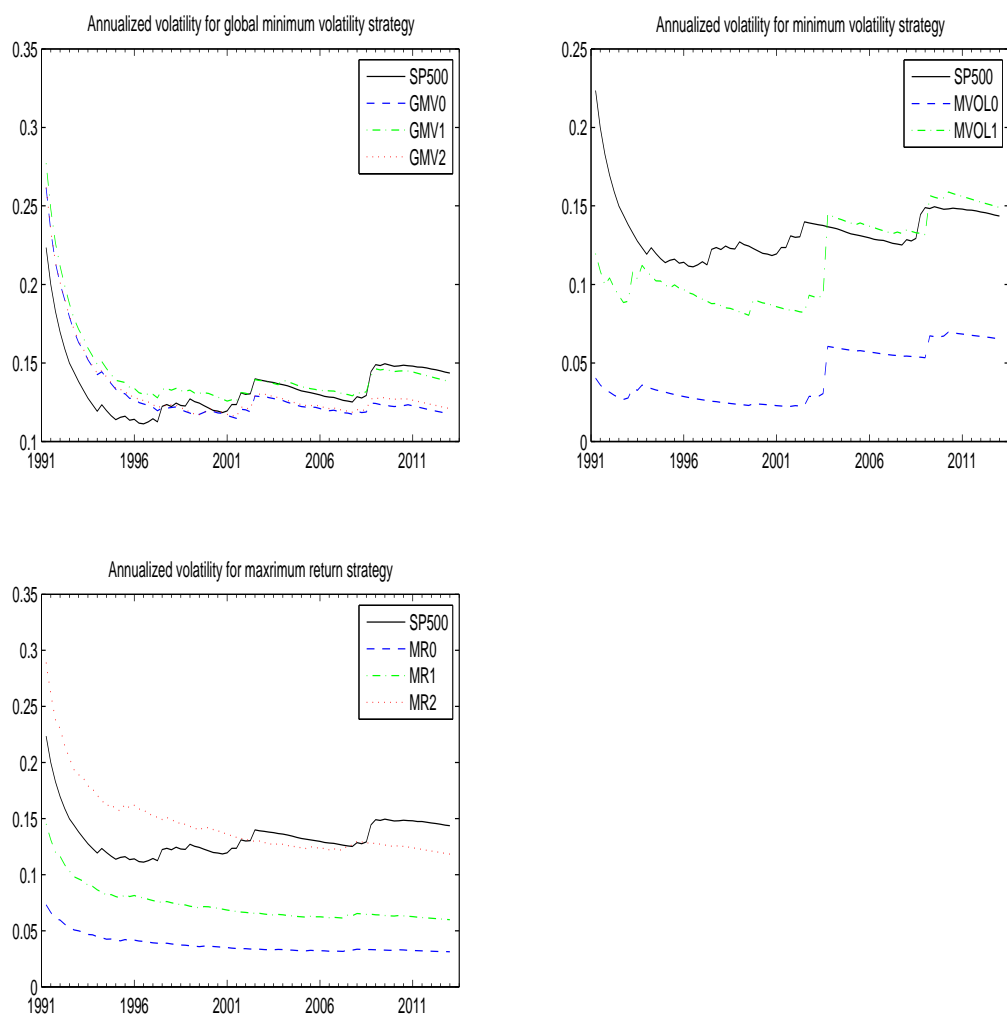


Figure 26: This figure shows the annualized volatility for three types of quarterly rebalancing strategies under model FVAR2 based on 22-industry data set. SP500 denotes the S&P 500 index. GMV0 is the global minimum volatility model without constraints, GMV1 is the global minimum volatility model with no-shorting constraint, and GMV2 is the global minimum volatility model with leverage constraint. MVOL0 denotes the minimum volatility model with target return of 0.5%, MVOL1 denotes the minimum volatility model with target return of 1%, MVOL2 denotes the minimum volatility model with target return of 4%. MR0 denotes the maximum return model with target volatility of 1%, MR1 denotes the maximum return model with target volatility of 2%, MR2 denotes the maximum return model with target volatility of 4%.

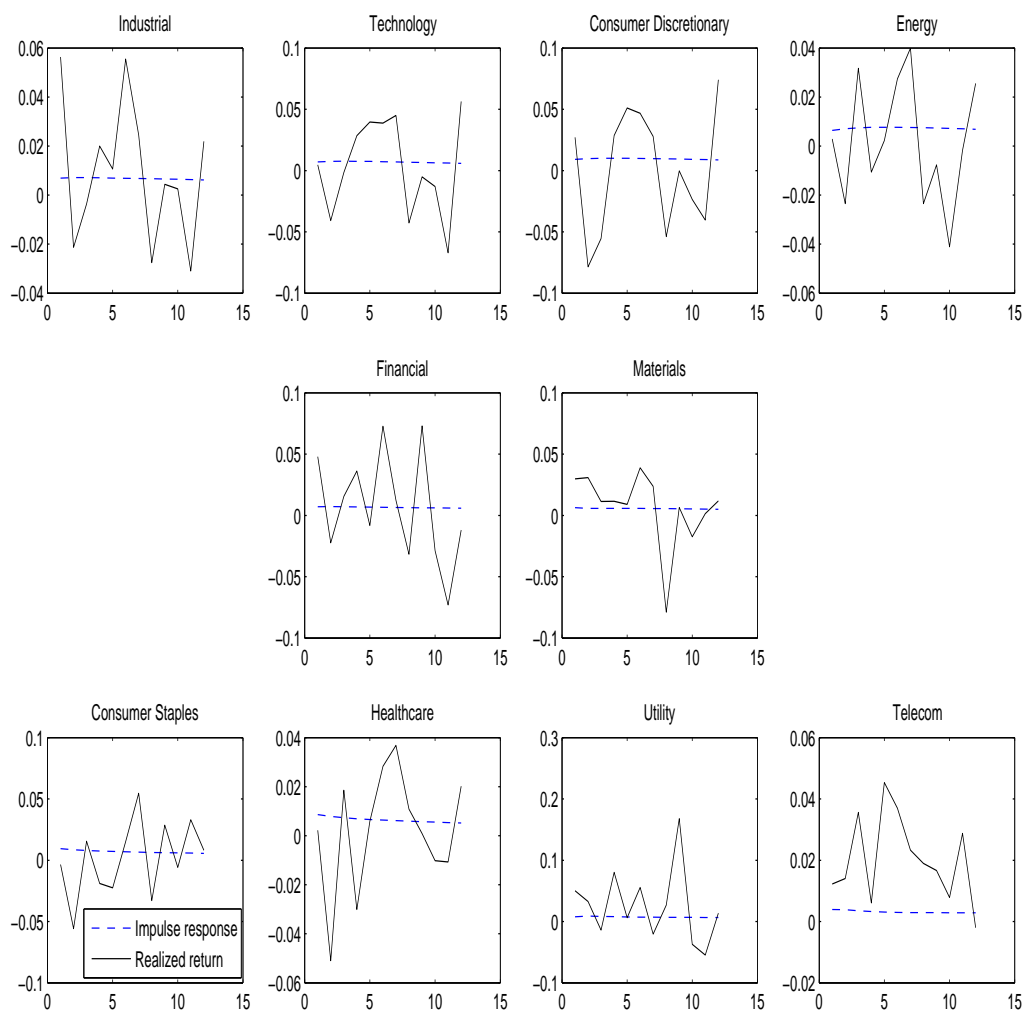


Figure 27: This figure shows the next 12 months impulse response of constant loading with stochastic volatility model FVAR1 for ten sectors on 06/2004 as the Fed starts to increase interest rate by a quarter point. Note that the impulse response is recorded in percentage returns.

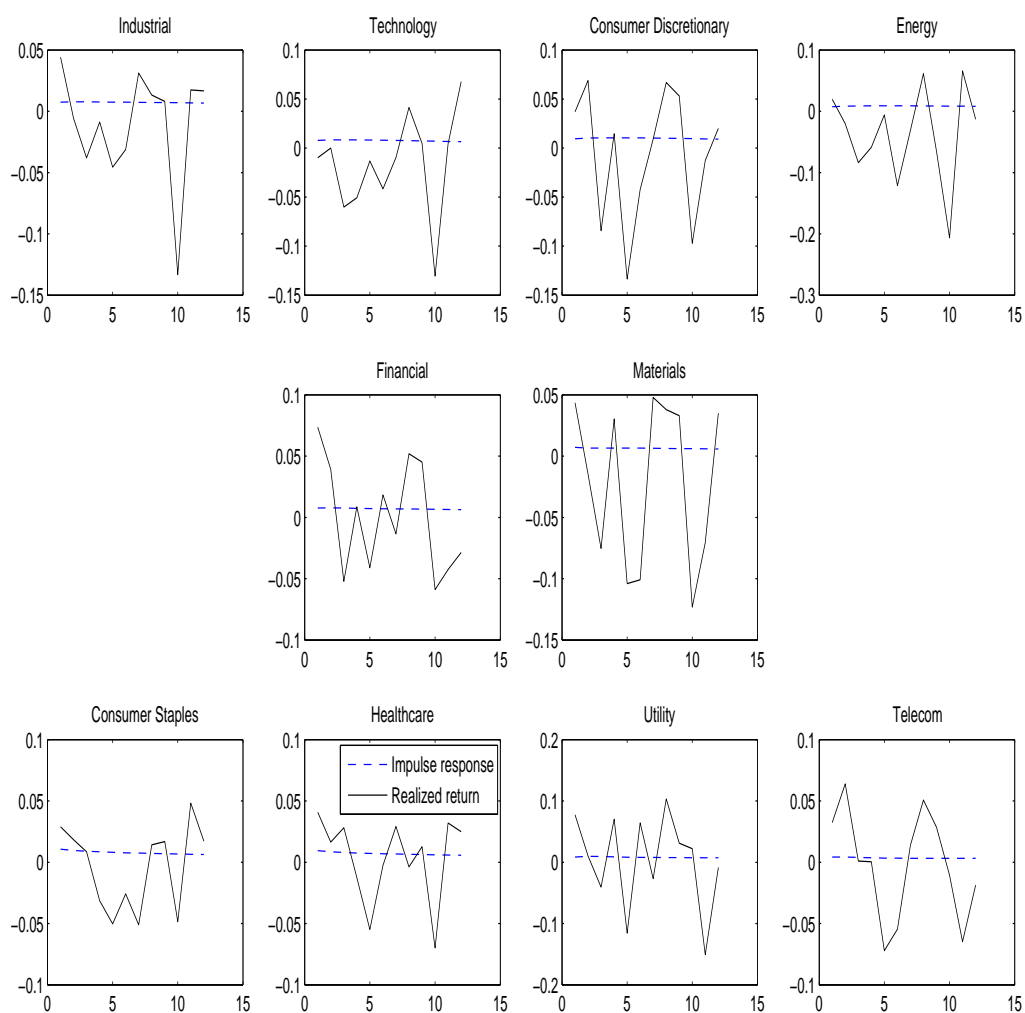


Figure 28: This figure shows the next 12 months impulse response of constant loading with stochastic volatility model FVAR1 for ten sectors on 09/2007 as the Fed cut interest rate by half point since June 2003. Note that the impulse response is recorded in percentage returns.

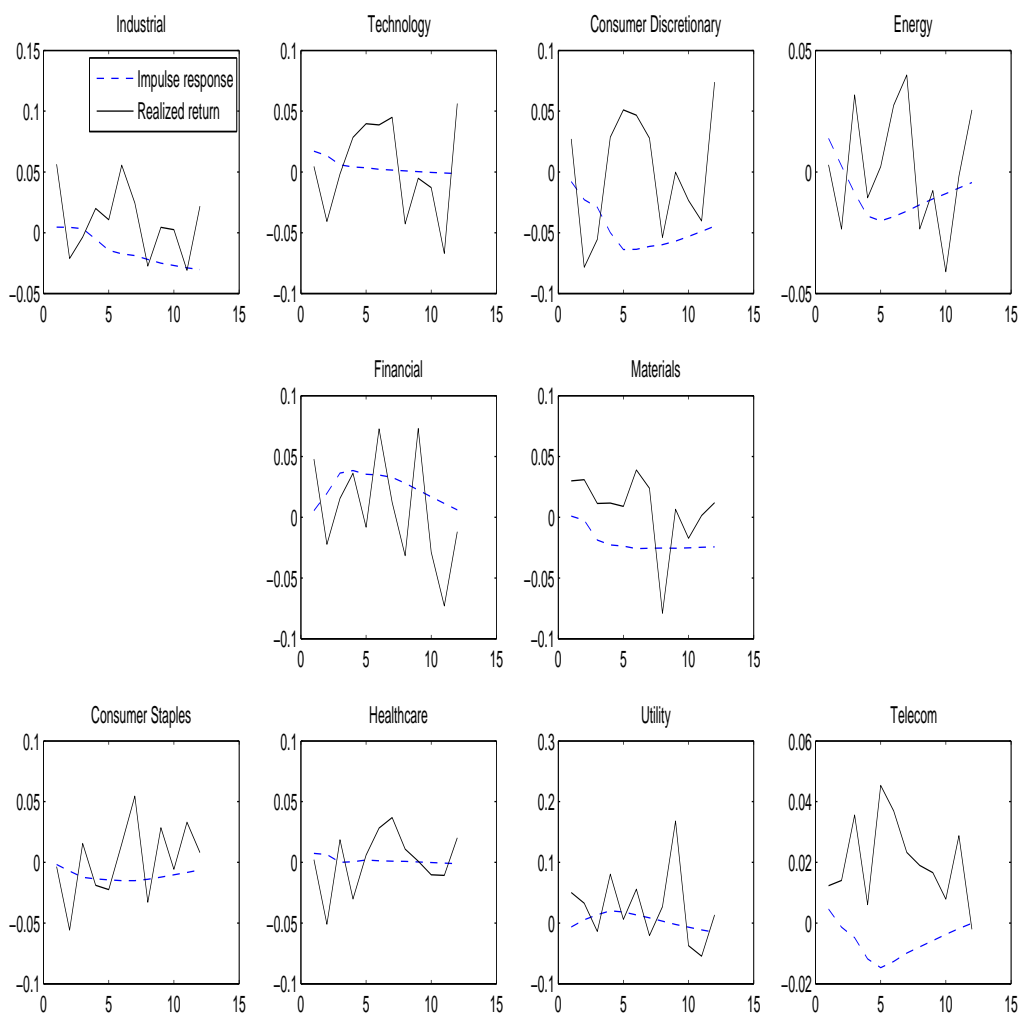


Figure 29: This figure shows the next 12 months impulse response of dynamic loading with stochastic volatility model DFVAR in (2) for ten sectors on 06/2004 as the Fed starts to increase interest rate by a quarter point. Note that the impulse response is recorded in percentage returns.

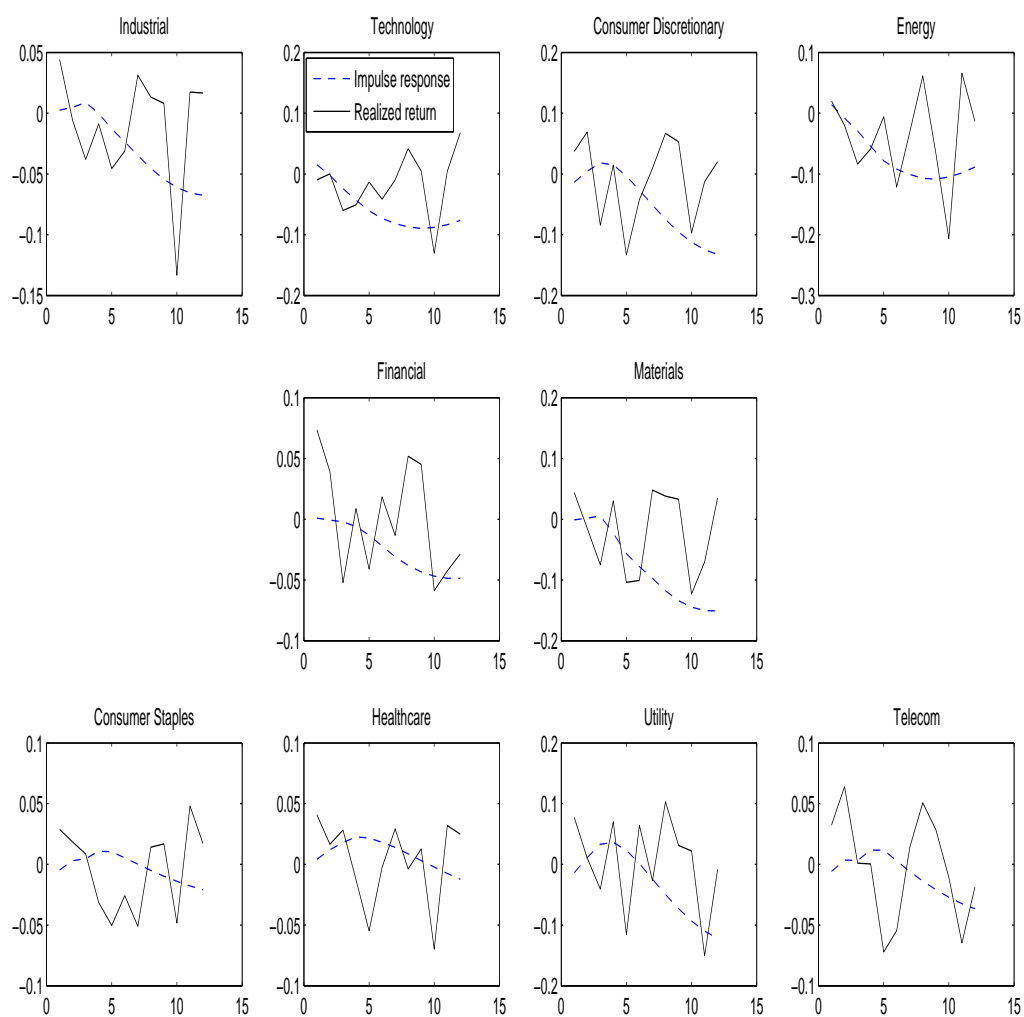


Figure 30: This figure shows the next 12 months impulse response of dynamic loading with stochastic volatility model DFVAR in (2) for ten sectors on 09/2007 as the Fed cut interest rate by half point since June 2003. Note that the impulse response is recorded in percentage returns.

Table 1: Monthly rebalancing portfolio performance under model FVAR0

This table reports the monthly rebalancing out-of-sample portfolio performance of model (15) for 10-sector data set, that is, when the factors follow a Gaussian distribution with stochastic volatility process. μ denotes the annualized return, σ denotes the annualized standard deviation, SR denotes the Sharpe ratio with risk-free rate of 0.5%, DD denotes the worst drawdown, Φ denotes the annualized performance fee, and notation "-" implies that the portfolio wealth is completely wiped out. BH represents the buy-and-hold strategy for holding the S&P 500 index. Under mean-variance framework, MV0 is the model (22) with risk-aversion coefficient of 6 without any constraints, MV1 is the model with no-shorting constraint, and MV2 is the model with leverage constraints. Under global minimum volatility framework, GMV0 is the model (23) without any constraint, GMV1 is the model with no-shorting constraint, and GMV2 is the model with leverage constraints. Under minimum volatility setting, MVOL0 is the model (24) with target expected return of 0.5%, MVOL1 is the model with target expected return of 1% and MVOL2 is the model with target expected return of 4%. Under maximum return setting, MR0 is the model (25) with target volatility of 1%, MR1 is the model with target volatility of 2%, and MR2 is the model with target volatility of 4%.

Monthly Rebalance							
Model	$\mu(\%)$	$\sigma(\%)$	SR	$DD(\%)$	$M2(bp)$	$\Phi(bp)$	BR(%)
BH	5.44	15.03	0.33	-18.56			
Mean-variance strategy							
MV0	-1.29	13.64	-0.13	-19.39	-691	-555	40.28
MV1	3.20	3.89	0.69	-12.26	541	316	39.93
MV2	-1.00	13.45	-0.11	-19.33	-661	-512	40.28
Global minimum volatility strategy							
GMV0	6.84	11.65	0.54	-12.76	316	360	48.06
GMV1	6.47	13.38	0.45	-17.66	180	217	47.70
GMV2	7.60	12.16	0.58	-13.09	376	400	48.76
Minimum volatility strategy							
MVOL0	-	-	-	-	-	-	42.05
MVOL1	-	-	-	-	-	-	39.58
MVOL2	-	-	-	-	-	-	41.34
Maximum return strategy							
MR0	1.58	4.87	0.22	-3.57	-165	138	40.28
MR1	-0.30	9.69	-0.08	-7.48	-616	-223	40.28
MR2	-4.63	19.35	-0.27	-15.29	-902	-1385	43.11

Table 2: Quarterly rebalancing portfolio performance under model FVAR0

This table reports the quarterly rebalancing out-of-sample portfolio performance of model (15) for 10-sector data set, that is, when the factors follow a Gaussian distribution with stochastic volatility process. μ denotes the annualized return, σ denotes the annualized standard deviation, SR denotes the Sharpe ratio with risk-free rate of 0.5%, DD denotes the worst drawdown, Φ denotes the annualized performance fee, and notation "-" implies that the portfolio wealth is completely wiped out. BH represents the buy-and-hold strategy for holding the S&P 500 index. Under mean-variance framework, MV0 is the model (22) with risk-aversion coefficient of 6 without any constraints, MV1 is the model with no-shorting constraint, and MV2 is the model with leverage constraints. Under global minimum volatility framework, GMV0 is the model (23) without any constraint, GMV1 is the model with no-shorting constraint, and GMV2 is the model with leverage constraints. Under minimum volatility setting, MVOL0 is the model (24) with target expected return of 0.5%, MVOL1 is the model with target expected return of 1% and MVOL2 is the model with target expected return of 4%. Under maximum return setting, MR0 is the model (25) with target volatility of 1%, MR1 is the model with target volatility of 2%, and MR2 is the model with target volatility of 4%.

Quarterly Rebalance							
Model	$\mu(\%)$	$\sigma(\%)$	SR	$DD(\%)$	$M2(bp)$	$\Phi(bp)$	BR(%)
BH	5.64	14.32	0.36	-26.87			
Mean-variance strategy							
MV0	1.77	4.95	0.26	-5.82	-143	75	39.78
MV1	3.68	1.58	2.02	-1.87	2377	317	38.71
MV2	1.77	4.93	0.26	-5.79	-1432	76	39.78
Global minimum volatility strategy							
GMV0	6.04	11.96	0.46	-18.29	143	220	49.46
GMV1	5.97	12.86	0.43	-23.22	100	148	44.09
GMV2	6.06	12.17	0.46	-17.97	143	212	48.39
Minimum volatility strategy							
MVOL0	-	-	-	-	-	-	40.86
MVOL1	-	-	-	-	-	-	40.86
MVOL2	-	-	-	-	-	-	43.01
Maximum return strategy							
MR0	2.59	2.87	0.73	-1.60	530	192	39.78
MR1	1.82	5.51	0.24	-4.00	-172	56	39.78
MR2	0.06	10.96	-0.04	-9.22	-573	-360	37.63

Table 3: Monthly rebalancing portfolio performance under model FVAR1

This table reports the monthly rebalancing out-of-sample portfolio performance of model (16) for 10-sector data set, that is, when the factors follow a VAR(1) with stochastic volatility process. μ denotes the annualized return, σ denotes the annualized standard deviation, SR denotes the Sharpe ratio with risk-free rate of 0.5%, DD denotes the worst drawdown, $M2$ denotes the risk-adjusted abnormal return, Φ denotes the annualized performance fee, and BR denotes the beat rate. BH represents the buy-and-hold strategy for holding the S&P 500 index. Under global minimum volatility framework, GMV0 is the model (23) without any constraint, GMV1 is the model with no-shorting constraint, and GMV2 is the model with leverage constraints. Under minimum volatility setting, MVOL0 is the model (24) with target expected return of 0.5%, MVOL1 is the model with target expected return of 1% and MVOL2 is the model with target expected return of 4%. Under maximum return setting, MR0 is the model (25) with target volatility of 1%, MR1 is the model with target volatility of 2%, and MR2 is the model with target volatility of 4%.

Monthly Rebalance							
Model	$\mu(\%)$	$\sigma(\%)$	SR	$DD(\%)$	$M2(bp)$	$\Phi(bp)$	$BR(\%)$
BH	5.44	15.03	0.33	-18.56			
Global minimum volatility strategy							
GMV0	6.59	12.00	0.51	-14.34	270	317	48.06
GMV1	5.79	13.20	0.40	-15.46	105	166	46.29
GMV2	5.19	12.89	0.36	-17.61	45	129	47.35
Minimum volatility strategy							
MVOL0	3.90	3.40	1.00	-9.71	1007	391	41.70
MVOL1	4.76	8.29	0.51	-21.31	271	332	43.46
MVOL2	-0.51	40.35	-0.03	-90.94	-541	-4383	47.00
Maximum return strategy							
MR0	4.59	4.99	0.82	-3.93	736	424	44.17
MR1	5.66	9.98	0.52	-8.19	285	340	43.46
MR2	7.06	19.97	0.33	-16.72	0	-302	46.64

Table 4: Quarterly rebalancing portfolio performance under model FVAR1

This table reports the quarterly rebalancing out-of-sample portfolio performance of model (16) for 10-sector data set, that is, when the factors follow a VAR(1) with stochastic volatility process. μ denotes the annualized return, σ denotes the annualized standard deviation, SR denotes the Sharpe ratio with risk-free rate of 0.5%, DD denotes the worst drawdown, $M2$ denotes the risk-adjusted abnormal return, Φ denotes the annualized performance fee, BR denotes the beat rate, and notation "-" implies that the portfolio wealth is completely wiped out. BH represents the buy-and-hold strategy for holding the S&P 500 index. Under global minimum volatility framework, GMV0 is the model without any constraint, GMV1 is the model with no-shorting constraint, and GMV2 is the model with leverage constraints. Under minimum volatility setting, MVOL0 is the model with target expected return of 0.5%, MVOL1 is the model with target expected return of 1% and MVOL2 is the model with target expected return of 4%. Under maximum return setting, MR0 is the model with target volatility of 1%, MR1 is the model with target volatility of 2%, and MR2 is the model with target volatility of 4%. N/A denotes a feasible solution couldn't be found.

Quarterly Rebalance							
Model	$\mu(\%)$	$\sigma(\%)$	SR	$DD(\%)$	$M2(bp)$	$\Phi(bp)$	$BR(\%)$
BH	5.64	14.32	0.36	-26.87			
Global minimum volatility strategy							
GMV0	5.74	12.54	0.42	-21.14	86	151	44.09
GMV1	5.92	13.27	0.41	-23.93	72	112	48.39
GMV2	5.81	12.53	0.42	-21.48	86	158	43.01
Minimum volatility strategy							
MVOL0	5.02	16.61	0.27	-36.02	-129	-496	40.86
MVOL1	3.23	37.85	0.07	-72.48	-415	N/A	46.24
MVOL2	-	-	-	-	-	-	-
Maximum return strategy							
MR0	2.82	2.89	0.80	-2.21	630	216	38.71
MR1	2.26	5.63	0.31	-5.68	-72	100	40.86
MR2	0.92	11.25	0.04	-12.61	-458	-285	39.78

Table 5: Monthly rebalancing portfolio performance under model FVAR2

This table reports the monthly rebalancing out-of-sample portfolio performance of model (17) for 10-sector data set, that is, when the factors follow a VAR(1) with simultaneous interactions among factors. μ denotes the annualized return, σ denotes the annualized standard deviation, SR denotes the Sharpe ratio with risk-free rate of 0.5%, DD denotes the worst drawdown, $M2$ denotes the risk-adjusted abnormal return, Φ denotes the annualized performance fee, and BR denotes the beat rate. BH represents the buy-and-hold strategy for holding the S&P 500 index. Under global minimum volatility framework, GMV0 is the model (23) without any constraint, GMV1 is the model with no-shorting constraint, and GMV2 is the model with leverage constraints. Under minimum volatility setting, MVOL0 is the model (24) with target expected return of 0.5%, MVOL1 is the model with target expected return of 1% and MVOL2 is the model with target expected return of 4%. Under maximum return setting, MR0 is the model (25) with target volatility of 1%, MR1 is the model with target volatility of 2%, and MR2 is the model with target volatility of 4%.

Monthly Rebalance							
Model	$\mu(\%)$	$\sigma(\%)$	SR	$DD(\%)$	$M2(bp)$	$\Phi(bp)$	$BR(\%)$
BH	5.44	15.03	0.33	-18.56			
Global minimum volatility strategy							
GMV0	6.60	11.33	0.54	-13.20	316	356	47.35
GMV1	6.29	12.68	0.46	-13.87	195	246	47.00
GMV2	6.53	12.15	0.50	-14.48	256	301	47.35
Minimum volatility strategy							
MVOL0	3.97	2.73	1.27	-6.27	1413	409	41.34
MVOL1	5.33	6.79	0.71	-14.12	571	442	44.17
MVOL2	9.00	33.31	0.26	-61.18	-105	-2133	43.46
Maximum return strategy							
MR0	4.40	4.50	0.86	-4.17	797	417	45.23
MR1	5.33	8.97	0.54	-8.35	316	356	44.88
MR2	6.58	17.94	0.34	-16.69	15	-143	46.64

Table 6: Quarterly rebalancing portfolio performance under model FVAR2

This table reports the quarterly rebalancing out-of-sample portfolio performance of model (17) for 10-sector data set, that is, when the factors follow a VAR(1) with simultaneous interactions among factors. μ denotes the annualized return, σ denotes the annualized standard deviation, SR denotes the Sharpe ratio with risk-free rate of 0.5%, DD denotes the worst drawdown, $M2$ denotes the risk-adjusted abnormal return, Φ denotes the annualized performance fee, BR denotes the beat rate, and notation "-" implies that the portfolio wealth is completely wiped out. BH represents the buy-and-hold strategy for holding the S&P 500 index. Under global minimum volatility framework, GMV0 is the model without any constraint, GMV1 is the model with no-shorting constraint, and GMV2 is the model with leverage constraints. Under minimum volatility setting, MVOL0 is the model with target expected return of 0.5%, MVOL1 is the model with target expected return of 1% and MVOL2 is the model with target expected return of 4%. Under maximum return setting, MR0 is the model with target volatility of 1%, MR1 is the model with target volatility of 2%, and MR2 is the model with target volatility of 4%.

Quarterly Rebalance							
Model	$\mu(\%)$	$\sigma(\%)$	SR	$DD(\%)$	$M2(bp)$	$\Phi(bp)$	$BR(\%)$
BH	5.64	14.32	0.36	-26.87			
Global minimum volatility strategy							
GMV0	5.80	12.41	0.43	-19.04	100	162	44.09
GMV1	5.56	13.69	0.37	-27.85	14	46	50.54
GMV2	5.77	12.10	0.44	-19.98	115	179	46.24
Minimum volatility strategy							
MVOL0	1.54	8.41	0.12	-18.02	-344	-89	39.78
MVOL1	-2.54	19.51	-0.16	-39.57	-745	-1390	40.86
MVOL2	-	-	-	-	-	-	-
Maximum return strategy							
MR0	2.47	2.69	0.73	-1.89	530	183	38.71
MR1	1.59	5.09	0.21	-4.85	-215	46	41.94
MR2	-0.35	10.07	-0.08	-11.07	-630	-349	39.78

Table 7: Monthly rebalancing portfolio performance under model FVAR1

This table reports the monthly rebalancing out-of-sample portfolio performance of model (16) for 22-industry data set, that is, when the factors follow a VAR(1) with stochastic volatility process. μ denotes the annualized return, σ denotes the annualized standard deviation, SR denotes the Sharpe ratio with risk-free rate of 0.5%, DD denotes the worst drawdown, $M2$ denotes the risk-adjusted abnormal return, Φ denotes the annualized performance fee, and BR denotes the beat rate. BH represents the buy-and-hold strategy for holding the S&P 500 index. Under global minimum volatility framework, GMV0 is the model (23) without any constraint, GMV1 is the model with no-shorting constraint, and GMV2 is the model with leverage constraints. Under minimum volatility setting, MVOL0 is the model (24) with target expected return of 0.5%, MVOL1 is the model with target expected return of 1% and MVOL2 is the model with target expected return of 4%. Under maximum return setting, MR0 is the model (25) with target volatility of 1%, MR1 is the model with target volatility of 2%, and MR2 is the model with target volatility of 4%.

Monthly Rebalance							
Model	$\mu(\%)$	$\sigma(\%)$	SR	$DD(\%)$	$M2(bp)$	$\Phi(bp)$	$BR(\%)$
BH	5.44	15.03	0.33	-18.56			
Global minimum volatility strategy							
GMV0	6.25	11.58	0.50	-11.49	256	310	45.58
GMV1	6.88	14.27	0.45	-17.33	180	192	48.06
GMV2	5.88	11.96	0.45	-13.16	180	252	45.23
Minimum volatility strategy							
MVOL0	3.82	2.05	1.62	-2.32	1939	402	40.99
MVOL1	5.03	5.23	0.87	-5.70	812	460	43.11
MVOL2	9.51	27.08	0.33	-26.01	0	-1001	44.88
Maximum return strategy							
MR0	5.27	5.45	0.88	-5.35	827	477	43.11
MR1	7.00	10.83	0.60	-10.70	406	420	46.29
MR2	9.60	21.64	0.42	-21.41	135	-254	46.29

Table 8: Quarterly rebalancing portfolio performance under model FVAR1

This table reports the quarterly rebalancing out-of-sample portfolio performance of model (16) for 22-industry data set, that is, when the factors follow a VAR(1) with stochastic volatility process. μ denotes the annualized return, σ denotes the annualized standard deviation, SR denotes the Sharpe ratio with risk-free rate of 0.5%, DD denotes the worst drawdown, $M2$ denotes the risk-adjusted abnormal return, Φ denotes the annualized performance fee, BR denotes the beat rate, and notation "-" implies that the portfolio wealth is completely wiped out. BH represents the buy-and-hold strategy for holding the S&P 500 index. Under global minimum volatility framework, GMV0 is the model without any constraint, GMV1 is the model with no-shorting constraint, and GMV2 is the model with leverage constraints. Under minimum volatility setting, MVOL0 is the model with target expected return of 0.5%, MVOL1 is the model with target expected return of 1% and MVOL2 is the model with target expected return of 4%. Under maximum return setting, MR0 is the model with target volatility of 1%, MR1 is the model with target volatility of 2%, and MR2 is the model with target volatility of 4%. N/A denotes a feasible solution couldn't be found.

Quarterly Rebalance							
Model	$\mu(\%)$	$\sigma(\%)$	SR	$DD(\%)$	$M2(bp)$	$\Phi(bp)$	$BR(\%)$
BH	5.64	14.32	0.36	-26.87			
Global minimum volatility strategy							
GMV0	5.74	12.34	0.43	-20.29	100	165	44.09
GMV1	6.17	14.12	0.40	-24.87	57	70	48.39
GMV2	5.07	12.91	0.35	-20.73	-14	64	46.24
Minimum volatility strategy							
MVOL0	4.85	4.51	0.96	-3.93	859	380	39.78
MVOL1	5.43	11.42	0.43	-11.68	100	141	45.16
MVOL2	-1.89	56.31	-0.04	-61.61	-573	N/A	43.01
Maximum return strategy							
MR0	2.90	3.20	0.75	-2.40	558	221	41.94
MR1	2.40	6.29	0.30	-6.05	-86	97	43.01
MR2	1.10	12.62	0.05	-13.35	-444	-348	40.86

Table 9: Monthly rebalancing portfolio performance under model FVAR2

This table reports the monthly rebalancing out-of-sample portfolio performance of model (17) for 22-industry data set, that is, when the factors follow a VAR(1) with simultaneous interactions among factors. μ denotes the annualized return, σ denotes the annualized standard deviation, SR denotes the Sharpe ratio with risk-free rate of 0.5%, DD denotes the worst drawdown, $M2$ denotes the risk-adjusted abnormal return, Φ denotes the annualized performance fee, and BR denotes the beat rate. BH represents the buy-and-hold strategy for holding the S&P 500 index. Under global minimum volatility framework, GMV0 is the model (23) without any constraint, GMV1 is the model with no-shorting constraint, and GMV2 is the model with leverage constraints. Under minimum volatility setting, MVOL0 is the model (24) with target expected return of 0.5%, MVOL1 is the model with target expected return of 1% and MVOL2 is the model with target expected return of 4%. Under maximum return setting, MR0 is the model (25) with target volatility of 1%, MR1 is the model with target volatility of 2%, and MR2 is the model with target volatility of 4%.

Monthly Rebalance							
Model	$\mu(\%)$	$\sigma(\%)$	SR	$DD(\%)$	$M2(bp)$	$\Phi(bp)$	$BR(\%)$
BH	5.44	15.03	0.33	-18.56			
Global minimum volatility strategy							
GMV0	6.71	11.14	0.56	-10.48	346	377	47.35
GMV1	5.60	14.45	0.35	-16.99	30	60	47.35
GMV2	5.85	11.62	0.46	-12.04	195	269	46.29
Minimum volatility strategy							
MVOL0	4.14	2.34	1.56	-1.81	1849	430	41.70
MVOL1	5.08	5.54	0.83	-4.55	752	456	43.11
MVOL2	8.31	26.35	0.30	-23.76	-45	-1014	43.82
Maximum return strategy							
MR0	4.45	4.72	0.84	-4.31	767	418	43.46
MR1	5.42	9.41	0.52	-8.91	286	345	44.88
MR2	6.67	18.82	0.33	-18.47	0	-219	47.00

Table 10: Quarterly rebalancing portfolio performance under model FVAR2

This table reports the quarterly rebalancing out-of-sample portfolio performance of model (17) for 22-industry data set, that is, when the factors follow a VAR(1) with simultaneous interactions among factors. μ denotes the annualized return, σ denotes the annualized standard deviation, SR denotes the Sharpe ratio with risk-free rate of 0.5%, DD denotes the worst drawdown, $M2$ denotes the risk-adjusted abnormal return, Φ denotes the annualized performance fee, BR denotes the beat rate, and notation "-" implies that the portfolio wealth is completely wiped out. BH represents the buy-and-hold strategy for holding the S&P 500 index. Under global minimum volatility framework, GMV0 is the model without any constraint, GMV1 is the model with no-shorting constraint, and GMV2 is the model with leverage constraints. Under minimum volatility setting, MVOL0 is the model with target expected return of 0.5%, MVOL1 is the model with target expected return of 1% and MVOL2 is the model with target expected return of 4%. Under maximum return setting, MR0 is the model with target volatility of 1%, MR1 is the model with target volatility of 2%, and MR2 is the model with target volatility of 4%.

Quarterly Rebalance							
Model	$\mu(\%)$	$\sigma(\%)$	SR	$DD(\%)$	$M2(bp)$	$\Phi(bp)$	$BR(\%)$
BH	5.64	14.32	0.36	-26.87			
Global minimum volatility strategy							
GMV0	4.90	11.68	0.38	-18.74	29	88	44.09
GMV1	5.00	13.74	0.33	-21.95	-43	-44	43.01
GMV2	4.72	12.03	0.35	-19.07	-14	49	46.24
Minimum volatility strategy							
MVOL0	2.52	6.51	0.31	-18.39	-72	104	39.78
MVOL1	0.87	14.82	0.03	-40.30	-473	-527	45.16
MVOL2	-	-	-	-	-	-	-
Maximum return strategy							
MR0	2.38	3.11	0.61	-2.21	358	173	40.86
MR1	1.39	5.95	0.15	-5.80	-301	11	41.94
MR2	-0.83	11.77	-0.11	-12.97	-673	-480	44.09

CHAPTER 2: OPTIMAL PORTFOLIO CHOICE AND CONSISTENT PERFORMANCE

I. Introduction

In a volatile market environment, successive adverse price movements and poor dynamic risk management systems can lead to substantial financial losses. In practice, a roller coaster financial performance could induce fund withdrawals and discourage potential investors. Many investors start to recognize the value of consistent performance and fund industry awards consistently well-performed funds, such as the Lipper Fund Award which highlights funds that have excelled in delivering consistently strong risk-adjusted performance. Therefore, consistent performance is the key element to success in asset management.¹⁴

A fund that performs well in one year may not show up in the five-year top listing or top performers in the past five years may turn out to be the worst in the next year. This implies that it is not very rewarding to rely on the analysis of historical returns over a single time instant. Instead, one should consider the historical performance over a long horizon and assign relative weights to the performance at different time points in order to better represent the true status of the fund performance and management skills.

¹⁴As John C. Bogle addresses it, "There is an important role that past performance can play in helping you to make your fund selections. While you should disregard a single aggregate number showing a fund's past long-term return, you can learn a great deal by studying the nature of its past return. Above all, look for consistency." (Excerpted from *Common Sense on Mutual Funds* by John C. Bogle, page 96.)

This paper examines portfolio choice problem with consistent performance requirement by imposing an endogenous wealth constraint, namely the *consistent performance constraint*, which claims that the current wealth never falls below a weighted average its historical positions from time zero to the present time. A weaker version of this constraint ensures that the *investment return in any investment period is greater than a fixed number*. We derive a general optimal policy and obtain a closed-form policy in a special case in which the optimal policy turns out to be the portfolio insurance strategy that has been studied extensively.¹⁵ The intuition of the solution under the consistent performance constraint is similar and straightforward: the investors use the benchmark as a capital reserve and invest a proportion of the cushion on the capital market, and thus the consistent performance is obtained.

There are three notable features for this consistent performance constraint. *Firstly*, it takes the entire historical path into account to build a subsistent level of portfolio wealth. By its very construction, the subsistent level highlights the cumulative investment performance over time instead of one particular extreme performance incurred at a certain time instant, such as the maximum drawdown constraint (See Grossman and Zhou (1993), Magdon-Ismai and Atiya (2004), and Pospisil and Vecer (2010)). Moreover, this constraint is dynamic and endogenous in comparison to other fixed exogenous constraints, i.e. Giacinto et al. (2011) and focuses on the consistency of wealth compared with the study of intolerance of declining consumption by Dybvig

¹⁵For instance, Black and Perold (1992), El Karoui and Jeanblanc-Picque (1998) and El Karoui, Jeanblanc-Picque and Lacoste (2005) examine the optimal portfolio choice problem under a deterministic wealth benchmark. For the portfolio choice problem with constraints, both the maximum drawdown and the leverage constraints (Grossman and Vila (1992)) lead to portfolio insurance strategies.

(1995) and Riedel (2009).

Secondly, the consistent performance constraint is strictly imposed in the sense that the wealth could stay at or above the consistent benchmark almost surely, which is in stark contrast to the probability-type constraint such as beating a benchmark in a confidence interval (see Boyle and Tian (2007, 2009), Cuoco, He and Isaenko (2008)). It is also known that the probability type constraint on the wealth often leads to a large position in the risky asset and can incur drastic losses in some extreme cases. Cuoco and Liu (2006) present a VaR-based analysis for bank capital. As shown in the recent financial crisis period 2007-2008, the bank capital calculated by a probability-based risk measure is not sufficient to cover the losses incurred under certain extreme adverse market conditions and can lead to severe financial and social consequences.

Thirdly, we find an interesting virtual function f in the general optimal policy in which the optimal policy looks very close to the classic intertemporal portfolio choice policy. One only need to replace the relative risk aversion of a Bernoulli function in the traditional Merton' case with the relative risk aversion of this virtual function f in the consistent performance constraint case. This virtual function internalizes the wealth constraint and implicitly describes investor's risk aversion, and thus can provide valuable insights about the status of investor's investment behavior.

The rest of the paper is organized as follows. Section 2 presents a continuous-time representative-agent economy in which a long-lived investor chooses the consumption-investment strategy under a consistent performance constraint. In Section 3 we derive a general optimal policy under this constraint, obtain a closed-form optimal policy in a special case, and then further investigate its features and implications. Section 4

concludes this paper and all proofs are presented in the Appendix.

II. The Economic Setting

Consider a representative agent with initial wealth W_0 at time zero and the following investment opportunities: one is the risk-free asset with constant return $r dt$ over time period $[t, t + dt]$, the other is a risky asset that has a rate of return $\mu dt + \sigma dz(t)$ over time period $[t, t + dt]$, where $z(t)$ is a one-dimensional standard Brownian motion. We assume that $\mu > r$, $c(t)$ is the consumption rate at time t , $\omega(t)$ is the fraction of the wealth that is invested in the risky asset. $W(t)$ is the agent's wealth at time t and governed by

$$dW(t) = rW(t)dt + \omega(t)W(t) [(\mu - r)dt + \sigma dz(t)] - c(t)dt. \quad (30)$$

The expected utility of consumption is defined as

$$\mathbb{E}_0 \int_0^\infty e^{-\rho t} u(c(t)) dt$$

where $\rho > 0$ is the pure rate of time preference and the function $u(x)$ is the felicity function. We consider an optimal dynamic investment and consumption policy in which the admissible policies $\{c(t), \omega(t) : t \geq 0\}$ are required to satisfy: (i) the consumption and investment decisions are adapted; (ii) $c(t) \geq 0, a.s.$ and the cumulative consumption is finite over any finite horizon, i.e., $\int_0^t c(s) ds < \infty, a.s.$; (iii) $W(t) \geq 0, a.s.$; and (iv) $W(t) \geq M(t), a.s.$, for all time t , where $M(t)$ is defined as the weighted average of the whole past wealth path $\{W(s) : 0 \leq s \leq t\}$ as follows.

$$M(t) = M_0 e^{-at} + b \int_0^t e^{-a(t-s)} W(s) ds \quad (31)$$

where $a \geq 0$, $b \geq 0$. We assume that $b \leq r + a$ and $0 \leq M_0 \leq W_0$. This assumption ensures that the set of admissible policies is non-empty and is proved in the Proposition 1.

Among these admissible conditions, (i) - (iii) are standard conditions to remove the doubling arbitrage opportunity (Dybvig and Huang (1988)). The last condition (iv) is the consistent performance constraint on the wealth.¹⁶ It states that the current wealth $W(t)$ is not allowed to fall below an exponential weighted average of wealth from time zero to the current time with a constant multiplier.

In equation (31), parameter a denotes the subjective time preference. As time goes, the recent performance has a higher weight than the remote performance. In one extreme case as $a = \infty$, this constraint is equivalent to $W_t \geq 0$ for all time t . In the other extreme case as $a = 0$, $M(t) = M_0 + b \int_0^t W(s)ds$ is an equally weighted average of the past wealth, that is, the performance at different past time instants has the same effect on the wealth benchmark. At any time instant, the greater value of parameter a , the less weight assigned to the performance and vice versa.

Parameter b denotes the effect of the cumulative historical performance. As $b = 0$, the subsistent level, $M(t) = M_0 e^{-at}$, is deterministic, which implies a guaranteed return rate from time 0 to time t . As $b > 0$, the equation (31) represents a dynamic stochastic benchmark and describes the cumulative effect of the entire historical performance on the current investment strategy.¹⁷

¹⁶In its discrete-time version, this constraint can be written as $W(t) \geq M_0 e^{-at} + bW(1)e^{-a(t-1)} + \dots + bW(t-1)e^{-a}$. In particular, $W(t)/W(t-1) \geq be^{-a}$ for all time t . That is the reason we use the terminology "consistent performance". The constraint (31) takes into account the whole performance path instead of one period performance.

¹⁷Dynamic deterministic benchmark for the portfolio wealth has been studied in El Karoui and Jeanblanc-Picque (1998), and El Karoui, Jeanblanc-Picque and Lacoste (2005). It has been shown

This consistent performance constraint can also be seen as a moderate drawdown control. Grossman and Zhou (1993) study the maximum drawdown constraint, i.e. $W(t) \geq \alpha \max_{0 \leq s \leq t} W_s, \forall t$. Obviously, the maximum drawdown constraint focuses on the extreme historical performance, while the condition (iv) emphasizes a moderate subsistent and consistent performance. To be precise, let $W_{max} = \max_{0 \leq s \leq t} W_s$ and $W_{min} = \min_{0 \leq s \leq t} W_s$, then as $a \neq 0$, equation (31) implies

$$M_0 e^{-at} + \frac{b}{a}(1 - e^{-at})W_{min} \leq M_t \leq M_0 e^{-at} + \frac{b}{a}(1 - e^{-at})W_{max}. \quad (32)$$

From equation (32), we can observe that the subsistent benchmark level is between the maximum and minimum wealth level over time. From the perspective of risk management, as $a \neq 0$, we can rewrite $M(t)$ as

$$M(t) = M_0 e^{-at} + b \left\{ \frac{W(t) - W_0 e^{-at}}{a} - \frac{1}{a} \int_0^t e^{-a(t-s)} dW(s) \right\}, \quad (33)$$

where dW represents the instantaneous wealth profit or loss. Then, as $a > b$, the constraint (iv) can be reformulated as

$$W(t) \geq \frac{aM_0 - bW_0}{a - b} e^{-at} - \frac{b}{a - b} \int_0^t e^{-a(t-s)} dW(s). \quad (34)$$

As $a < b$, the constraint (iv) can be represented as

$$W(t) \leq \frac{bW_0 - aM_0}{b - a} e^{-at} + \frac{b}{b - a} \int_0^t e^{-a(t-s)} dW(s). \quad (35)$$

As $a = b$, the constraint (iv) implies that $W_0 - M_0 \geq - \int_0^t e^{as} dW(s)$. From equations (34) and (35), the consistent dynamic constraint indicates that the current wealth

that, under the dynamic deterministic constraint $W_t \geq L_t$, the optimal strategy is equivalent to a Merton's optimal portfolio plus an American-type put option on Merton's optimal portfolio. See also Grossman and Zhou (1996) when L_t is a constant.

falls in a range with lower and upper bounds, depending on the parameter values of a and b .

From the perspective of asset management, portfolio manager's performance is often tracked over time by his supervisor in practice. The managed portfolio would incur gains or losses at different time instants due to the future investment uncertainty. Thus, the constraint (iv) could offer an appealing benchmark to monitor the portfolio performance and be implemented as an investment strategy for practitioners as well.

In this paper, the optimal admissible policy $\{c(t), \omega(t)\}$ and the associated derived utility are defined by

$$J(W_0, M_0) \equiv \sup_{c(t), \omega(t)} \mathbb{E}_0 \int_0^\infty e^{-\rho t} u(c(t)) dt \quad (36)$$

and it is assumed that $u(c) = \frac{c^\gamma}{\gamma}$, $\gamma < 1$, $\gamma \neq 0$.¹⁸

III. A General Optimal Policy

This section solves the general optimal policy under the consistent performance constraint. By using the solution of a nonlinear ordinary differential equation as an auxiliary function, we present the optimal policy explicitly. Moreover, we find a closed-form optimal policy under the consistent performance constraint in a special case and further investigate its properties and demonstrate its implications.

Proposition 1 *It is assumed that $(b-a)\gamma - \rho < 0$, then there exists a unique optimal*

¹⁸Note that when $\gamma \rightarrow 0$, the felicity function is reduced to be the log-utility. Since the log utility is not homogeneous, the two-argument value function cannot be reduced to one-argument function, hence the PDE could not be transformed to the associated ODE. More technique details are shown in the Appendix.

consumption and trading strategy, where $\{C^*(t), \omega^*(t)\}$ is given by

$$C^*(t) = M(t)f'(u)^{1/(\gamma-1)} \quad (37)$$

and

$$\omega^*(t) = -\frac{\mu - r}{\sigma^2} \frac{f'(u)}{uf''(u)} \quad (38)$$

where $u = \frac{W(t)}{M(t)}$, and the auxiliary function $f(u)$ satisfies the following nonlinear ordinary differential equation with $u \in [1, \infty)$

$$-\frac{1}{2} \frac{(\mu - r)^2}{\sigma^2} \frac{[f'(u)]^2}{f''(u)} + [(bu - a)\gamma - \rho]f(u) + f'(u)u[r - (bu - a)] + \frac{1 - \gamma}{\gamma} [f'(u)]^{\frac{\gamma}{\gamma-1}} = 0 \quad (39)$$

subject to the following boundary conditions:

$$f(1) = \frac{[a + r - b]^\gamma}{\gamma(\rho - (b - a)\gamma)}, \quad (40)$$

$$f'(1) = (a + r - b)^{\gamma-1}. \quad (41)$$

It is noted that we need condition $b \leq a + r$ to ensure the existence of optimal policy, e.g. equation (G-15) in the appendix. Thus, $a + r$ is the upper bound of parameter b . Furthermore, we could find a closed-form optimal policy as $b = a + r$, which is demonstrated by the following corollary.

Proposition 2 *As $b = a + r$, let $f(u) = \frac{h^{\gamma-1}}{\gamma}(u - 1)^\gamma \geq 0$ since for nonnegative consumption, the value function $J(W, M) = M^\gamma f(u) \geq 0$, where*

$$h \equiv \frac{1}{1 - \gamma} \left(\rho + a\gamma - \frac{\gamma(\mu - r)^2}{2(1 - \gamma)\sigma^2} \right) \geq 0, \quad (42)$$

Then there exists a unique optimal policy such that

$$c^*(t) = h(W(t) - M(t)), \quad (43)$$

and

$$\omega^*(t)W(t) = m(W(t) - M(t)) \quad (44)$$

where $m \equiv \frac{\mu-r}{(1-\gamma)\sigma^2} > 0$ and the corresponding derived value function is

$$J(W(t), M(t)) = \frac{h^{\gamma-1}}{\gamma} (W(t) - M(t))^\gamma. \quad (45)$$

This Proposition implies that to meet the consistent performance requirement, the agent first builds a capital cushion, $W(t) - M(t)$, invests m fraction of this cushion into risky asset and consumes a constant percentage h of the cushion, and finally put the remaining amount $W(t) - (h + m)(W(t) - M(t))$ into the risk-free asset. This optimal strategy is similar to the one in other contexts, such as the constant proportional portfolio insurance in Black and Perold (1992), the drawdown constraint in Grossman and Zhou (1993), the ratcheting constraint in Dybvig (1995), and the portfolio insurance in Grossman and Zhou (1996).

Note that as $b = a + r$, $\frac{f'(u)}{f''(u)} = \frac{u-1}{\gamma-1}$, so $\lim_{u \rightarrow 1} \frac{f'(u)}{f''(u)} = 0$. At the boundary in the general case, we have $C^*(t) = M(t)(f'(1))^{\frac{1}{\gamma-1}} = 0$ since $\gamma < 1$ and $\omega^* = -\frac{\mu-r}{\sigma^2(\gamma-1)} \frac{f'(1)}{f''(1)} = 0$, which also match the optimal policy of special case, e.g. equations (43) and (44) in the Proposition 2.

It is interesting to observe that the general optimal policy looks very close to the Merton's optimal policy. For example, one only need to replace the relative risk aversion of Bernoulli utility in the Merton's optimal weight policy with the relative

risk aversion of endogenous function $f(u)$ in the optimal weight policy in the general case. Intuitively, this virtual function $f(u)$ represents the investor's tolerance of wealth drawdown magnitude, i.e. the variable u denotes the ratio of current wealth of subsistent wealth level, implying the potential wealth change magnitude. Furthermore, the first derivative and second derivative of $f(u)$ indicates the changing speed and accelerating speed of wealth tolerance change, which implicitly describes investor's relative risk aversion. In other words, the virtual function $f(u)$ could internalize the wealth constraint and provide valuable information to disclose investor's relative risk aversion.

From the perspective of optimal consumption policy, let $W_m(t)$ be the optimal wealth and $c_m(t)$ be the optimal consumption rate in Merton's model, and then the wealth and consumption dynamics can be described by

$$\frac{dW_m(t)}{W_m(t)} = \left[\frac{r - \rho}{1 - \gamma} + \frac{(2 - \gamma)(\mu - r)^2}{2(1 - \gamma)^2\sigma^2} \right] dt + m\sigma dz(t) \quad (46)$$

and

$$c_m(t) = \frac{1}{1 - \gamma} \left(\rho - r\gamma - \frac{\gamma(\mu - r)^2}{2(1 - \gamma)\sigma^2} \right) W_m(t). \quad (47)$$

Comparing equation (43) with equation (47), when the utility displays less risk aversion than logarithmic utility ($\gamma < 0$), the agent consumes more in no consistent performance case, while when the utility displays more risk aversion than logarithmic utility ($\gamma > 0$), then the agent consumes more in consistent performance case. This observation suggests that as the agent becomes more risk averse and worries about the consistency of his portfolio wealth, he consumes more with the consistent constraint,

but less without the consistent constraint and postpones to realize his utility.

Let M_m be the corresponding subsistent level by equation (31) in Merton's model, then M_m is a combination of the so called Yor's process and a geometrical Brownian motion. Thus, there are always positive probabilities such that $W_m(t) < M_m(t)$. (See Yor (1992) and Panel A in Figure 1.) We can observe from Panel A in Figure 1 that there are always positive probabilities such that the wealth falls below the consistent performance benchmark in Merton's model, while as illustrated in the Panel B of Figure 1, the optimal wealth stays above the consistent performance constraint almost surely. Furthermore, the optimal wealth demonstrates an *upward* trend in the consistent performance case. An explicit characterization of W_t , as shown by Proposition 4 below, explains the reason clearly why the consistent performance is preserved almost surely. We will demonstrate theoretically that subsistent level has a positive growth rate in Proposition 4. Hence, *the optimal portfolio generates an upward trend.*

For comparison purposes, we also plot the maximum drawdown benchmark for non-consistent performance case and consistent performance case in Panel C and Panel D, respectively. As depicted in Panel C, there are positive probabilities such that the maximum drawdown benchmark is violated. On the other hand, the maximum drawdown benchmark is largely satisfied in Panel D. The intuition is that the consistent performance constraint captures the whole historical wealth path and can avoid drastic wealth change in a short time period.

In the general case, however, the function $f(u)$ has to be solved numerically. We can reformulate the second-order initial value differential equation as a system of two

first-order equations as follows

$$f'(u) = y, \quad (48)$$

$$y'(u) = \frac{(\mu - r)^2}{2\sigma^2} y^2 \left[[(bu - a)\gamma - \rho]f(u) + yu(a + r - bu) + \frac{1 - \gamma}{\gamma} y^{\frac{\gamma}{\gamma-1}} \right]^{-1}. \quad (49)$$

The Runge-Kutta method of order 4 can be used to solve this system of first-order equations efficiently. The numerical value for each parameter satisfies the conditions of $b < r + a$ and $(b - a)\gamma - \rho < 0$.

In Figure 32, Panel A shows that as the ratio u of wealth to its subsistent level rises, the weight in risky asset increases. The reason is that as capital cushion becomes larger, it can protect the higher position in the risky asset from potential loss in order to ensure the wealth can always be greater than its consistent performance benchmark, thus the investor tends to invest larger portion in risky assets. This finding is also consistent with the one of special case in which a larger capital cushion indicates a greater weight in risky assets. The effect of the parameter a on the weight in the risky asset is mixed in the general situation, as depicted in the Panel A of Figure 32. Panel B of Figure 32 demonstrates similar patterns for different risk-free rate environments r as parameter a is fixed.

The following proposition gives an upper bound for the instantaneous wealth return rate when the wealth is fairly close to the benchmark in the general case.

Proposition 3 *As the consistent performance benchmark approaches to the wealth, the instantaneous expected return of wealth converges to $b - a$. Precisely,*

$$\lim_{u_t \rightarrow 1} \frac{\mathbb{E} \left[\frac{dW(t)}{W(t)} \right]}{dt} = b - a.$$

By Proposition 3, the instantaneous expected return converges to $b - a$ when the consistent performance benchmark approaches the wealth. As b is bounded by $a + r$, the limit of the expected return is bounded by the risk-free rate. Therefore, the instantaneous expected portfolio return is bounded by the risk-free rate (consistent with the arbitrage-free principle).

III.1 The Cost of Consistent Performance Constraint

We next examine the cost of consistent performance constraint on the investor's derived utility. The derived utility under consistent performance constraint is given by equation (45) and the capital cushion dynamics is described by equation (54). The derived utility for Merton's model is written as $J_m(W_m(t)) = \frac{h_m^{\gamma-1}}{\gamma} W_m^\gamma(t)$, where $h_m = \frac{1}{1-\gamma} \left(\rho - r\gamma - \frac{\gamma(\mu-r)^2}{2(1-\gamma)\sigma^2} \right) > 0$.

By straightforward derivation, we can obtain

$$\begin{aligned} \frac{J(W(t), M(t))}{J_m(W_m(t))} &= \left(\frac{h}{h_m} \right)^{\gamma-1} \left(\frac{W(t) - M(t)}{W_m(t)} \right)^\gamma \\ &= \left(\frac{h}{h_m} \right)^{\gamma-1} \left(\left(1 - \frac{M(0)}{W(0)} \right) e^{(n-n_m)t} \right)^\gamma \end{aligned} \quad (50)$$

where $n_m = \frac{r-\rho}{1-\gamma} + \frac{(2-\gamma)(\mu-r)^2}{2(1-\gamma)^2\sigma^2}$ is the expected return for Merton's model. Clearly, $J(W(t), M(t)) < J_m(W_m(t))$.

When the investor's utility displays more risk aversion than logarithmic utility ($0 < \gamma < 1$), if parameter a increases, then h increases, so by equation (50) the ratio $\left(\frac{h}{h_m} \right)^{\gamma-1}$ decreases. Moreover, if a increases, then n decreases, hence the product $\left(\left(1 - \frac{M(0)}{W(0)} \right) e^{(n-n_m)t} \right)^\gamma$ decreases. Therefore, the utility ratio $\frac{J(W(t), M(t))}{J_m(W_m(t))}$ decreases. In other words, the cost of consistent performance constraint is reduced as a increases.

Similarly, as $\gamma < 0$, if a increases, the cost of consistent performance constraint also increases. Overall, as investor tends to be more risk-averse, higher value of parameter a (less cushion) could reduce the cost of constraint; as investor tends to be less risk-averse, higher value of parameter a could increase the cost of constraint.

III.2 Optimal Wealth Process and Subsistent Level

The following proposition characterizes explicitly the dynamics of optimal wealth and the corresponding consistent performance benchmark.

Proposition 4 *Assume that $W_0 > M_0 > 0$ and a geometrical Brownian motion is given as*

$$Y(t) \equiv Y(0) \exp \left\{ \left(n - \frac{m^2 \sigma^2}{2} \right) t + m \sigma z(t) \right\}, Y(0) = W_0 - M_0.$$

Then the optimal wealth $W^(t)$ is given by*

$$W^*(t) = M_0 e^{rt} + Y(t) + (r + a) \int_0^t e^{r(t-s)} Y(s) ds. \quad (51)$$

The consistent performance benchmark is expressed as

$$M^*(t) = M_0 e^{rt} + (r + a) \int_0^t e^{r(t-s)} Y(s) ds. \quad (52)$$

According to Proposition 4, the optimal wealth is equivalent to a combination of three components: the initial benchmark with a growth rate of risk-free rate r , capital cushion, and a proportion of the cumulative capital cushion with a growth rate of risk-free rate r . Proposition 4 clearly shows that the consistent performance condition is satisfied almost surely and indicates a remarkable point: *the endogenous subsistent*

level is always upward. Specifically, for any time $t_1 < t_2$, equation (52) implies that

$$M^*(t_2) = M^*(t_1)e^{r(t_2-t_1)} + (r+a) \int_{t_1}^{t_2} e^{r(t_2-s)} Y(s) ds > M^*(t_1)e^{r(t_2-t_1)}. \quad (53)$$

and the growth rate of the subsistent level must be greater than the risk-free rate. Therefore, the portfolio wealth demonstrates an upward trend under the consistent performance constraint.

III.3 Probability Distribution of Drawdown Ratio

According to Proposition 2, the dynamics for the capital cushion can be obtained as follows,

$$W(s) - M(s) = (W(t) - M(t)) \exp \left\{ \left(n - \frac{m^2 \sigma^2}{2} \right) (s - t) + m \sigma (z(s) - z(t)) \right\}, \quad (54)$$

where $n \equiv -\frac{\rho+a}{1-\gamma} + \frac{(2-\gamma)(\mu-r)^2}{2(1-\gamma)^2\sigma^2}$ and $s > t$. From equation (54), the capital cushion follows a geometrical Brownian motion with expected return n . Furthermore, as long as the $W_0 > M_0$, the wealth is as great as the consistent performance benchmark almost surely. If at any particular time, the portfolio wealth is identical to the consistent benchmark, say, $W(t) = M(t)$, then the optimal strategy is to put all wealth into the risk-free asset. Moreover, if $n < \frac{m^2 \sigma^2}{2}$, then $W(t) - M(t) \rightarrow 0, a.s.$ as $t \rightarrow \infty$. In other words, the wealth converges to the consistent benchmark almost surely. Thus, it is reasonable to assume that $n \geq \frac{m^2 \sigma^2}{2}$. As a matter of fact, a stronger condition, $n > r + m^2 \sigma^2$, is required to ensure the existence of a stationary distribution, which is shown in Proposition 5 below.

In order to examine the optimal portfolio under the consistence performance constraint in details, we first derive the stationary probability distribution for the draw-

down ratio, and then present the optimal wealth dynamics explicitly. Let $\varphi(t) = \frac{W(t)}{Y(t)} = \frac{W(t)}{W(t)-M(t)}$ denote the drawdown ratio, the ratio of the total wealth to the capital cushion, and $\psi(t) = \frac{M(t)}{W(t)}$ be the ratio of the subsistent level over the current wealth, and then $\varphi(t)$ and $\psi(t)$ can be represented by the following relationship

$$\psi(t) = \frac{\varphi(t) - 1}{\varphi(t)}.$$

The stationary probability distributions for both $\varphi(t)$ and $\psi(t)$ can be obtained by the following proposition.

Proposition 5 *From Proposition 2 and it is assumed that*

$$n - r - m^2\sigma^2 > 0. \quad (55)$$

Then $\varphi(t)$ has a stationary probability distribution with density

$$p_\varphi = \kappa(\varphi - 1)^{\frac{2(r-n)}{m^2\sigma^2}} e^{-\frac{2(a+r)}{m^2\sigma^2} \frac{1}{\varphi-1}}, \quad 1 < \varphi < \infty \quad (56)$$

where

$$\kappa^{-1} = \left[\frac{m^2\sigma^2}{2(a+r)} \right]^{\frac{2(n-r-m^2\sigma^2)}{m^2\sigma^2}+1} \Gamma \left[\frac{2(n-r-m^2\sigma^2)}{m^2\sigma^2} + 1 \right] \quad (57)$$

and $\Gamma(\cdot)$ is the gamma function. The expected mean of $\varphi(t)$ is a constant that is expressed as

$$\mathbb{E}[\varphi] = \frac{a+n-m^2\sigma^2}{n-m^2\sigma^2-r}. \quad (58)$$

The stationary density function of ψ is obtained as

$$p_\psi = p_{\varphi(\psi)} \frac{d\varphi}{d\psi} = \kappa \psi^{\frac{2(r-n)}{m^2\sigma^2}} (1-\psi)^{\frac{2(n-r-m^2\sigma^2)}{m^2\sigma^2}} e^{-\frac{2(a+r)}{m^2\sigma^2} \frac{1-\psi}{\psi}}. \quad (59)$$

The expected drawdown ratio $\mathbb{E}[\varphi] = \frac{a+r}{n-m^2\sigma^2-r} + 1$ shows that the expected draw-

down ratio increases as parameter a increases, implying that the subsistent level rises and the cushion becomes thinner as parameter a increases. Thus, there is less amount of wealth to invest in the risky assets, leading to less expected return. This observation also matches the implication of Proposition 3, that is, the instantaneous expected return decreases as parameter a increases.

From the perspective of constraint cost discussed in section 3.1, as investor becomes more risk averse, he seeks an investment strategy to keep most value of his wealth and tends to invest smaller amount of his wealth in the risky assets, implying the thinner cushion and higher drawdown ratio, that is, higher value of a . Since the consistent performance constraint matches this investor's intention of keeping his wealth safe, the cost of consistent constraint is reduced as parameter a increases. This observation aligns with the implication of the constraint cost discussed in section 3.1 as well.

We could also represent the wealth dynamics and calculate its moments in terms of the probability distribution of drawdown ratio. By Proposition 2 and equation (30), the optimal wealth movement can be described by

$$\frac{dW(t)}{W(t)} = [r + (n + a)(1 - \psi)] dt + m\sigma(1 - \psi)dz(t). \quad (60)$$

Then, we could obtain

$$\frac{\mathbb{E} [dW(t)/W(t)]}{dt} = n + a + r - (n + a) \int_0^1 \psi p_\psi d\psi \quad (61)$$

and

$$\frac{Var [dW(t)/W(t)]}{dt} = (m\sigma)^2 \int_0^1 (1 - \psi)^2 p_\psi d\psi. \quad (62)$$

IV. Conclusion

This paper solves an optimal portfolio choice problem under a consistent performance constraint. This consistent performance constraint represents a "*dynamic consistent return*" which would be attractive in a volatile financial market and have rich practical implications. A remarkable feature of this constraint is to take the entire past return records into account, instead of focusing on the performance at a specific time instant. In particular, the investment return over any time period is greater than a fixed benchmark return under this constraint.

It is noteworthy to compare the consistent performance constraint with the moving average strategy implemented in the technical analysis. Moving average crossover or other geometrical shapes in historical price charts are often employed exogenously to infer the buying or selling signals of risky assets. Zhou and Zhu (2009) examine the optimal portfolio choice among *exogenous* moving average trading strategies on the underlying risky assets. This paper solves the optimal portfolio choice problem under an *endogenous* consistent performance constraint, hence it would be appealing to investigate whether those technical analysis rules are optimal in the setting of portfolio selection under this constraint.

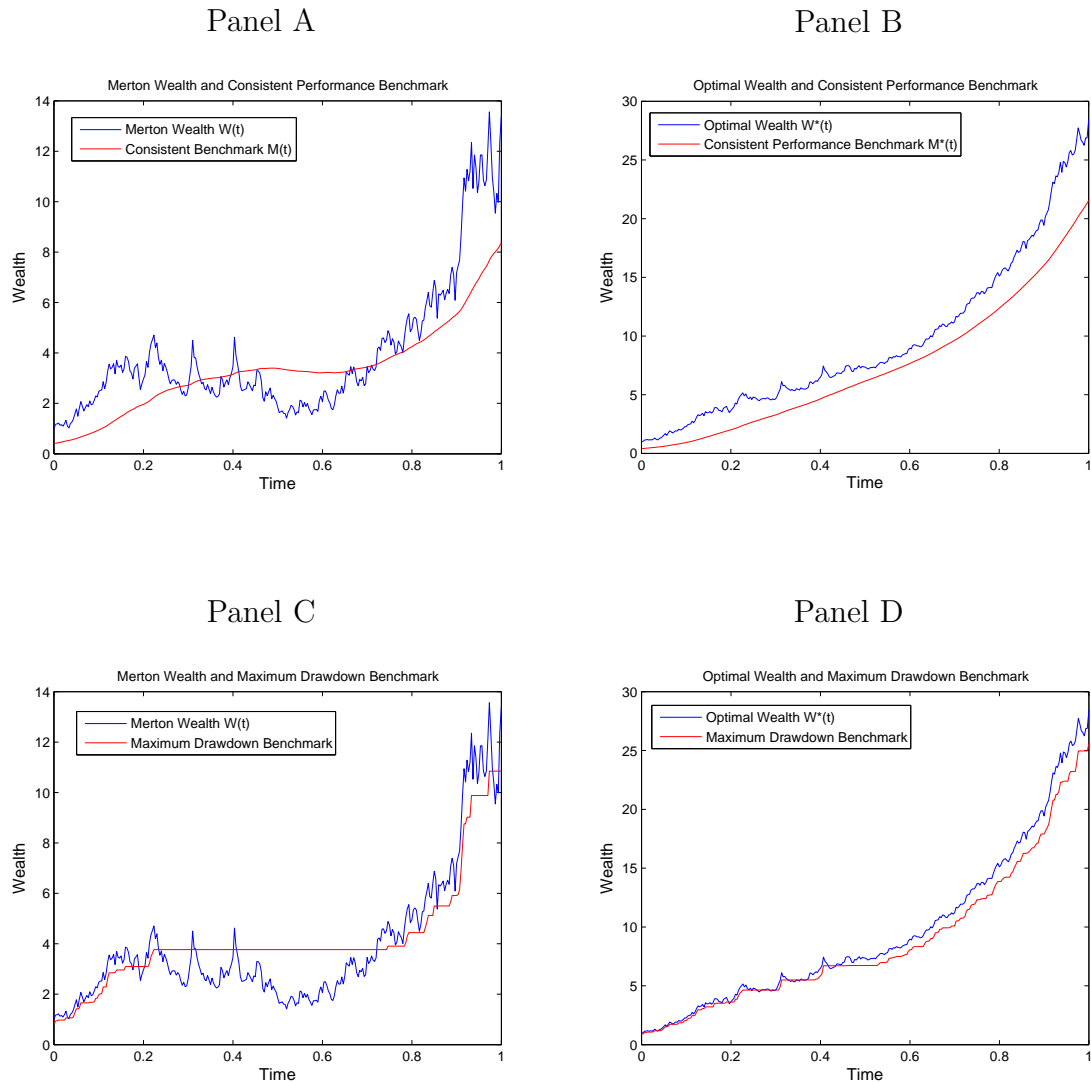


Figure 31: The figure in Panel A depicts wealth process and the consistent performance benchmark in Merton's model. Parameters are: $\mu = 0.07, \sigma = 0.2, r = 0.5\%, \rho = 0.25, \gamma = 0.8$, and $W_0 = 1$. The consistent performance benchmark parameters are chosen as $M_0 = 0.4, a = 0.01, b = r + a = 0.015$. Wealth $W(t)$ is characterized by equation (46) and the consistent performance benchmark $M(t)$ is calculated by equation (H-2). The figure in Panel B depicts the optimal wealth and the consistent performance benchmark. Both optimal wealth $W(t)$ and the consistent performance benchmark $M(t)$ are characterized by Proposition 4. The figures in Panel C and Panel D depict the Merton's wealth process and optimal wealth process with maximum drawdown benchmark $\alpha \max_{0 \leq s \leq t} W_t$, where $\alpha = 80\%$, respectively.

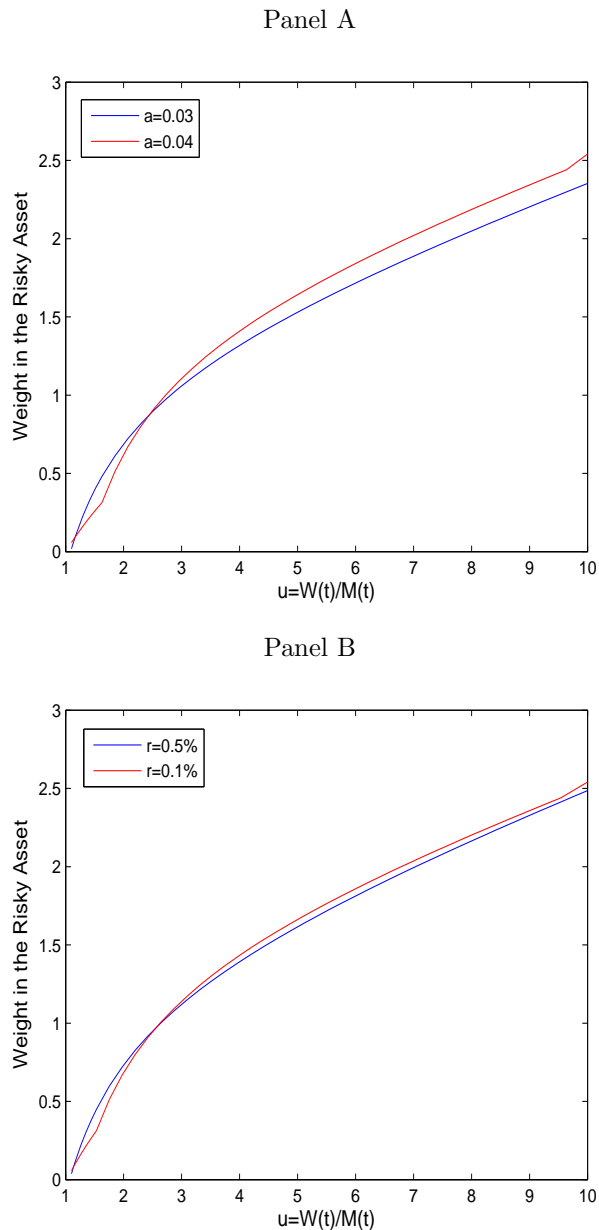


Figure 32: The figure in Panel A depicts the position in risky assets versus the ratio of wealth to the consistent performance benchmark for different values of parameter a . The parameters used in this example are chosen as $\mu = 0.08$, $\sigma^2 = 0.1$, $r = 0.5\%$, $\rho = 0.035$, $\gamma = 0.8$, $b = 0.03$, with $a = 0.03$ and 0.04 , respectively. The figure in Panel B depicts the position in risky assets versus the ratio of wealth to the consistent performance benchmark for different values of parameter r . The parameters used in this example are: $\mu = 0.08$, $\sigma^2 = 0.1$, $\rho = 0.035$, $\gamma = 0.8$, $a = 0.03$, $b = 0.03$, with $r = 0.5\%$ and 1% , respectively.

CHAPTER 3: WHAT MATTERS MOST? IT'S THE CONSISTENCY!

I. Introduction

What matters most in asset management? It's not delivering high returns in a short time period. Instead, it's about generating stable returns consistently over time including both expanding and contracting economy. It is not unusual to hear about the stories of the rise and fall of star funds in the past several decades. Investors gradually appreciate the value of consistent performance in the long run instead of chasing short-term pleasure. As John C. Bogle addresses it: *There is an important role that past performance can play in helping you to make your fund selections. While you should disregard a single aggregate number showing a fund's past long-term return, you can learn a great deal by studying the nature of its past return. Above all, look for consistency.* (Bogle, 1999).

How to implement an investment strategy to obtain a consistent performance? In Chapter 2, we propose a consistent performance strategy in an optimal portfolio choice setting. The key ingredient in this consistent performance strategy is a so called "consistent performance constraint", that is, $w_t \geq m_t$ for all time t , where w_t is the wealth at time t and m_t is a moving average of the wealth path from starting date to current date t . The consistent performance strategy is the optimal one among all alternatives given the consistent benchmark constraint. There are three notable

features by following the consistent performance strategy: (1) The investors could achieve a consistently stable return of portfolio wealth, more precisely, $w_{t+1}/w_t \geq c$ for all time t and c is a positive constant number; (2) $m_{t+1}/m_t > r$ for all time t and r is a constant risk-free interest rate. Both features demonstrate the “upward” trend of the wealth portfolio. Moreover, (2) ensures that the growth rate of the benchmark beats the interest rate; (3) This strategy demonstrates a *capital protection and low volatility* oriented investment philosophy, which could have rich implications for various types of asset management funds, i.e., pension funds, endowment funds, mutual funds and so on.

II. The Consistent Performance Strategy (CPS)

To illustrate the consistent performance strategy (see Appendix for its details), we use a traditional intertemporal asset allocation policy as a benchmark. The traditional intertemporal asset allocation policy is to consume a *constant proportion* of wealth and invest a *constant proportion* of wealth in a risky asset, i.e., an index or exchange-trade-fund (ETF). As shown in Panel A of Figure 33, the portfolio wealth generated from the traditional intertemporal policy has a high likelihood to fall below the consistent benchmark. In other words, the consistent benchmark constraint is not satisfied under a traditional portfolio choice setting.

By contrast, the graph in Panel B of Figure 33 shows that the portfolio wealth following the consistent performance strategy could always stay above the consistent performance benchmark. The consistent performance strategy is implemented as follows: an investor first builds a wealth cushion $w_t - m_t$, where m_t is a weighted average

of the historical wealth records $\{w_s; 0 \leq s \leq t\}$, invests a constant proportion of this cushion in the risky asset, consumes another constant proportion of this cushion, and then puts the remaining amount into a risk-free asset. In addition, the investor has many options to construct this strategy according to his own investment perception and risk appetite.

Intuitively, this consistent performance strategy could be viewed as a capital-protection and steady-growth oriented strategy. To illustrate it, Figure 34 depicts the trading positions on assets in one possible wealth scenario. Panel A of Figure 34 shows that the traditional investment strategy is to borrow from riskless asset and invest the proceeds into the risky asset. In the long run, the amount of investment in risky asset declines over a 30-year span associated with decreasing total portfolio wealth, as shown in Panel A of Figure 35. The borrowing peak occurs around the sixth year as the total portfolio value hits record high. Despite the total portfolio wealth starts to decline, the conventional strategy still suggests borrowing the riskless bond and invest them in the risky asset. On the other hand, in Panel B of Figure 34, the consistent performance strategy implies that the investor stops borrowing from riskless bond at the early years of the investment horizon and then gradually reduces the investment in the risky asset although the total portfolio wealth achieves the highest value around the sixth year.

The dynamic consumption rule is displayed in Figure 35. In Panel A of Figure 35, the consumption is always a constant proportion of portfolio wealth by construction. In contrast, as shown in Panel B of Figure 35, the dynamics of portfolio wealth and consumption rule have different shapes since the agent consumes only a constant

proportion of the buffer instead of the wealth itself. Note that the wealth buffer tends to shrink over time as shown in Panel B of Figure 33, implying a larger position in risky asset and higher spending at the early stage of investing and then a reduced position in risky asset and less consumption at the later stage of investing. Through this investment process, the agent always invests and consumes some constant portion of the capital buffer and then puts the remaining capital into riskless asset. Having capital buffer is crucial in this strategy in order to reduce future uncertainty and obtain stable wealth growth and also the key difference from the traditional investing strategy.

To compare the consistent performance strategy and the traditional strategy in a more intuitive way we plot the comparisons of consumption and risky investment position for traditional and consistent strategies, respectively in Figure 36. Panel A shows the consumption difference between these two strategies. It's interesting to see that the consistent performance requirement doesn't sacrifice investor's consumption, but in fact can provide a relatively higher spending budget than the traditional strategy. The stable cash flows from riskless bond investment could make a difference, in comparison to the aggressive investment in the risky asset from a traditional strategy. Panel B of Figure 36 can further shed light on the causes: The traditional investment shorts a large amount of riskless bond and invests them in the risky asset, as the investment suffers the setbacks, the total portfolio wealth also declines since there is no other sources to offset the losses, hence the consumption drops accordingly; on the other hand, the consistent performance strategy instead of putting all money in the risky asset but constantly invests a certain amount of wealth in the riskless asset to

generate a steady stream of cash flows for spending.

II.1 Portfolio Performance

We now demonstrate the portfolio performance in terms of its expected return, variance, Sharpe ratio and leverage. The corresponding parameters calibration is explained in Appendix. Table 11 reports the expected return, variance, Sharpe ratio and leverage of the portfolio when the tuning parameter a changes from 0.005 to 0.05. In the top of Table 11, we study the case as $r = 1.817\%$ and in the bottom investigate the case as $r = 1.5\%$. When $r = 1.817\%$, as shown in Table 11, the expected gross return moves around 2.016% as $a \in [0.005, 0.05]$. The expected mean of the return rate tends to decrease as a increases. The intuition is that low value of a leads to a flatter consistent performance benchmark, so the investor has more freedom to meet the constraint by investing larger position in risky asset and thereby increasing the expected return rate of the wealth. Similarly, rising a leads to a decreasing expected return rate of the wealth and a decreasing variance of the return rate as well.

A remarkable point is that the variance of the return rate drops more significantly with respect to the expected return rate, as a consequence, the corresponding Sharpe ratio measure increases. In fact, the Sharpe ratio can be as large as 1.74 when a is chosen as 0.05. Therefore, the consistent constraint on the wealth indeed improves the performance of the portfolio return under several portfolio performance measures. From the perspective of Sharpe ratio measure, the proposed consistent performance strategy generates a robust "*low risk and high return*" trading strategy for a relatively steeper benchmark curve. If the interest rate drops to $r = 1.5\%$, the risky asset

becomes more attractive as the risk-free rate is lower. Hence both instantaneous expected mean rate and variance rate increase associated with increasing Sharpe ratio.

II.2 Leverage Position

The investment in the risky asset is a constant, k (see Appendix), proportion of the capital buffer. Thus, the portfolio weight of the total wealth in the risky asset is $\alpha_t \equiv k(1 - m_t/w_t)$. If $k \leq 1$, then $0 < \alpha_t < 1$. Then there is no short position in the risky asset and risk-free asset. If the expected return of the risky asset is large enough, or the volatility is sufficiently low, or the investor is less risk-averse, then the proportion k can be greater than one, implying a short position. So the weight α_t can be greater than one and the investor has a leverage position by borrowing.

We explain under what conditions the leverage position exists in average, i.e., $E[\alpha_t] > 1$, where $E[\cdot]$ denotes the expectation and the associated probability distribution function is shown in Proposition 5 in Chapter 2. The last column in Table 11 reports the expected value of the weight in risky assets, $E[\alpha_t]$ with respect to a in two different scenarios of interest rate: $r = 1.817\%$ and 1.5% . As shown from Table 11, as a increases, $E[\alpha_t]$ decreases regardless of the value of interest rate. The intuition is the same as that in the last section. The smaller value of parameter a means the investor tends to have a larger position in risky investment, that is, $E[\alpha]$ increases with decreasing a . When the interest rate drops, from $r = 1.817\%$ to $r = 1.5\%$, the risky asset becomes more attractive, so $E[\alpha_t]$ increases. Our numerical result reported in Table 11 supports this intuition. Indeed, as interest rate drops the investor tends

to borrow cheaper capitals to finance their risky leverage positions.

III. The Implementation of CPS

The consistent performance strategy can be implemented as follows.

Step 1: Calibrate parameters and construct the consistent performance benchmark.

Step 2: Calculate the capital cushion between the current portfolio wealth and benchmark.

Step 3: Invest a fixed portion of the capital cushion in the risky assets.

Step 4: Consume a fixed portion of the current capital cushion.

Step 5: Invest the remaining capital in the riskless bond.

Step 6: Go to step 2 for next time period investment.

III.1 The Effect of Parameter a

Panel A of Figure 37 shows that as parameter a increases, the capital cushion presents a steeper downward trend, implying that the average capital cushion tends to decrease. The drawdown ratio is defined as the ratio of portfolio wealth to the capital cushion. A larger drawdown ratio implies a smaller capital cushion and thereby less investment in risk asset and consumption, and it can be shown that the average value of drawdown ratio is positively related to the parameter a . Hence, as parameter a increases, the average drawdown ratio increases, and therefore the capital cushion drops in average and thereby a steeper downward slope for capital cushion. From another perspective, a greater value of parameter a , a steeper upward slope for consistent performance benchmark, implying the agent allocates more wealth into riskless bond. Hence, the choice of parameter a depends on the agent's individual risk pref-

erence and his priority of capital safety, and it can be determined in a similar way as for parameter γ shown in the Appendix.

On the other hand, the consumption portion h increases as a rises presented in the Appendix. Thus, the overall effect of increasing a on the spending amount is determined by the tradeoff from decreasing capital cushion and increasing consumption portion. Panel B of Figure 37 indicates that the effect of increasing consumption proportion dominates the effect of shrinking capital cushion, that is, as a increases, the amount of consumption also increases. In other words, the consumption portion h is more sensitive to parameter a than capital cushion.

Panel A of Figure 38 shows the investment in the risky asset for different values of a . It can be seen that the graph has a similar pattern as Panel A of Figure 37, since the proportion to invest in the risky asset is a fixed amount of capital cushion regardless of parameter a . Thus, as parameter a increases, the investment in risky asset in average has a steeper downward slope. On the other hand, Panel B of Figure 38 suggests that as a increases, the capital cushion decreases and the investment amount in risky asset drops, so the amount in riskless bond increases. Therefore, the parameter a can be intuitively thought as the extent of priority of "*capital-protection*". A more capital-protection oriented investor may require a higher value of parameter a .

III.2 The Effect of Volatility

Panel A of Figure 39 shows that as the volatility increases, the average capital cushion increases in general. Where does the incremental capital cushion go? Panel

B of Figure 39 shows that the consumption budget increases as volatility rises since the consumption portion is positively related to the volatility. On the other hand Panel A of Figure 40 implies that the agents reduces the investment amount in the risky asset. As the constant investment proportion m in the risky asset is negatively related to the volatility, but at the same time the risky asset investment is positively correlated with capital cushion. Hence, the investment amount in risky asset is determined by the tradeoff from increasing capital cushion and decreasing investment portion. The graph shows that the effect of decreasing investment portion in risky asset dominates the effect of increasing capital cushion. In other words, the investment portion in risky asset is more sensitive to volatility than capital cushion.

Because the incremental consumption only consists of a marginal proportion of the incremental capital cushion and the investment in risky asset drops, the remaining incremental capital flows into the riskless bond as demonstrated in Panel B of Figure 40. In other words, the agent under consistent performance constraint chooses the safe bet and at the same time slightly raises the quote for spending budget, implying that the joy derived from the realized consumption as to the agent outweighs the potential gain from the risky investment in front of high uncertainties. Furthermore, it demonstrates the "*low-volatility*" preference feature of the proposed consistent performance strategy.

III.3 The Effect of Risk Aversion

As Panel A of Figure 41 shown, as the agent becomes more risk-averse, he requires more capital cushion. The capital cushion depends on the investing opportunities

and investor's risk preference. Based on the past 30 years market characteristics, it's interesting to see that the investor needs to increase the capital cushion and thereby puts more portfolio wealth into the risky asset since the risky asset investment portion m is positively related to the risk-aversion as demonstrated in Panel A of Figure 42.

The consumption amount depends on the combined effect from the consumption proportion h and capital cushion. Panel B of Figure 41 implies that the agent consumes more as he becomes risk-averse, which is similar to the case of increasing volatility. On the other hand, as the agent becomes more risk-averse, at the first few years of the investing horizon he tends to short the riskless bond and later on steadily invests in the riskless bond. As indicated by Panel B of Figure 42, the upward slope is steeper as he becomes more risk-averse. This experiment discloses an interesting implication that based on the past 30 years market characteristics, an investor with a capital-protection oriented mind needs more participation in the equity market in order to generate a return that is greater than the risk-free rate.

VI. Conclusion

We introduce a consistent performance strategy that could generate consistently growing portfolio wealth. An attractive feature of this strategy is its upward growing trend of the portfolio wealth in spite of good or bad times in the market. Another distinctive difference of consistent strategy from the traditional investing strategies is that the consistent strategy saves a capital cushion first and both the investment in risky asset and consumption activities derive from the capital buffer. Moreover, the growth rate of this capital buffer is greater than the risk-free rate as well. Overall,

this consistent performance strategy can be viewed as a capital-protection and low-volatility oriented investing strategy which could have appealing features and rich implications for practical investors.

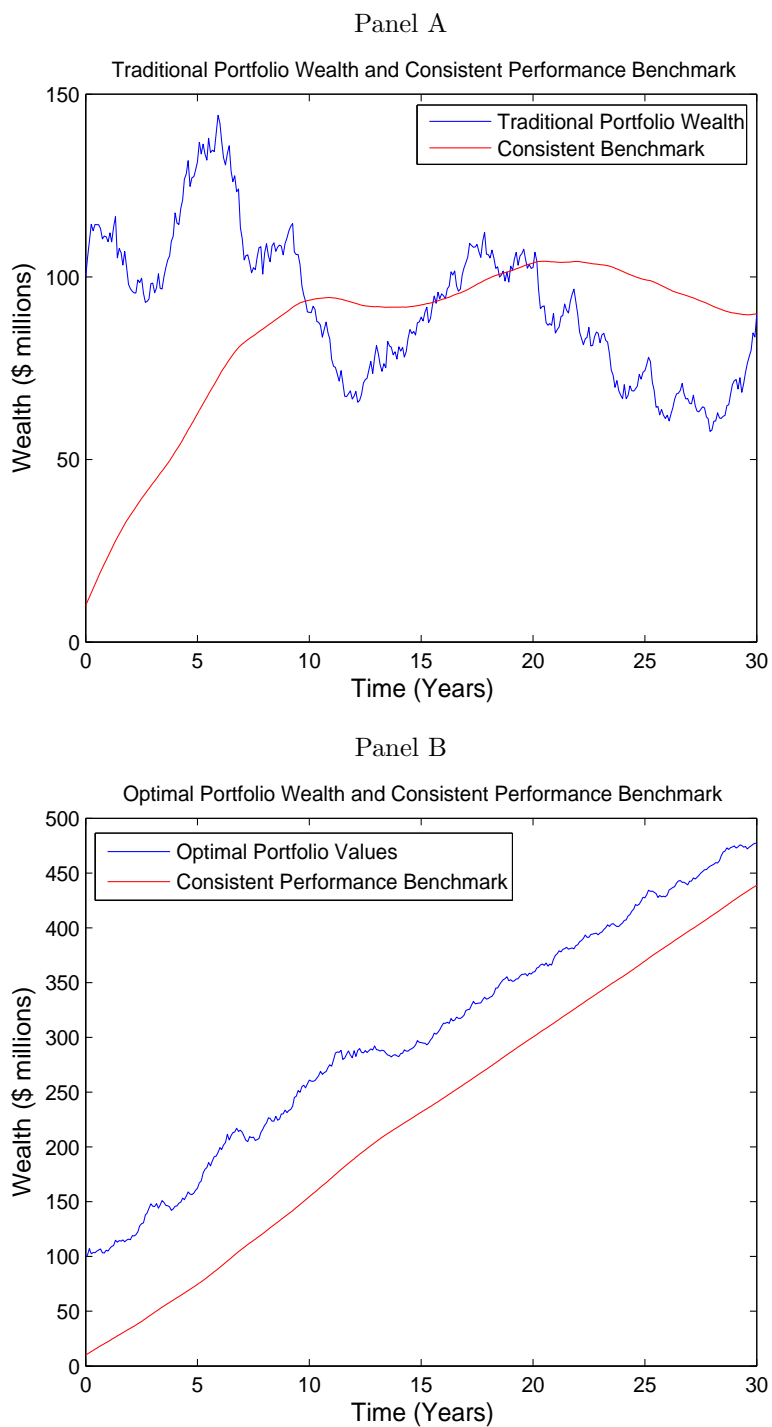


Figure 33: The figure in Panel A depicts the dynamics of portfolio wealth under traditional intertemporal policy. The parameters used in this example are chosen as $\mu = 6.46\%$, $\sigma = 18.35\%$, $r = 1.817\%$, $\rho = 0.05$, $\gamma = 0.3$, $a = 0.01$. The figure in Panel B depicts the optimal wealth dynamics under the consistent performance constraint with the same parameters.

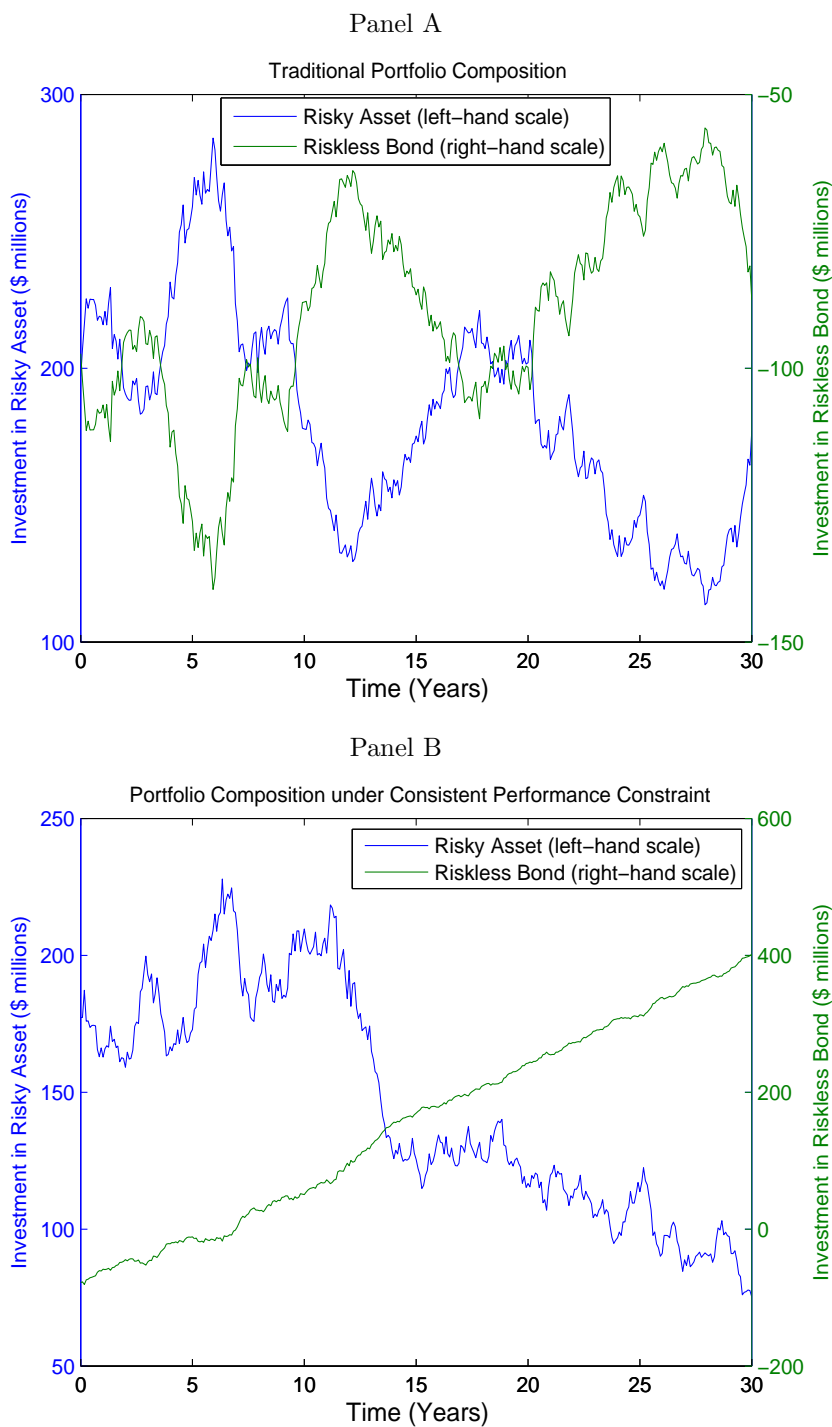


Figure 34: The figure in Panel A depicts the composition of portfolio wealth under traditional intertemporal policy. The parameters used in this example are chosen as $\mu = 6.46\%$, $\sigma = 18.35\%$, $r = 1.817\%$, $\rho = 0.05$, $\gamma = 0.3$, $a = 0.01$. The figure in Panel B depicts the composition of portfolio under the consistent performance constraint with the same parameters.

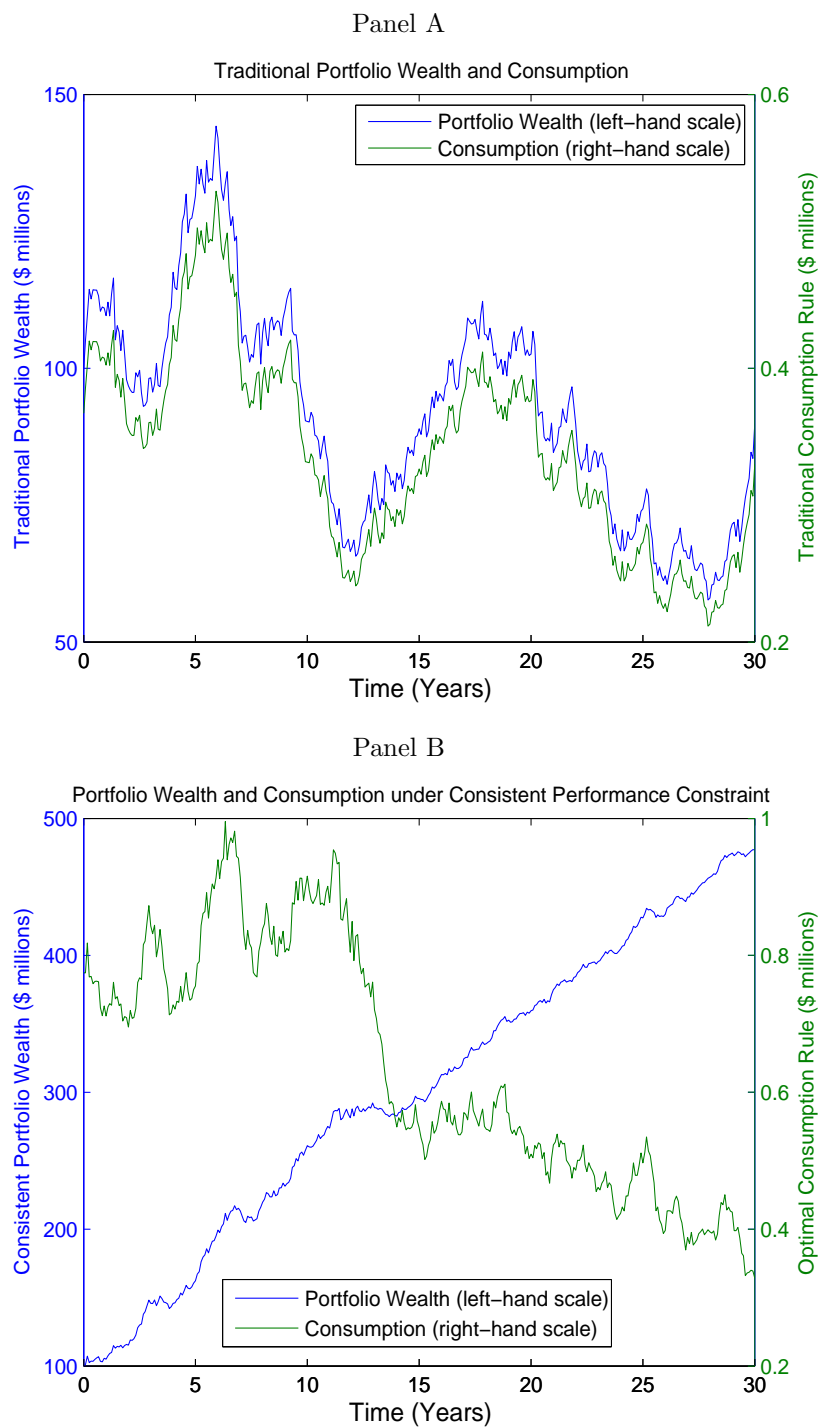


Figure 35: The figure in Panel A depicts the dynamics of portfolio wealth and consumption rule under traditional intertemporal policy. The parameters used in this example are chosen as $\mu = 6.46\%$, $\sigma = 18.35\%$, $r = 1.817\%$, $\rho = 0.05$, $\gamma = 0.3$, $a = 0.01$. The figure in Panel B depicts the dynamics of portfolio wealth and consumption under the consistent performance constraint with the same parameters.

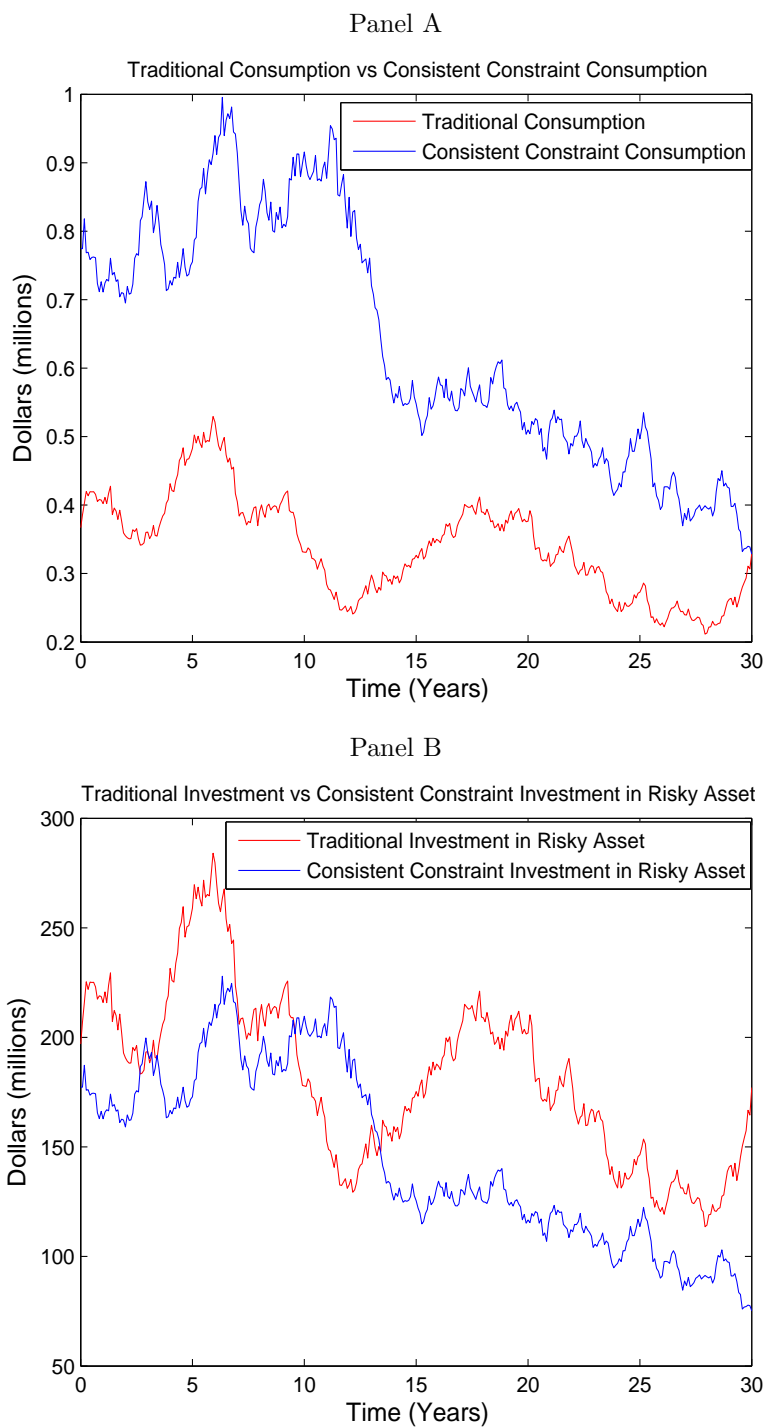


Figure 36: The figure in Panel A depicts the comparison of traditional consumption policy and the optimal consumption policy under consistent performance constraint. The parameters used in this example are chosen as $\mu = 6.46\%$, $\sigma = 18.35\%$, $r = 1.817\%$, $\rho = 0.05$, $\gamma = 0.3$, $a = 0.01$. The figure in Panel B depicts the comparison of traditional investment policy in the risky asset and the one under consistent performance constraint with the same parameters.

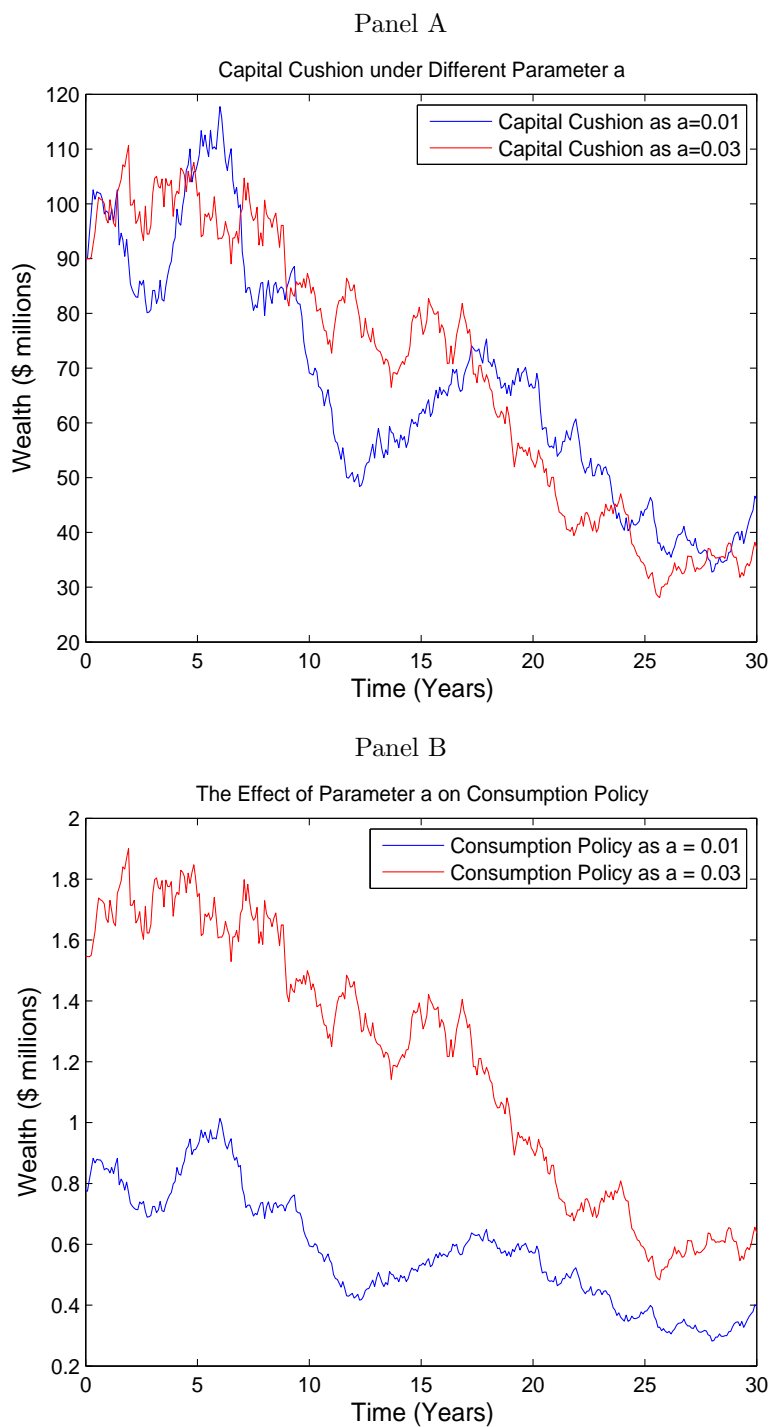


Figure 37: The figure in Panel A depicts the capital cushion under the consistent performance constraint for different values of parameter a . Other parameters used in this example are chosen as $\mu = 6.46\%$, $\sigma = 18.35\%$, $r = 1.817\%$, $\rho = 0.05$, $\gamma = 0.3$. The figure in Panel B depicts the optimal consumption policy under the consistent performance constraint with the same parameters.

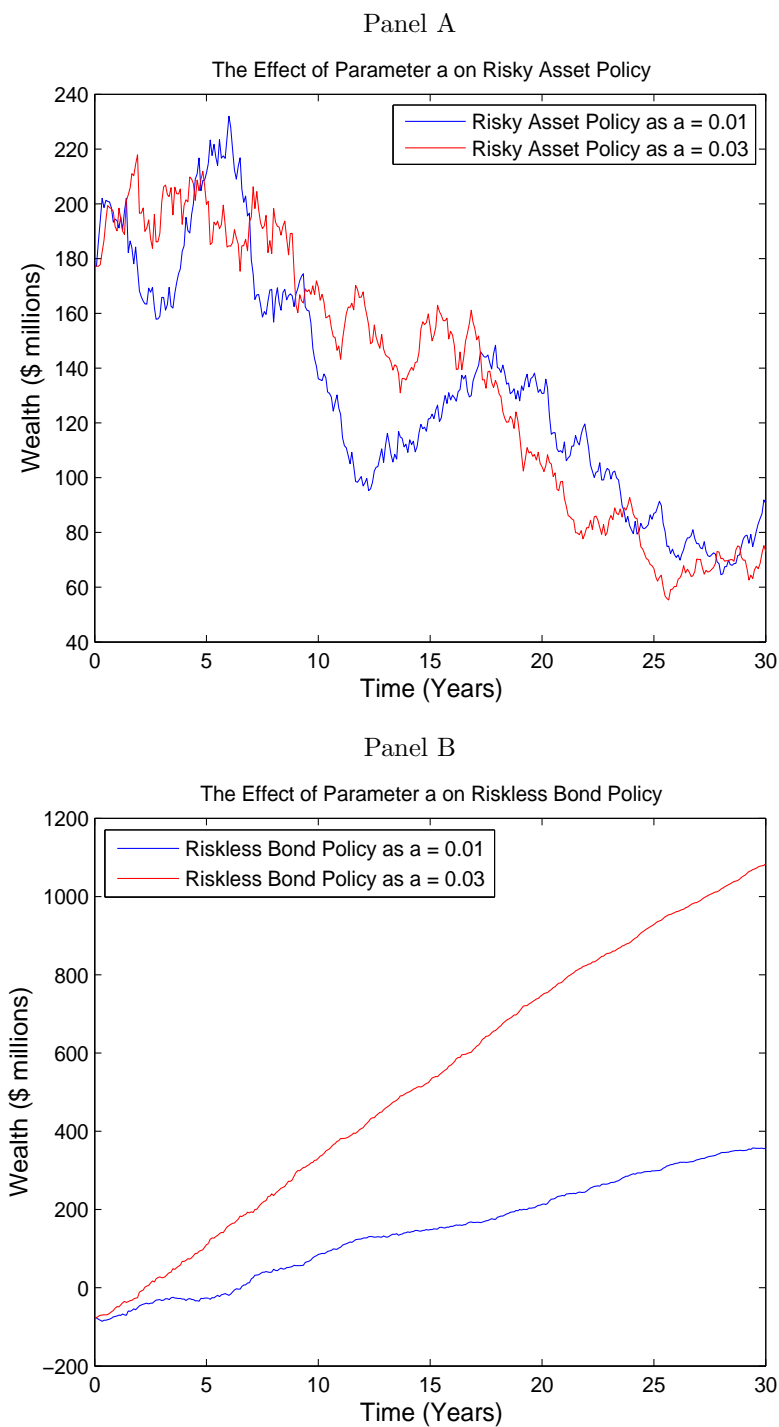


Figure 38: The figure in Panel A depicts optimal risky asset investment policy under the consistent performance constraint for different values of parameter a . Other parameters used in this example are chosen as $\mu = 6.46\%$, $\sigma = 18.35\%$, $r = 1.817\%$, $\rho = 0.05$, $\gamma = 0.3$. The figure in Panel B depicts optimal riskless investment policy under the consistent performance constraint with the same parameters.

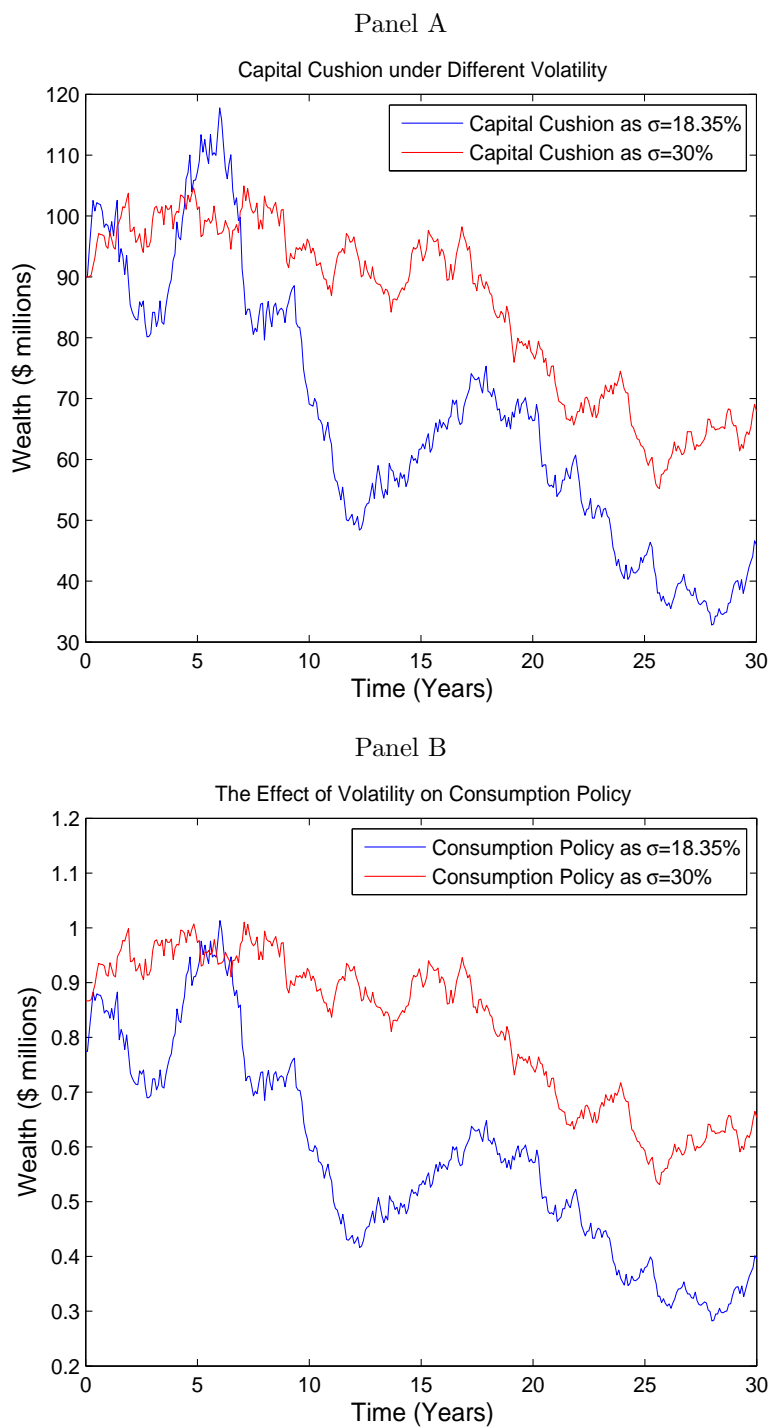


Figure 39: The figure in Panel A depicts the capital cushion under the consistent performance constraint for different volatility values. Other parameters used in this example are chosen as $\mu = 6.46\%$, $r = 1.817\%$, $\rho = 0.05$, $\gamma = 0.3$, $a = 0.01$. The figure in Panel B depicts the optimal consumption policy under the consistent performance constraint with the same parameters.

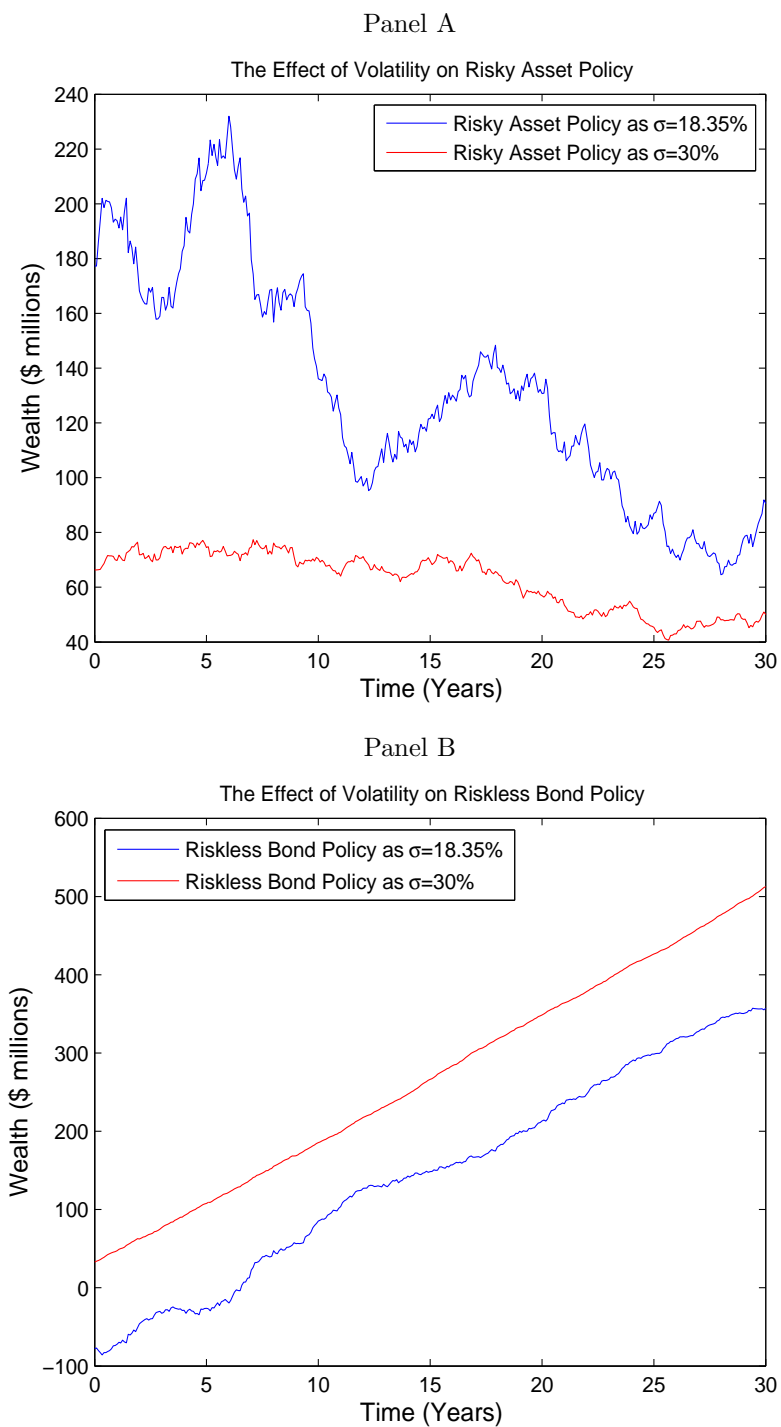


Figure 40: The figure in Panel A depicts optimal risky asset investment policy under the consistent performance constraint for different volatility values. Other parameters used in this example are chosen as $\mu = 6.46\%$, $r = 1.817\%$, $\rho = 0.05$, $\gamma = 0.3$, $a = 0.01$. The figure in Panel B depicts optimal riskless investment policy under the consistent performance constraint with the same parameters.

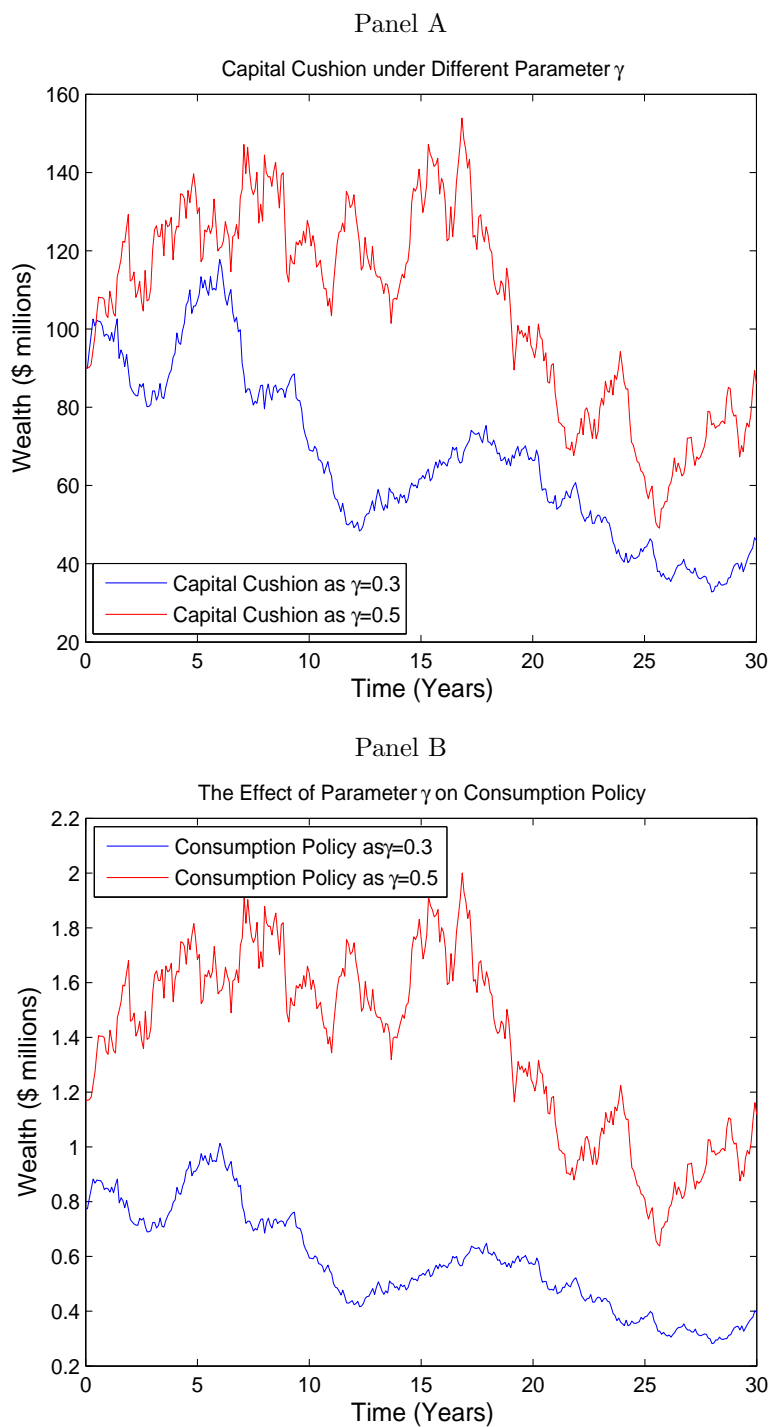


Figure 41: The figure in Panel A depicts the capital cushion under the consistent performance constraint for different values of parameter γ . Other parameters used in this example are chosen as $\mu = 6.46\%$, $\sigma = 18.35\%$, $r = 1.817\%$, $\rho = 0.05$, $a = 0.01$. The figure in Panel B depicts the optimal consumption policy under the consistent performance constraint with the same parameters.

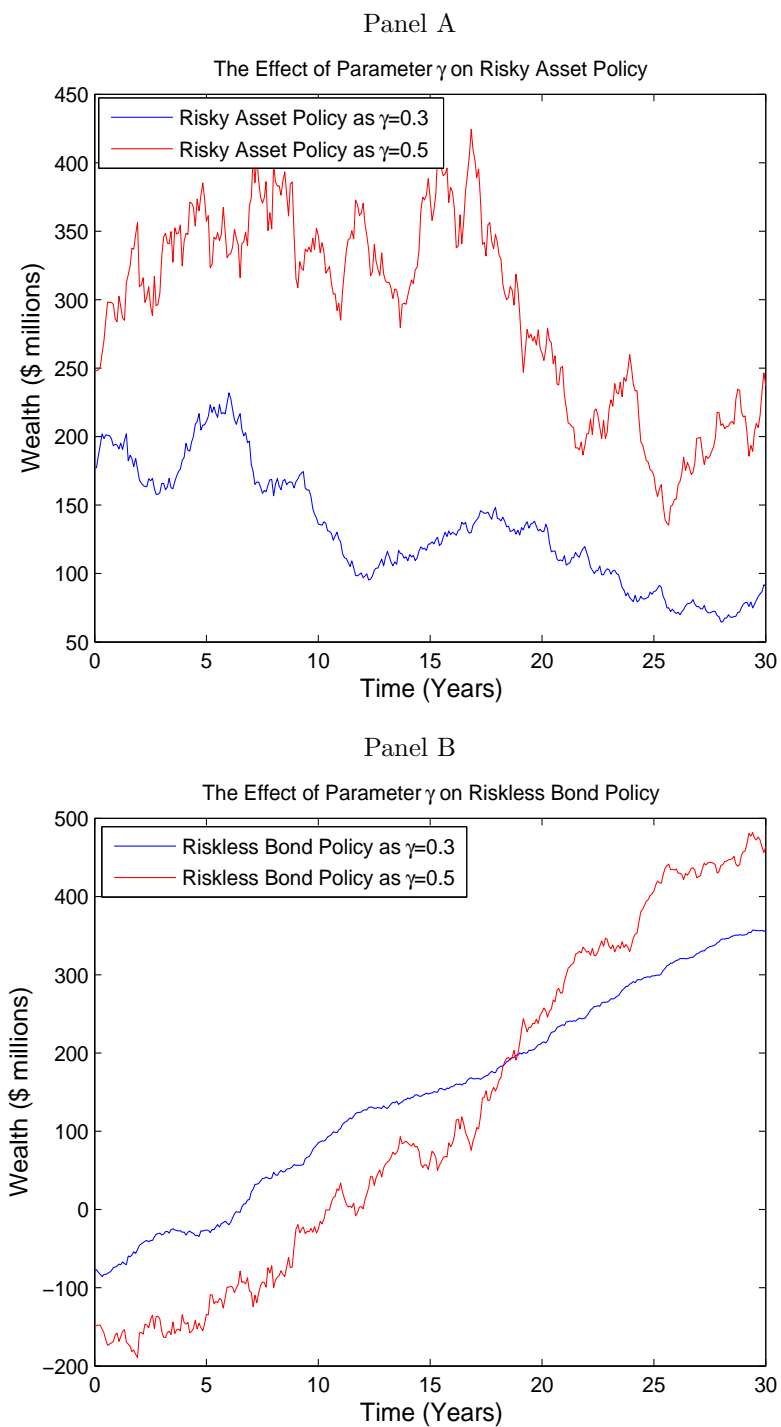


Figure 42: The figure in Panel A depicts optimal risky asset investment policy under the consistent performance constraint for different values of parameter γ . Other parameters used in this example are chosen as $\mu = 6.46\%$, $\sigma = 18.35\%$, $r = 1.817\%$, $\rho = 0.05$, $a = 0.01$. The figure in Panel B depicts optimal riskless investment policy under the consistent performance constraint with the same parameters.

Table 11: Measures of the portfolio performance under consistent performance constraint

This table reports the expected return rate, variance, Sharpe ratio and leverage position when $r = 1.817\%$, and $r = 1.5\%$, respectively.

$r = 1.817\%$				
a	Expected return	Standard deviation	Sharpe ratio	Leverage
0.005	2.0168%	0.3105%	0.6434	0.7743
0.010	2.0166%	0.2607%	0.7656	0.6481
0.015	2.0165%	0.2248%	0.8875	0.5574
0.020	2.0165%	0.1974%	1.0103	0.4889
0.025	2.0164%	0.1763%	1.1316	0.4355
0.030	2.0164%	0.1591%	1.2533	0.3925
0.035	2.0164%	0.1450%	1.3754	0.3573
0.040	2.0164%	0.1331%	1.4975	0.3279
0.045	2.0163%	0.1231%	1.6196	0.3030
0.050	2.0163%	0.1144%	1.7417	0.2815
$r = 1.5\%$				
a	Expected return	Standard deviation	Sharpe ratio	Leverage
0.005	2.0191%	0.7439%	0.6978	2.0118
0.010	2.0182%	0.6248%	0.8295	1.6826
0.015	2.0178%	0.5385%	0.9613	1.4462
0.020	2.0174%	0.4731%	1.0936	1.2681
0.025	2.0172%	0.4219%	1.2258	1.1292
0.030	2.0170%	0.3807%	1.3580	1.0177
0.035	2.0169%	0.3467%	1.4908	0.9263
0.040	2.0168%	0.3185%	1.6227	0.8500
0.045	2.0167%	0.2944%	1.7549	0.7853
0.050	2.0166%	0.2738%	1.8871	0.7297

REFERENCES

- Aguilar, O., and M. West, 2000 July, Bayesian Dynamic Factor Models and Portfolio Allocation, *Journal of Business and Economic Statistics* 18(3), 338-357.
- Andersen, T., L. Benzoni, and J. Lund, 2002 June, An Empirical Investigation of Continuous-Time Equity Return Models, *Journal of Finance*, Vol. LVII, No. 3, 1239-1284.
- Ang, A., and G. Bekaert, 2007, Stock Return Predictability: Is It There?, *Review of Financial Studies* 20(3), 651-707.
- Avramov, D., 2002, Stock Return Predictability and Model Uncertainty, *Journal of Financial Economics* 64, 423-458.
- Barberis, N., 2000, Investing for the Long Run When Returns Are Predictable, *Journal of Finance* 55, 225-264.
- Basak, S., and A. Shapiro, 2001, Value-at-Risk Based Risk Management: Optimal Policies and Asset Prices, *Review of Financial Studies* 14, 371-405.
- Bengtsson, T., P. Bickel, and B. Li, 2008, Curse-of-Dimensionality Revisited: Collapse of the Particle Filter in Very Large Scale Systems *Probability and Statistics: Essays in honor of David Freedman*, 316-334.
- Bernanke, B. S., and J. Boivin, 2003, Monetary Policy in a Data-rich Environment, *Journal of Monetary Economics* 50, 525-546.
- Bernanke, B. S., J. Boivin, and P. Elias, 2005 February, Measuring the Effects of Monetary Policy: A Factor-Augmented Vector Autoregressive (FAVAR) Approach. *Quarterly Journal of Economics* 120, 387-422.
- Black, F., and R. Litterman 1991, Asset Allocation: Combining Investor Views with Market Equilibrium, *Journal of Fixed Income* 1(2), 7-18.
- Black, F., and A. Perold, 1992, Theory of Constant Proportion Portfolio Insurance, *Journal of Economic Dynamics and Control* 16, 403-426.
- Bogle J., 1999, *Common Sense on Mutual Funds - New Imperatives for the Intelligent Investor*, John Wiley and Sons, Inc., New York.
- Bollerslev, T., 1990, Modelling the Coherence in Short-run Nominal Exchange Rates: A Multivariate Generalized ARCH Approach, *Review of Economics and Statistics* 72, 498-505.

- Bouchard B., Elie, R. and C. Imbert, 2012 Optimal Control under Stochastic Target Constraints. *SIAM Journal on Control and Optimization* 48(5), 3501-3531.
- Boudoukh, J., M. Richardson, and R.F. Whitelaw 2008, The Myth of Long-Horizon Predictability, *Review of Financial Studies* 21(4), 1577-1605.
- Boyle, P., and W. Tian, 2007, Portfolio Choice with Constraints. *Mathematical Finance* 17, 319-343.
- Boyle, P., and W. Tian, 2009, Optimal Design of Equity-Linked Structured Products with a Probabilistic Constraint. *Scandinavian Actuarial Journal* 4, 253-280.
- Brandt, M. W., A. Goyal, P. Santa-Clara, and J. R. Stroud 2005, A Simulation Approach to Dynamic Portfolio Choice with an Application to Learning About Predictability, *Review of Financial Studies* 18, 831-873.
- Brennan, M., Cheng, X., and F. Li, 2012, Agency and Institutional Investment. *European Financial Management* 18 (1), 1 - 27.
- Carter, C. K., and R. Kohn, 1994, On Gibbs Sampling for State Space Models, *Biometrika* 81(3), 541-553.
- Chan, L. K.C., J. Karceski, and J. Lakonishok, 1998, The Risk and Return From Factors, *Journal of Financial and Quantitative Analysis* 33(2), 159-188.
- Chib, S, and E. Greenberg, 1995, Understanding the Metropolis-Hastings Algorithm, *The American Statistician* 49, 327-335.
- Chib, S, and E. Greenberg, 1998, Analysis of Multivariate Probit Models, *Biometrika* 85(2), 347-361.
- Chib, S, F. Nardari, and N. Shephard, 2006, Analysis of High Dimensional Multivariate Stochastic Volatility Models, *Journal of Econometrics* 134, 341-371.
- Cogley, T., and T. Sargent, 2005, Drifts and Volatilities: Monetary Policies and Outcomes in the Post WWII U.S., *Review of Economic Studies* 8, 262-302.
- Constantinides, G, 1990, Habit Formation: A Resolution of the Equity Premium Puzzle, *Journal of Political Economy* 98, 519-543.
- Couco, D., and H. Liu, 2006, An Analysis of VaR-based Capital Regulation, *Journal of Financial Intermediation* 15, 362-394.
- Cremers, M., 2002, Stock Return Predictability: A Bayesian Model Selection

- Procedure, *Review of Financial Studies* 15, 1223-1575.
- Cuoco, D., H. He., S. Isaenko, 2008, Optimal Dynamic Trading Strategies with Risk Limits, *Operations Research* 56, 358-368.
- Dangl, T. and M. Halling, 2012, Predictable Regressions with Time-Varying Coefficients, *Journal of Financial Economics* 106, 157-181.
- Doucet, A., N. De Freitas, and N. Gordon, 2001, Sequential Monte Carlo Methods in Practice, *Springer: New York*.
- Duffie, D., J. Pan and K. Singleton, 2000 June, Transform Analysis and Asset Pricing for Affine Jump-Diffusions, *Econometrica*, Vol. 68, 1343-1376.
- Dybvig, P, 1995, Dusenberry's Ratcheting of Consumption: Optimal Dynamic Consumption and Investment Given Intolerance for any Decline in Standard of Living, *Review of Economic Studies* 62, 287-313.
- Dybvig, P, 1999, Using Asset Allocation to Protect Spending, *Financial Analysts Journal* January/February, 49-62.
- Dybvig, P., and C. Huang, 1988, Nonnegative Wealth, Absence of Arbitrage, and Feasible Consumption Plans, *Review of Financial Studies* 1, 377-401.
- Engle, R.F., 2002, Dynamic Conditional Correlation: A Simple Class of Multivariate GARCH Models, *Journal of Business and Economic Statistics* 20, 339-350.
- Eraker, B., M. Johannes and N. Polson, 2003 June, The Impact of Jumps in Volatility and Returns, *Journal of Finance*, Vol. LVIII, No. 3, 1269-1300.
- Ferson, W., and C. Harvey, 1991, The Variation of Economic Risk Premiums, *Journal of Political Economy* 99(2), 385-415.
- Fleming, J., C. Chris, and B. Ostdiek, 2001, The Economic Value of Volatility Timing, *Journal of Finance* 56, 329-352.
- Frühwirth-Schnatter, S, 1994, Data Augmentation and Dynamic Linear Models, *Journal of Time Series Analysis* 15, 183-202.
- Geweke, J., 1992, Evaluating the Accuracy of Sampling-Based Approaches to the Calculation of Posterior Moments, *Bayesian Statistics Vol 4*, New York: Oxford University Press, 169-188.
- Giacinto, M., Federico, S., and F. Gozzi, 2011, Pension Funds with a Minimum Guarantee: A Stochastic Control Approach, *Finance and Stochastics* 15,

297-342.

- Goldberg D, 1989, Genetic Algorithms in Search Optimization and Machine Learning, Reading MA: Addison Wesley.
- Goldman Sachs, June 1998, Using the Black-Litterman Global Asset Allocation Model: Three Years of Practical Experience, Fixed Income Research.
- Greenspan, A., 2004, Risk and Uncertainty in Monetary Policy, *American Economic Review, Papers and Proceedings* 94(2), 33-40.
- Grossman, S., and J. Vila, 1992, Optimal Dynamic Trading with Leverage Constraints, *Journal of Financial and Quantitative Analysis* 27, 151-168.
- Grossman, S., and Z. Zhou, 1993, Optimal Investment Strategies for Controlling Drawdowns, *Mathematical Finance* 3, 241-276.
- Grossman, S., and Z. Zhou, 1996, Equilibrium Analysis of Portfolio Insurance, *Journal of Finance* 51 (4), 1379-1403.
- Han, Y, 2006, Asset Allocation with a High Dimensional Latent Factor Stochastic Volatility Model, *Review of Financial Studies* 19(1), 237-271.
- Johannes, M., A. Korteweg and N. Polson, 2014 April, Sequential Learning, Predictability, and Optimal Portfolio Returns, *Journal of Finance* LXIX(2), 611-644.
- de Jong, P., and N. Shephard, 1995, The Simulation Smoother for Time Series Models, *Biometrika* 82(2), 339-350.
- Jones, C.S., and S. Tuzel, 2013, New Orders and Asset Prices, *Review of Financial Studies* 26(1), 115-157.
- Kandel, S., and R. F. Stambaugh 1996, On the Predictability of Stock Returns: An Asset-Allocation Perspective, *Journal of Finance* 51(2), 385-424.
- El Karoui, N., and M. Jeanblanc-Picque., 1998, Optimization of Consumption with Labor Income, *Finance and Stochastics* 2, 409-440.
- El Karoui, N., M. Jeanblanc-Picque., and V. Lacoste, 2005, Optimal Portfolio Management with American Capital Guarantee, *Journal of Economic Dynamics and Control* 29, 449-468.
- Kim, S., N. Shephard, and S. Chib, 1998, Stochastic Volatility: Likelihood Inference and Comparison with ARCH Models, *Review of Economic Studies* 65, 361-393.

- Leippold, M., F. Trojani and P. Vanini, 2006, Equilibrium Impact of Value-at-Risk, *Journal of Economic Dynamics and Control*, 30, 1277-1313.
- Lettau, M., S.C. Ludvigson, and J.A. Wachter, 2008, The Decling Equity Premium: What Role Does Macroeconomic Risk Play?, *Review of Financial Studies* 21(4),1653-1687.
- Ludvigson, S., and S. Ng, 2007, The Empirical Risk-Return Relation: A Factor Analysis Approach, *Journal of Financial Economics* 83, 171-222.
- Maior, P., 2014, Don't Fight the Fed!, *Review of Finance* 18, 623-679.
- Magdon-Ismail, M., and A. Atiya, 2004, Maximum Drawdown, *Risk* 17 (10), 99-102.
- Markowitz, H. M., 1952, Portfolio Selection, *Journal of Finance* 7(1), 77-91.
- Merton, R., 1971, Optimum Consumption and Portfolio Rules in a Continuous-Time Model, *Journal of Economic Theory* 3, 373-413.
- Modigliani, F., and L. Modigliani 1997, Risk-Adjusted Performance, *Journal of Portfolio Management* Winter, 45-54.
- Pitt, M.K., and N. Shephard, 1999, Filtering via Simulation: Auxiliary Particle Filters, *Journal of the American Statistical Association* 94(446), 590-599.
- Pospisil, L., and J. Vecer, 2010, Portfolio Sensitivity to the Changes in the Maximum and the Maximum Drawdown, *Quantitative Finance* 10(6), 617-627.
- Primiceri, G., 2005, Time Varying Structural Vector Autoregressions and Monetary Policy, *Review of Economic Studies* 72, 821-852.
- Stock, J.H., and M.W. Watson, 2002 April, Macroeconomic Forecasting Using Diffusion Indexes, *Journal of Business and Economic Statistics* 20(2), 147-162.
- Rapach, D.E., J.K. Strauss and G. Zhou, 2010, Out-of-Sample Equity Premium Prediction: Combination Forecasts and Links to the Real Economy, *Review of Financial Studies* 23(2), 821-862.
- Riedel, F., 2009, Optimal Consumption Choice with Intolerance for Declining Standard of Living, *Journal of Mathematical Economics* 45, 449-464.
- Schroder, M., and C. Skiadas, 2002, An Isomorphism Between Asset Pricing Models With and Without Linear Habit Formation, *Review of Financial Studies* 15,

1189-1221.

- Snyder, C., Bengtsson T., P. Bickel, and J. Anderson, 2008, Obstacles to High-Dimensional Particle Filtering, *Monthly Weather Review* 136(12), 4629-4640.
- Shanken, J., and M. Weinstein 2006, Economic Forces and the Stock Market Revisited, *Journal of Empirical Finance* 13(2), 129-144.
- Taylor, J., 2007, Housing and Monetary Policy, *Proceedings of FRB of Kansas city*, 463-476.
- Welch, I., and A. Goyal 2008, A Comprehensive Look at the Empirical Performance of Equity Premium Prediction, *Review of Financial Studies* 21(4), 1455-1508.
- Wong, E., 1964, The Construction of a Class of Stationary Markoff Processes, *Proceedings of Symposia in Applied Mathematics* Vol. 16. Providence, R.I.: American Mathematical Society.
- Xia, Y., 2001, Learning About Predictability: The Effect of Parameter Learning on Dynamic Asset Allocation, *Journal of Finance* 56, 205-246.
- Yor, M., 1992, On Some Exponential Functionals of Brownian Motion, *Advances in Applied Probability*, 24, 509-531.
- Zhou, G., and Y. Zhu, 2009, Technical Analysis: An Asset Allocation Perspective on the Use of Moving Averages, *Journal of Financial Economics* 92, 519-544.

APPENDIX A: SIMULATION SMOOTHER

Lower case letters are used to denote column vectors and upper case letters are used to denote matrices. Conditional on $\omega = (\omega_0; \omega_1; \dots; \omega_n)$, it is supposed that y_t is generated by the following state space model.

$$\begin{aligned} y_t &= X_t\beta + Z_t\alpha_t + G_tu_t \\ \alpha_{t+1} &= W_t\beta + T_t\alpha_t + H_tu_t \end{aligned} \tag{A-1}$$

where $\alpha_0 = 0$. The coefficients matrices may depend on ω and u_t are independent $N(0, I)$ variables.

We first run the Kalman filter for $t = 1, 2, \dots, T$ as follows

$$\begin{aligned} e_t &= y_t - X_t\beta - Z_t\alpha_t \\ D_t &= Z_tP_tZ_t' + G_tG_t' \\ K_t &= (T_tP_tZ_t' + H_tG_t')D_t^{-1} \\ \alpha_{t+1} &= W_t\beta + T_t\alpha_t + K_te_t \\ P_{t+1} &= T_tP_tL_t' + H_tJ_t' \end{aligned}$$

where $a_1 = W_0\beta$, $P_1 = H_0H_0'$, $L_t = T_t - K_tZ_t$ and $J_t = H_t - K_tG_t$

Then we set $r_n = 0$ and $U_n = 0$, and assume $G_tH_t' = 0$. For $t = n, n-1, \dots, 1$, we

run the following procedures

$$C_t = \Omega_t - \Omega_t U_t \Omega_t$$

$$\varepsilon_t \sim N(0, C_t)$$

$$V_t = \Omega_t U_t L_t$$

$$r_{t-1} = Z_t' D_t^{-1} e_t + L_t' r_t - V_t' C_t^{-1} \varepsilon_t$$

$$U_{t-1} = Z_t' D_t^{-1} Z_t + L_t' U_t L_t + V_t' C_t^{-1} V_t$$

where $\Omega_t = H_t H_t'$ and $\eta_t = \Omega_t r_t + \varepsilon_t$ is a draw from $p(H_t u_t | y, \omega)$.

APPENDIX B: AUXILIARY PARTICLE FILTER

We apply one of sequential Monte Carlo methods, called the auxiliary particle filter (APF) (Pitt and Shephard (1999) and the the book review of Doucet (2001)), to estimate the predictive density of conditional variance and mean discussed in the above asset allocation part. Generally speaking, particle filters incorporate the advantages of sequential feature of Kalman filters and flexibility of MCMC samplers and avoid some their disadvantages. The essential idea of APF is to use auxiliary indicators to mark the particles with high conditional likelihood so that the particles that have very low likelihoods will not be sampled in the second stage and the statistical efficiency of sampling could be improved. A general implementation procedure is shown as follows. In the empirical analysis, we set $M=50,000$ and $R=500,000$. A larger number of $M=100,000$ and $R=1,000,000$ has been tested as well, there is no material difference in the empirical results.¹⁹

1. We first sample the proposal values as follows. Given values $\{h_{t-1}^{(1)}, \alpha_{t-1}^{(1)}, \sigma_{t-1}^{(1)}, Y_{t-1}^{(1)}, \dots, h_{t-1}^{(M)}, \alpha_{t-1}^{(M)}, \sigma_{t-1}^{(M)}, Y_{t-1}^{(M)}\}$ generated from $(h_{t-1}, \alpha_{t-1}, \sigma_{t-1}, Y_{t-1} | \mathcal{F}_{t-1}, \Gamma^*)$, we can have

¹⁹The program for large number of particles is tested in the supercomputer center at University of North Carolina - Charlotte as it's computationally expensive. The command is written in shell scripts which are submitted to Torque scheduler running in the Portable Batch System (PBS).

the proposed values as follows

$$\begin{aligned}\hat{h}_t^{*(g)} &= E(h_t^{(g)} | h_{t-1}^{(g)}) \\ \hat{\alpha}_t^{*(g)} &= E(\alpha_t^{(g)} | \alpha_{t-1}^{(g)}) \\ \hat{\sigma}_t^{*(g)} &= E(\sigma_t^{(g)} | \sigma_{t-1}^{(g)}) \\ \hat{Y}_t^{*(g)} &= E(Y_t^{(g)} | Y_{t-1}^{(g)}) \\ \omega_g &= N_n(r_t | B\hat{Y}_t^{*(g)}, \Psi_t(\hat{h}_t^{*(g)}, \hat{Y}_t^{*(g)}), \Gamma^*),\end{aligned}$$

with $g=1, \dots, M$, and then sample R times the integers $1, 2, \dots, M$ with normalized probability $\bar{\omega}_t^g = \omega_g / \sum_{j=1}^M \omega_j$. The proposal values usually could be chosen as mean or mode, here we choose the mean as the proposal value. Let k_1, \dots, k_R be the sampled indexes associated with $\{\hat{h}_t^{*(k_1)}, \hat{\alpha}_t^{*(k_1)}, \hat{\sigma}_t^{*(k_1)}, \hat{Y}_t^{*(k_1)}, \dots, \hat{h}_t^{*(k_R)}, \hat{\alpha}_t^{*(k_R)}, \hat{\sigma}_t^{*(k_R)}, \hat{Y}_t^{*(k_R)}\}$.

2. For each k_g in step 1, we could obtain the propagated values

$\{h_t^{*(1)}, \alpha_t^{*(1)}, \sigma_t^{*(1)}, Y_t^{*(1)}, \dots, h_t^{*(R)}, \alpha_t^{*(R)}, \sigma_t^{*(R)}, Y_t^{*(R)}\}$ from

$$\begin{aligned}h_{j,t}^{*(g)} &= h_{j,t-1}^{(k_g)} + \sigma_{h_j} u_{h_{j,t}}^g \\ \alpha_{j,t}^{*(g)} &= \alpha_{j,t-1}^{(k_g)} + \sigma_{\alpha_j} u_{\alpha_{j,t}}^g \\ \sigma_{j,t}^{*(g)} &= \sigma_{j,t-1}^{(k_g)} + \sigma_{\sigma_j} u_{\sigma_{j,t}}^g \\ Y_t^{*(g)} &= y_{t-1}^{(k_g)'} \beta_t^{*(k_g)} + (A_t^{*(k_g)})^{-1} \sum_t^{*(k_g)} u_{y_t}^g\end{aligned}$$

with $g = 1, \dots, R$ and $u_{h_{j,t}}^g \sim N(0, 1)$, $u_{\alpha_{j,t}}^g \sim N(0, 1)$, $u_{\sigma_{j,t}}^g \sim N(0, 1)$, and $u_{y_t}^g \sim N(0, I_m)$.

3. We then resample

$$\{h_t^{*(1)}, \alpha_t^{*(1)}, \sigma_t^{*(1)}, Y_t^{*(1)}, \dots, h_t^{*(R)}, \alpha_t^{*(R)}, \sigma_t^{*(R)}, Y_t^{*(R)}\}$$

M times with replacement by using the following probabilities

$$\omega_g^* = \frac{N_n(r_t | BY_t^{*(g)}, \Psi_t(h_t^{*(g)}, Y_t^{*(g)}))}{N_n(r_t | B\hat{Y}_t^{*(k_g)}, \Psi_t(\hat{h}_t^{*(k_g)}, \hat{Y}_t^{*(k_g)}))}$$

to have the desired filtered sample

$$\{h_t^{(1)}, \alpha_t^{(1)}, \sigma_t^{(1)}, Y_t^{(1)}, \dots, h_t^{(M)}, \alpha_t^{(M)}, \sigma_t^{(M)}, Y_t^{(M)}\}$$

from $(h_t, \alpha_t, \sigma_t, Y_t | \mathcal{F}_t, \Gamma^*)$.

APPENDIX C: ESTIMATION PROCEDURES

We conduct a two-step estimation procedure. In the first step, we extract a key principal component, that is, the representing economic factor, from a block of closely related time series. The second step is a Bayesian estimation approach. This two-step estimation method can be viewed as a semiparametric approach, that is, a nonparametric way to uncover the underlying important economic factors in the first step and then a parametric way to estimate the evolution of factors and corresponding parameters in the second step.

As a large set of time series are measured on widely differing ranges and units, we first standardize them in order to avoid the issue of having one variable with large variance that dominates others and thereby affecting the determination of loading factors. Principal components are used to extract important information from a large number of series. The underlying intuition of principal components is to rotate the original axes so that the axes could align in the directions of maximum variation in the new coordinates. Thus the majority part of dynamics and the interactions among variables could be described in a handful components.

In this paper, instead of extracting components from all kinds of series, i.e., Stock and Watson (2002), Bernanke and Boivin (2003), and Bernanke et al. (2005), we categorize time series into several representing groups according to their economic features. We assume that one major representing factor could be used to reflect the majority of the information content for each segment. One way to check the effect of the principal component is to look at the percentage of variation explained by the first

factor. For our case of five factors, the first component is able to account for variation from 67.27% to 92.96%. Thus, one representing factor assumption seems reasonable. On the other hand, we could always divide the segment into smaller groups so that the extracted component could account for larger variation in the smaller group. To keep model parsimony and easier to understand, we only extract five representing fundamental factors with reasonable explaining power in our study.

The first step is to extract a standard principal component. As shown in equation (2), the coefficients are in fact unidentified.²⁰ We follow the standard normalization in principal components literature (see also Bernanke et al. 2005) to make the standardized components as $\hat{C} = \sqrt{T}\hat{Z}$, where \hat{Z} are the eigenvectors of the largest eigenvalues of XX' where X is a block of time series from which the economic factor is extracted.

The second step is to estimate the factor evolution equations and model parameters. let $\theta = (\Sigma_b, \Sigma_\beta, \Sigma_\alpha, \Sigma_\sigma, \Sigma_h)$ denote the hyperparameters. The priors of covariance diagonal matrix are assumed to be the inverse gamma distribution with reasonable values, the initial state of various time-varying variables are assumed to be zero, and the algorithm is fairly robust to the prior specification and initial values. The MCMC simulation is run for 30,000 iterations after discarding the burn-in 3,000 samples. Our Gibbs sampling algorithm for the general dynamic model is summarized as follows.

- i) Initialize $b, h, \alpha, \beta, \sigma, \theta$
- ii) Sample $b|h, \theta$
- iii) Sample $h|b, \theta$

²⁰Let $\hat{\Lambda}^f = \Lambda^f T$ and $\hat{f}_t = T^{-1} f_t$, where T is a $k \times k$ nonsingular matrix then $\{\hat{\Lambda}^f, \hat{f}_t\}$ also satisfy equation (2). Thus we couldn't distinguish these two solutions.

- iv) Sample $\beta|\alpha, \sigma, \theta$
- v) Sample $\alpha|\beta, \sigma, \theta$
- vi) Sample $\sigma|\alpha, \beta, \theta$
- vii) Sample $\theta|b, h, \alpha, \beta, \sigma$

1) Sampling b : Since under the conditional independence of the errors, we could sample the parameters and log-volatilities series-by-series. In other words, the model is scalable in both the number of assets n and the number of factors k . As $b_{i,t}$ denotes the row elements of $B_{i.,t}$, we could sample $b_{i,t}$ by using the simulation smoother. If we treat $b_{i,t} = b_i$ as constant coefficient, that is, the return can be represented as $r_{i,t} = b_i' Y_{i,t} + \epsilon_{i,t}$ and the prior distribution for $b_i \sim N_m(b_0, B_0)$, then we could sample b_i as

$$b_i \sim N_m(\bar{b}_i, B_1) \quad (\text{C-1})$$

where $B_1 = [B_0^{-1} + \sum_{t=1}^n \frac{Y_{i,t} Y_{i,t}'}{e^{h_{i,t}}}]^{-1}$ and $\bar{b}_i = B_1 [B_0^{-1} b_0 + \sum_{t=1}^n \frac{Y_{i,t} r_{i,t}}{e^{h_{i,t}}}]$.

2) Sampling h : consider

$$r_t - B_t Y_t = \hat{r}_t^* \quad (\text{C-2})$$

and the fact that \hat{r}_t^{*2} could be a very small number, thus we add an offset constant \bar{c} , i.e., $\bar{c} = 10^{-6}$ and approximate the state space form as follows

$$\hat{r}_t^{**} = h_t + \eta_t \quad (\text{C-3})$$

$$h_{t+1} = h_t + u_{ht} \quad (\text{C-4})$$

where $\hat{r}_{i,t}^{**} = \log[(\hat{r}_{i,t}^*)^2 + \bar{c}]$ and $\eta_{i,t} = \log(\epsilon_{i,t}^2)$ for $i = 1, \dots, n$. Note that this system is a linear but non-Gaussian state space form as $\log(\epsilon_{i,t}^2) \sim \log \chi_1^2$. We follow Kim et

al. (1998) to use seven normal components with component probabilities q_j , means $m_j - 1.2704$ and variances ν_j^2 to match a number of moments of $\log \chi_1^2$ distribution.

The seven normal components are shown as follows.

ω	$Pr(\omega = j)$	m_j	ν_j^2
1	0.00730	-10.12999	5.79596
2	0.10556	-3.97281	2.61369
3	0.00002	-8.56686	5.17950
4	0.04395	2.77786	0.16735
5	0.34001	0.61942	0.64009
6	0.24566	1.79518	0.34023
7	0.25750	-1.08819	1.26261

Note that the covariance of the idiosyncratic noise in the measurement equation is an identity matrix, so we could estimate the state space system equation by equation.

We first sample indicator s_j conditional on \hat{r}_t^{**}, h as follows

$$\pi(s_{i,t} = j | \hat{r}_{i,t}^{**}, h_{i,t}) \propto q_j \phi(\hat{r}_{i,t}^{**} | h_{i,t} + m_j - 1.2704, \nu_j^2), j = 1, \dots, 7; i = 1, \dots, T. \quad (\text{C-5})$$

Then we sample the state h according to the simulation smoother of de Jong and Shephard (1995) which indirectly sample state distribution through the error distribution instead of directly sampling state distribution such as Carter and Kohn (1994) and Frühwirth-Schnatter (1994). One of the advantages of simulation smoother is that it could avoid the degeneracies inherent in state samplers. We run the simulation

smoother with the corresponding variables to equation (A-1) as follows.

$$\begin{aligned}
 X_t \beta &= 0 \\
 Z_t &= 1 \\
 G_t &= (\nu_j, 0) \\
 W_t \beta &= 0 \\
 T_t &= 1 \\
 H_t &= (0, \Sigma_{h_i}^{1/2}) \\
 H_0 &= (0, \Sigma_{h_{i0}}^{1/2})
 \end{aligned} \tag{C-6}$$

3. Sampling β : consider equation (6), and we could have the factor state space equations as follows

$$Y_t = y'_{t-1} \beta_t + A_t^{-1} \Sigma_t u_{yt} \tag{C-7}$$

$$\beta_{t+1} = \beta_t + u_{\beta t} \tag{C-8}$$

Thus, we could run the simulation smoother with the corresponding variables to

equation (A-1) as follows.

$$\begin{aligned}
X_t\beta &= \mathbf{0}_m \\
Z_t &= y'_{t-1} \\
G_t &= (A_t^{-1}\Sigma_t, \mathbf{0}_m) \\
W_t\beta &= \mathbf{0}_m \\
T_t &= \mathbf{I}_m \\
H_t &= (\mathbf{0}_m, \Sigma_\beta^{1/2}) \\
H_0 &= (\mathbf{0}_m, \Sigma_{\beta 0}^{1/2})
\end{aligned} \tag{C-9}$$

4. Sampling α : after sampling β , we could then transfer the state space equations according to the special lower triangular trait of matrix A_t as follows

$$\hat{Y}_t = \hat{K}_t\alpha_t + \Sigma_t u_{yt} \tag{C-10}$$

$$\alpha_{t+1} = \alpha_t + u_{\alpha t} \tag{C-11}$$

where $\hat{Y}_t = Y_t - y'_{t-1}\beta_t$ and

$$\hat{K}_t = \begin{pmatrix} 0 & 0 & 0 & 0 & \cdots & 0 \\ -\hat{Y}_{1t} & 0 & 0 & 0 & \cdots & 0 \\ 0 & -\hat{Y}_{1t} & -\hat{Y}_{2t} & 0 & \cdots & 0 \\ 0 & 0 & 0 & -\hat{Y}_{1t} & \cdots & \vdots \\ \vdots & & & \ddots & 0 & \cdots & 0 \\ 0 & \cdots & & 0 & -\hat{Y}_{1t} & \cdots & -\hat{Y}_{m-1,t} \end{pmatrix} \tag{C-12}$$

Hence, we could run the simulation smoother with the corresponding variables to

equation (A-1) as follows.

$$\begin{aligned}
X_t\beta &= \mathbf{0}_m \\
Z_t &= \hat{K}_t \\
G_t &= (\Sigma_t, \mathbf{0}_m) \\
W_t\beta &= \mathbf{0}_m \\
T_t &= \mathbf{I}_m \\
H_t &= (\mathbf{0}_m, \Sigma_\alpha^{1/2}) \\
H_0 &= (\mathbf{0}_m, \Sigma_{\alpha_0}^{1/2})
\end{aligned} \tag{C-13}$$

5) Sampling σ : as for the stochastic volatility σ , we could transfer the state space equations as follows

$$\hat{Y}_t^* = \sigma_t + \epsilon_t \tag{C-14}$$

$$\sigma_{t+1} = \sigma_t + u_{\sigma t} \tag{C-15}$$

where $\hat{Y}_t^* = \log[A_t(Y_t - y'_{t-1}\beta_t) + \bar{c}]^2$ and $\epsilon_{i,t} = \log \chi_1^2$. Similarly, we can follow the previous step 2 to use the seven normal components to approximate the $\log \chi_1^2$ and run the simulation smoother equation by equation to estimate $\sigma_{i,t}$ for $i = 1, \dots, m$ as

follows

$$\begin{aligned}
 X_t \beta &= 0 \\
 Z_t &= 1 \\
 G_t &= (\nu_j, 0) \\
 W_t \beta &= 0 \\
 T_t &= 1 \\
 H_t &= (0, \Sigma_{\sigma_i}^{1/2}) \\
 H_0 &= (0, \Sigma_{\sigma_{i_0}}^{1/2})
 \end{aligned} \tag{C-16}$$

6) Sampling the hyperparameters θ : Since the hyperparameters of the model are the diagonal blocks, we use the standard conjugate inverse gamma distribution to sample the conditional posterior distribution for each block of variance.

APPENDIX D: SIMULATION STUDY

We run a simulation study for an univariate series to examine the effectiveness of our estimation procedure, which could be directly applied to multivariate series since the procedure is scalable in the number of assets. Suppose an univariate time series r_t can be simulated as follows

$$r_t = f_B' B + f_\alpha \alpha_t + \epsilon_t$$

where $f_B = (f_{B1}, f_{B2})'$ is a vector of two factors with constant loading $B = (B_1, B_2)'$, while $f_\alpha = (f_{\alpha_1}, f_{\alpha_2})'$ is a vector of two factors with dynamic loading $\alpha_t = (\alpha_{1t}, \alpha_{2t})$ such that

$$\alpha_t = \alpha_{t-1} + \nu_t,$$

where $\nu_t \sim N(0, \Sigma_\alpha)$ for $t = 1, \dots, n$, and $\epsilon_t \sim N(0, e^{h_t})$ such that

$$h_t = h_{t-1} + u_t,$$

where $u_t \sim N(0, \sigma_h^2)$ for $t = 1, \dots, n$.

Note that this model setting includes both time-varying loading and stochastic volatility features. If we treat $\alpha_t = \alpha$, i.e., the constant loading, then this model can be seen as a constant loading with stochastic volatility model. Furthermore, if we set $\epsilon_t \sim N(0, \sigma^2)$, that is, a constant volatility, then we could also obtain the combination of constant loading with constant volatility, and time-varying loading with constant volatility accordingly. The factors are generated from uniform distribution as $f_B \sim U(-0.5, 0.5)$ and $f_\alpha \sim U(-0.5, 0.5)$ and the true parameters are specified as $B =$

$(3, -0.1)'$, $\alpha_0 = (-2, -2)'$, $h_0 = -5$, $\Sigma_\alpha = \text{diag}(0.4, 0.05)$, $\sigma_h = 0.2$, where diag denotes the diagonal matrix with the numbers in the main diagonal. The simulated series with $n = 200$ are shown in the Panel A of Figure 1.

By following the estimation procedure described in the appendix, after discarding the initial burn-in 3,000 samples, we then draw 30,000 samples with prior such as $B \sim N(0, 5 * I_2)$, $\Sigma_\alpha \sim IW(2, 20 * I_2)$, $\sigma_h^2 \sim IG(2, 0.02)$, where I_2 refers to the identity matrix with two dimensions, IW refers to the inverse Wishart distribution, and IG refers to the inverse Gamma distribution. The sample autocorrelation function, sample draws, and the posterior densities are shown in the Panel B of Figure 1, from which we could observe that the sample autocorrelations are quite low after 300 draws and the sample draws look stable, suggesting that the estimates seem satisfactory.

We also summarize the the estimation results in Table 12, in which the IF denotes the inefficiency factor which is the inverse of the relative numerical efficiency (Geweke 1992). It is defined as $1 + 2 \sum_{s=1}^{\infty} \rho_s$, where ρ_s represents the s -th sample autocorrelation. Suppose n_1 uncorrelated samples is required to obtain a reasonable posterior estimate and the inefficiency factor is equal to n_2 , then we need to run the MCMC for at least $n_1 * n_2$ times to get the satisfactory posterior estimate. From the estimated results, we could see that the posterior means are quite close to the true values and the inefficiency factors are quite low. Although the IF for σ_h is around 135, total 30,000 samples would generate about 220 uncorrelated samples, which would be sufficient to produce a satisfactory estimate.

Figure 2 depicts the estimation outcomes and the 99% confidence interval for the state variables. From the plot, we could observe that the trajectory of the posterior

Table 12: This table summarizes the estimation results for the simulated data.

Parameter	True	Mean	Std. dev	99% Interval	IF
B_1	3	2.9615	0.0537	[2.8526,3.0639]	10.50
B_2	-0.1	-0.1718	0.0552	[-0.2802,-0.0636]	8.35
Σ_{11}	0.4	0.3752	0.0859	[0.2282,0.5639]	27.37
Σ_{22}	0.05	0.0297	0.0117	[0.0127,0.0581]	34.69
σ_h	0.2	0.2280	0.0825	[0.1053,0.4190]	135.56

mean could closely catch up with the true processes of the state variables and the 99% confidence interval can fully contain the trajectories of the true state variables. Overall, the estimation procedure we implemented is efficient and effective to track both static and dynamic variables in a structural setting, and all empirical analysis in this paper is based on the estimation procedure we discussed previously.

APPENDIX E: DATA DESCRIPTION

Transformation code: 0 - no transformation; 1 - first difference; 2 - logarithm; 3 - first difference of logarithm

Real Economic Factor

#	Mnemonic	Description	T-Code
1	INDPRO	Indu. Prod. Index	3
2	IPMAN	Indu. Prod.: Manufacturing	3
3	IPCONGD	Indu. Prod.: Consumer Goods	3
4	IPMAT	Indu. Prod.: Materials	3
5	IPMINE	Indu. Prod.: Mining	3
6	IPBUSEQ	Indu. Prod.: Business Equipment	3
7	IPUTIL	Indu. Prod.: Electric and Gas Util.	3
8	IPDMAN	Indu. Prod.: Durable Manufacturing	3
9	IPNMAN	Indu. Prod.: Nondurable Manu.	3
10	IPDCONGD	Indu. Prod.: Dur. Consumer Goods	3

#	Mnemonic	Description	T-Code
11	IPNCONGD	Indu. Prod.: Nondur. Consu. Goods	3
12	IPDMAT	Indu. Prod.: Dur. Materials	3
13	IPNMAT	Indu. Prod.: Nondur. Materials	3
14	IPFINAL	Indu. Prod.: Final Products	3
15	MCUMFN	Cap. Util.: Manu. (%)	0
16	TCU	Cap. Util.: Total Industry (%)	0
17	CE	Civilian Employment	3
18	CIVPART	Civi. Lab. Force Parti. Rate (%)	0
19	EMRATIO	Civi. Employment-Popu. Ratio (%)	0
20	UNRATE	Civi. Unemployment Rate (%)	0
21	UEMPMEAN	Ave. (Mean) Duration of Unempl.	0
22	UEMPLT5	Civi. Unempl. - Less Than 5 Weeks	0
23	UEMP5TO14	Civi. Unempl. for 5 - 14 Weeks	0
24	UEMP15T26	Civi. Unempl. for 15 - 26 Weeks	0
25	UEMP27OV	Civi. Unempl. for 27 Weeks and Over	0
26	UEMP15OV	Civi. Unempl. for 15 Weeks and Over	0
27	CEU	All Employees: Total Private	3
28	PAYEMS	All Empl.: Total Nonfarm	3
29	USPRIV	All Empl.: Tot. Private Ind.	3
30	MANEMP	All Empl.: Manu.	3
31	USCONS	All Empl.: Constr.	3

#	Mnemonic	Description	T-Code
32	USGOVT	All Employees: Government	3
33	DMANEMP	All Empl.: Dura. Goods	3
34	USGOOD	All Empl.: Goods-Producing Indu.	3
35	USFIRE	All Empl.: Financial Acti.	3
36	USTRADE	All Empl.: Retail Trade	3
37	USWTRADE	All Empl.: Wholesale Trade	3
38	USEHS	All Empl.: Edu. and Health Serv.	3
39	SRVPRD	All Empl.: Serv.-Providing Indu.	3
40	USINFO	All Empl.: Info. Services	3
41	NDMANEMP	All Empl.: Nondur. Goods	3
42	USPBS	All Empl.: Profe. and Busi. Serv.	3
43	USLAH	All Empl.: Leisure and Hosp.	3
44	USMINE	All Empl.: Mining and Logging	3
45	USSERV	All Empl.: Other Services	3
46	USTPU	All Empl.: Trade, Transp. and Uti.	3
47	AHEM	Ave. Hourly Earnings: Manu.	0
48	AHECONS	Ave. Hourly Earnings: Constr.	0
49	AWHMAN	Ave. Weekly Hours: Manu.	0
50	AWOTMAN	Ave. Weekly Overtime Hours: Manu.	0
51	PI	Personal Income	3
52	DSPI	Real Disposable Personal Income	3

#	Mnemonic	Description	T-Code
53	PCE	Personal Consump. Expen.	3
54	PCEDG	Personal Consump. Expen.: Dur. Goods	3
55	PCEND	Personal Consump. Expen.: Nondur. Goods	3
56	PCES	Personal Consump. Expen.: Ser.	3
57	HOUST	Hous. St.: Tot.: New Pri. Owned Hous.	2
58	HOUSTNE	Hous. St. in Northeast Census Region	2
59	HOUSTMW	Hous. St. in Midwest Census Region	2
60	HOUSTS	Hous. St. in South Census Region	2
61	HOUSTW	Hous. St. in West Census Region	2
62	IR	Import (End Use): All Commodities	3
63	IQ	Export (End Use): All Commodities	3

Price Factor

#	Mnemonic	Description	T-Code
64	PCEPI	Pers. Consump. Exp.: Chain Price Index	3
65	CPIAUCSL	CPI for All Urb. Consu.: All Items	3
66	CPIAPPSL	CPI for All Urb. Consu.: Apparel	3
67	CPITRNSL	CPI for All Urb. Consu.: Transp.	3
68	CPIMEDSL	CPI for All Urb. Consu.: Med. Care	3
69	CUSRSAC	CPI for All Urb. Consu.: Commodities	3
70	CUSRSAS	CPI for All Urb. Consu.: Services	3
71	CUSRSAD	CPI for All Urb. Consu.: Durables	3
72	CPIULFSL	CPI for All Urb. Consu.: All-Food	3
73	CUSRSALS	CPI for All Urb. Consu.: All-Shelter	3
74	CUSRSALM	CPI for All Urb. Consu.: All-Med. Care	3
75	PPIACO	Producer Price Index: All Commodities	3
76	PPIFGS	PPI: Finished Goods	3
77	PPIFCF	PPI: Finished Consu. Foods	3
78	PPIFCG	PPI: Finished Consu. Goods	3
79	PFCGEF	PPI: Finished Consu. Goods Excl. Foods	3
80	PPICPE	PPI: Finished Goods: Capital Equipment	3
81	PPIITM	PPI: Interme. Materials: Suppl. and Compo.	3
82	PPICRM	PPI: Crude Materials for Further Proce.	3
83	OILPRICE	Spot Oil Price: West Texas Interme.	3

Interest Rate Factor

#	Mnemonic	Description	T-Code
84	TB3MS	3-Month T Bill: Sec. Market Rate	0
85	TB6MS	6-Month T Bill: Sec. Market Rate	0
86	GS1	1-Year T Constant Maturity Rate	0
87	GS3	3-Year T Constant Maturity Rate	0
88	GS5	5-Year T Constant Maturity Rate	0
89	GS10	10-Year T Constant Maturity Rate	0
90	AAA	Moody's Seas. Aaa Corp. Bond Yield	0
91	BAA	Moody's Seas. Baa Corp. Bond Yield	0
92	STB3FF	Spread TB3MS - FEDFUNDS	0
93	STB6FF	Spread TB6MS - FEDFUNDS	0
94	SGS1FF	Spread GS1 - FEDFUNDS	0
95	SGS3FF	Spread GS3 - FEDFUNDS	0
96	SGS5FF	Spread GS5 - FEDFUNDS	0
97	SGS10FF	Spread GS10 - FEDFUNDS	0
98	SAAAFF	Spread AAA - FEDFUNDS	0
99	SBAAFF	Spread BAA - FEDFUNDS	0
100	MPRIME	Bank Prime Loan Rate	0
101	EXJPUS	Japan/U.S. Foreign Ex. Rate	3
102	EXCAUS	Canada/U.S. Foreign Ex. Rate	3
103	EXSZUS	Swiss/U.S. Foreign Ex. Rate	3
104	EXUSUK	U.S./U.K. Foreign Ex. Rate	3

Money and Credit Factor

#	Mnemonic	Description	T-Code
105	M1	M1 Money Stock	3
106	CURRENCY	Currency Component of M1	3
107	M2	M2 Money Stock	3
108	MBCURRCIR	Mone. Base: Curr. in Circu.	3
109	BOGAMBSL	Mone. Base, Adj. Cha. in Res. Req.	3
110	CURRCIR	Currency in Circulation	3
111	TOTRESNS	Tot. Res. of Depo. Ins.	3
112	RESBALNS	Tot. Res. Bal. with Fed. Res. banks	3
113	TRARR	Total Res., Adj. Changes in Res. Req.	3
114	REQRESNS	Required Res. of Depo. Inst.	3
115	NONBORRES	Res. of Depo. Inst., Nonborrowed	3
116	EXCSRESNS	Excess Res. of Depo. Inst.	3
117	BOGNONBR	Non-Borrowed Res. of Depo. Inst.	3
118	TCDSL	Tot. Checkable Deposits	3
119	USGDCB	U.S. Gov. Demand Depo. at Comme. Banks	3
120	USGVDDNS	U.S. Gov. Demand Depo. Note Bal.-Tot.	3
121	DEMDEPSL	Demand Depo. at Comme. Banks	3
122	STDCBSL	Small Time Depo. at Comme. Banks	3
123	SVGCBSL	Savings Depo. at Comme. Banks	3
124	STDSL	Small Time Deposits - Total	3

#	Mnemonic	Description	T-Code
125	SAVINGSL	Savings Deposits - Total	3
126	OTHSEC	Other Secu. at Comme. Banks	3
127	CONSUMER	Consumer Loans at Comme. Banks	3
128	BUSLOANS	Comme. and Indu. L., Comme. Banks	3
129	REALLN	Real Estate Loans at Comm. Banks	3
130	TOTALSL	Tot. Consu. Cre. Own. Secu., Outst.	3
131	NONREVSL	Tot. Nonrev. Cre. Own. Secu., Outst.	3
132	LOANS	Lo. and Leas. in Bank Cre., Comme. Banks	3
133	USGSEC	Treas. and Agen. Secu. at Comme. Banks	3
134	INVEST	Secu. in Bank Cre. at Comme. Banks	3
135	NFORBRES	Net Free or Borr. Res. of Depo. Inst.	1
136	BORROW	Tot. Borro. of Dep. Inst. from Fed. Res.	3

Expectation Factor

#	Mnemonic	Description	T-Code
137	MICH	Univ. of Mich. Inf. Expec. (%)	0
138	PMI	ISM Manu.: PMI Compo. Index (%)	0
139	NAPMNOI	ISM Manu.: New Orders Index (%)	0
140	NAPMEI	ISM Manu.: Employment Index (%)	0
141	NAPMII	ISM Manu.: Inventories Index (%)	0
142	NAPMPI	ISM Manu.: Production Index (%)	0
143	NAPMSDI	ISM Manu.: Suppl. Deli. Index (%)	0
144	NAPMPRI	ISM Manu.: Prices Index (%)	0
145	NAPMEXI	ISM Manu.: New Exp. Orders Index (%)	0
146	NAPMIMP	ISM Manu.: Imports Index (%)	0

Monetary Instrument

#	Mnemonic	Description	T-Code
147	FEDFUNDS	Effective Federal Funds Rate	0

APPENDIX F: A HYBRID MODEL

We run a simulation study for an univariate series to demonstrate the effectiveness of our algorithm, which could be directly extended to multivariate framework and the estimation algorithms are shown next. Assume an univariate time series y_t with constant and dynamic loading, stochastic volatility, time-varying jump, and heavy tail has the following structure.

$$y_t = x_t' \beta + z_t \alpha_t + k_t q_t + u_t \quad (\text{F-1})$$

$$\alpha_t = \alpha_{t-1} + \xi_t$$

$$h_t = h_{t-1} + \eta_t$$

where $x_t = (x_{1t}, x_{2t})'$ is a vector of two variables with constant loading β , $z_t = (z_{1t}, z_{2t})$ is a vector of two factors with dynamic loading α_t and $\xi_t \sim N(0, \Sigma_\alpha)$, k_t refers to the time-varying jump magnitude as a jump occurs, i.e., $\psi_t \equiv \log(1 + k_t) \sim N(-0.5\delta^2, \delta^2)$ (Anderson et al., 2002) and q_t is a Bernoulli random variable with parameter κ such that $P(q_t = 1) = \kappa$ and $P(q_t = 0) = 1 - \kappa$, which refers to the jump intensity. $u_t = \lambda_t^{-\frac{1}{2}} \epsilon_t$ refers to the heavy tail where λ_t follows i.i.d. Gamma($\nu/2, \nu/2$) and $\epsilon_t \sim N(0, e^{h_t})$ with $\eta_t \sim N(0, \sigma_h^2)$.

Note that this structural dynamic model contains hybrid stylized facts in financial data, i.e., stochastic volatility, jumps, and heavy tails. It can also be seen as a discretization of the popular Lévy process with jumps model used in continuous finance literature (Duffie et al., 2000 and Eraker et al., 2003). Other types of model with desired features can be selected accordingly as a subset of this model, i.e., a

model with constant loading, stochastic volatility and jumps or a model with dynamic loading, constant volatility and heavy tail.

Time series are generated from the uniform distributions such as $x_t \sim U(-0.5, 0.5)$ and $z_t \sim U(-0.5, 0.5)$ and the true parameters are specified as $\beta = (1, -0.3)'$, $\alpha_0 = (-0.5, -0.5)'$, $h_0 = -7$, $\Sigma_\alpha = \text{diag}(0.02, 0.04)$, $\sigma_h = 0.15$, where diag denotes the diagonal matrix with the numbers in the main diagonal, $\delta = 0.04$, $\kappa = 0.03$ and $\nu = 12$. The simulated series with $n = 200$ are shown in the Panel A of Figure 43.

By following the estimation procedure described next, after discarding the initial burn-in 3,000 samples, we then draw 30,000 samples with prior such as $B \sim N(0, 5 * I_2)$, $\Sigma_\alpha \sim IW(2, 20 * I_2)$, $\sigma_h^2 \sim IG(2, 0.02)$, where I_2 refers to the identity matrix with two dimensions, IW refers to the inverse Wishart distribution, and IG refers to the inverse Gamma distribution, and $\nu_0 = 8$, $\delta_0 = 0.01$, $\kappa_0 = 0.01$. The sample autocorrelation function, sample draws, and the posterior densities are shown in the Panel B of Figure 43, from which we could observe that the sample autocorrelations are quite low after 300 draws and the sample draws look stable, suggesting that the estimates seem satisfactory.

We also summarize the the estimation results in Table 13, in which the IF denotes the inefficiency factor which is the inverse of the relative numerical efficiency (Geweke 1992).

Figure 44 depicts the estimation outcomes and the 99% confidence interval for the state variables. From the plot, we could observe that the trajectory of the posterior mean could closely catch up with the true processes of the state variables and the 99% confidence interval can fully contain the trajectories of the true state variables.

Table 13: Estimation results summary for the simulated data including heavy tail and jump.

Parameter	True	Mean	Std. dev	99% Interval	IF
β_1	0.1	0.0969	0.0246	[0.0485,0.1452]	10.12
β_2	-0.3	-0.2816	0.0241	[-0.3287,-0.2342]	6.40
Σ_{11}	0.02	0.0297	0.0072	[0.0183,0.0459]	11.87
Σ_{22}	0.04	0.0374	0.0088	[0.0230,0.0576]	16.91
σ_h	0.15	0.1274	0.0483	[0.0629,0.2461]	117.18
δ	0.04	0.0253	0.0286	[0.0008,0.0925]	1.65
κ	0.03	0.0347	0.0234	[0.0045,0.0925]	6.64
ν	12	12.4953	2.6423	[7.8672,18.1819]	17.19

Overall, the estimation procedure we implemented is efficient and effective to track both static and dynamic variables in a structural setting.

The estimation steps are shown as follows.

- 1) Initialize ν , λ_t , q_t , and h_t
- 2) Sample constant loading β by using the standard normal distribution and α_t by using the simulation smoother.
- 3) Sample mixture distribution indicator s_t as follows

$$P(s_t|y_t^*, h_t) \propto P(s_t)N(y_t^*|h_t + \mu_{s_t}, \nu_{s_t}^2) \quad (\text{F-2})$$

where μ_{s_t} and $\nu_{s_t}^2$ are the corresponding mean and variance of the mixture component at time t.

- 4) Then we could sample the volatility states $\{h_t\}$ by using simulation smoother.
- 5) (5.a) Sample $\nu|\lambda$ as follows: the conditional posterior distribution of ν is given by

$$\pi(\nu|\lambda) \propto \pi(\nu) \frac{(\frac{\nu}{2})^{\frac{n\nu}{2}}}{[\Gamma(\frac{\nu}{2})]^n} \prod_{t=1}^n \lambda_t^{\frac{\nu}{2}} e^{-\frac{\nu}{2} \sum_{t=1}^n \lambda_t} \quad (\text{F-3})$$

And let $\ell(\nu) = \log \pi(\nu|\lambda)$ and apply Taylor second order expansion to $\ell(\nu)$ at $\hat{\nu}$ as follows

$$\ell(\nu) \approx \ell(\hat{\nu}) + \ell'(\hat{\nu})(\nu - \hat{\nu}) + \frac{1}{2}\ell''(\hat{\nu})(\nu - \hat{\nu})^2 \equiv h(\nu) \quad (\text{F-4})$$

where $\hat{\nu}$ is the mode of the conditional posterior density, $\ell'(\hat{\nu})$ and $\ell''(\hat{\nu})$ are the first and second derivative of $\ell(\nu)$ evaluated at $\nu = \hat{\nu}$. We sample ν from $N(\mu_\nu, \sigma_\nu^2)$, where $\mu_\nu = \hat{\nu} - \ell'(\hat{\nu})/\ell''(\hat{\nu})$ and $\sigma_\nu^2 = -1/\ell''(\hat{\nu})$, and then apply a Metropolis-Hastings algorithm.

(5.b) Sample $\lambda_t|y_t, h_t, \beta_t, \psi_t, q_t, \nu$ as follows

$$\lambda_t|y_t, h_t, \beta_t, \psi_t, q_t, \nu \sim \text{Gamma} \left(\frac{\nu + 1}{2}, \frac{\nu + (y_t - x_t' \beta_t - (e^{\psi_t} - 1)q_t)^2 / e^{h_t}}{2} \right) \quad (\text{F-5})$$

6) (6.a) Sample $q_t|y_t, h_t, \beta_t, \nu, \kappa$ as follows

$$P(q_t = 1|y, h_t, \beta, \nu, \kappa) \propto \kappa f_t(y_t|x_t' \beta_t + k_t, e^{h_t}, \nu) \quad (\text{F-6})$$

$$P(q_t = 0|y, h_t, \beta, \nu, \kappa) \propto (1 - \kappa) f_t(y_t|x_t' \beta_t, e^{h_t}, \nu) \quad (\text{F-7})$$

where $f_t(\cdot)$ denotes univariate-t probability density function.

(6.b) Sample $\kappa|q_t$ as follows

$$\kappa|q_t \sim \text{Beta}(n_{k1} + n_1, n_{k0} + n_0) \quad (\text{F-8})$$

where n_{k1} denotes the prior value of jump indicator of 1, n_{k0} denotes the prior value of jump indicator of 0, n_0 is the count of $q_t = 0$, and $n_1 = n - n_0$ is the count of $q_t = 1$.

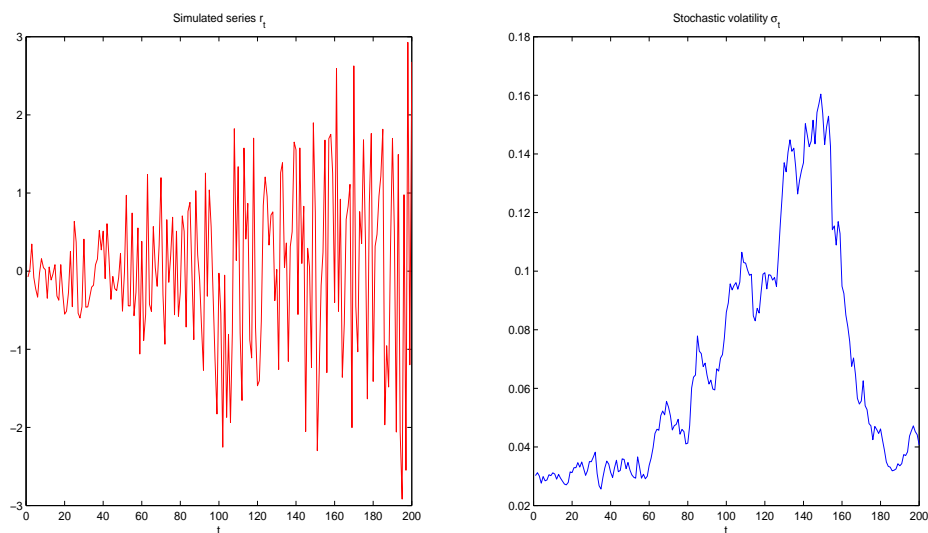
7) By following similar procedures in step 5, we could sample jump magnitude parameter δ , and then sample the jump magnitude ψ_t as follows: if $q_t = 0$, draw ψ_t

from $N(-\frac{\delta^2}{2}, \delta^2)$; and if $q_t = 1$, draw ψ_t from $N(\psi_\mu, \psi_{\sigma^2})$, where $\psi_{\sigma^2} = \frac{1}{\delta^2} + \frac{\lambda_t q_t^2}{e^{h_t}}$ and

$$\psi_\mu = \frac{1}{\psi_{\sigma^2}} \left(-\frac{1}{2} + \frac{y_t q_t \lambda_t}{e^{h_t}} \right).$$

8) Repeat from step 2 to step 7.

Panel A



Panel B

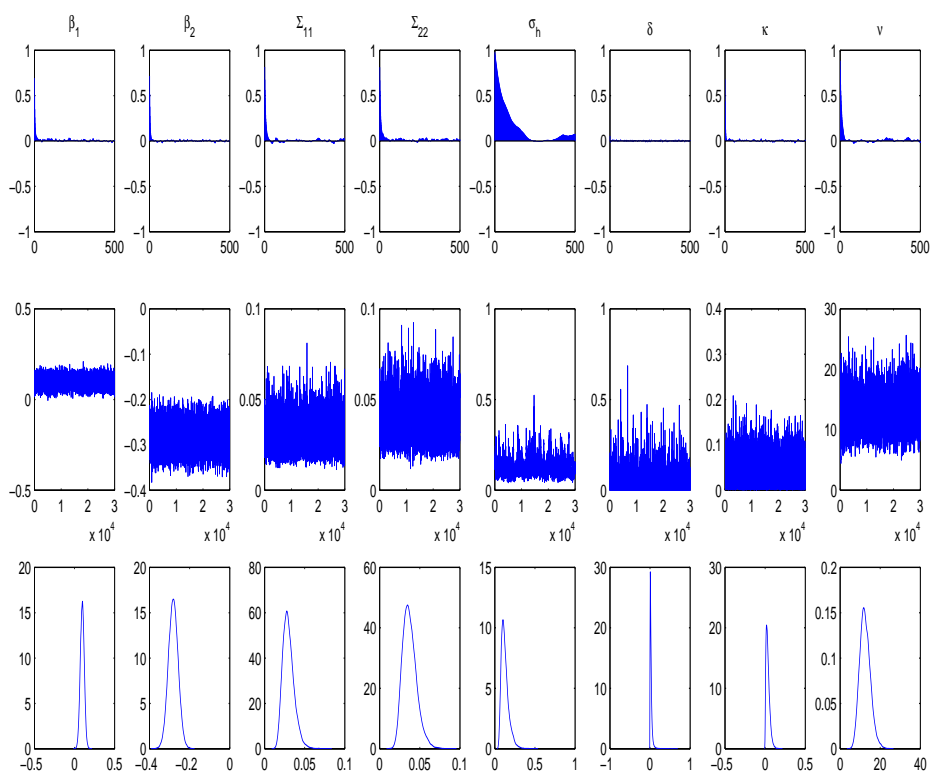


Figure 43: The figure in Panel A depicts the simulated series and stochastic volatility. The figure in Panel B depicts the sample autocorrelation function, sample draws and posterior densities for simulated data

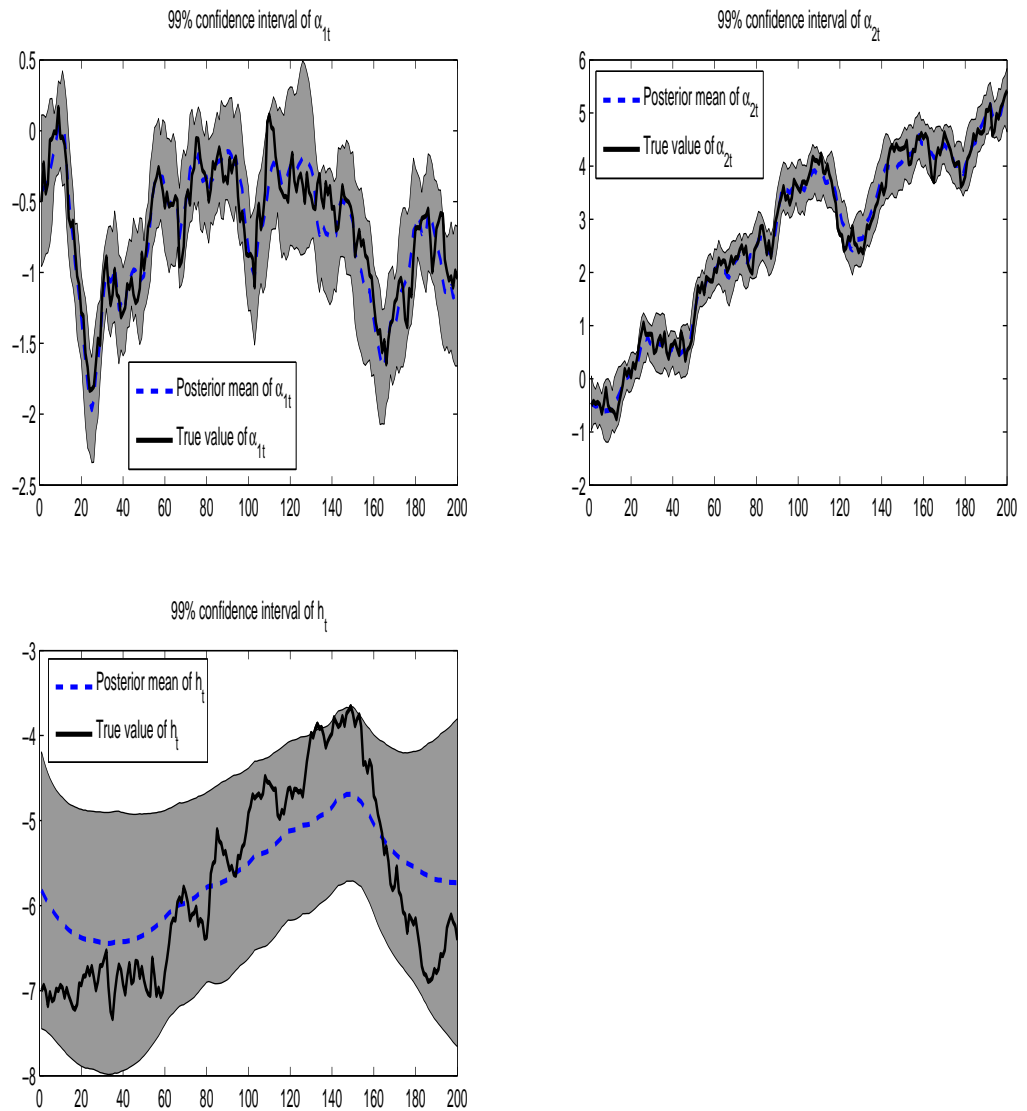


Figure 44: This figure shows the estimation results of α_{1t} , α_{2t} and h_t for the simulated data. The gray area represents the 99% confidence interval. The solid line denotes the true value of the state variable and the dashes line denotes the posterior mean.

APPENDIX G: CHAPTER 2 PROOFS

Before proving Proposition 1, we need the following lemma whose proof is evident and omitted.

Lemma 1 *The value function $J(W, M)$ is homogeneous degree of γ , that is, for all nonnegative constant $k > 0$, we can obtain $J(kW, kM) = k^\gamma J(W, M)$.*

Proof of Proposition 1.

Suppose there exists a candidate value function $\hat{J}(W, M)$ which solves the bellman equation such that

$$\begin{aligned} 0 = & -\rho\hat{J} + \sup_{c(t), \omega(t)} \left\{ \frac{C^\gamma(t)}{\gamma} + [\omega(t)(\mu - r)W(t) + rW(t) - C(t)] \hat{J}_W \right. \\ & \left. + [bW(t) - aM(t)] \hat{J}_M + \frac{1}{2} \omega^2 \sigma^2 W^2 \hat{J}_{WW} \right\}. \end{aligned} \quad (\text{G-1})$$

Define an infinitesimal generator \mathcal{L}^α as follows

$$\mathcal{L}^\alpha \hat{J} = [\omega(t)(\mu - r)W(t) + rW(t) - C(t)] \hat{J}_W + [bW(t) - aM(t)] \hat{J}_M + \frac{1}{2} \omega^2 \sigma^2 W^2 \hat{J}_{WW} \quad (\text{G-2})$$

where $\alpha = \{c, \omega\}$ is a control policy in the set of admissible trading strategies \mathcal{A} .

Then equation (G-1) can be expressed as

$$0 = -\rho\hat{J} + \sup_{\alpha \in \mathcal{A}} \left\{ \frac{C^\gamma(t)}{\gamma} + \mathcal{L}^\alpha \hat{J} \right\} \quad (\text{G-3})$$

Applying Itô's formula to $e^{-\rho t} \hat{J}(W, M)$ between 0 and T , we can obtain

$$\begin{aligned} \mathbb{E}[e^{-\rho T} \hat{J}(W_T, M_T)] &= \hat{J}(W, M) + \mathbb{E} \left[\int_0^T e^{-\rho u} [\mathcal{L}^{\alpha_u} \hat{J}(W_u, M_u) - \rho \hat{J}(W_u, M_u)] du \right] \\ &\leq \hat{J}(W, M) - \mathbb{E} \left[\int_0^T e^{-\rho u} \frac{C^\gamma(u)}{\gamma} du \right] \end{aligned}$$

The inequality comes from equation (G-3). By sending T to infinity and applying the transversality condition, the dominated convergence theorem yields

$$\hat{J}(W, M) \geq \mathbb{E} \left[\int_0^\infty e^{-\rho t} \frac{C^\gamma(t)}{\gamma} dt \right], \forall \alpha \in \mathcal{A} \quad (\text{G-4})$$

Hence, we have $\hat{J}(W, M) \geq J(W, M)$.

By last lemma, we can define $\hat{J}(W, M) = M^\gamma f(u)$, where $u = \frac{W}{M}$. Then the first order condition can give a policy $\hat{\alpha} = \{\hat{c}, \hat{\omega}\}$, where $\{\hat{c}, \hat{\omega}\}$ are shown in the equation (37) and (38), respectively. By plugging this policy, we can obtain the following nonlinear ODE in terms of $f(u)$ as

$$-\frac{1}{2} \frac{(\mu - r)^2}{\sigma^2} \frac{[f'(u)]^2}{f''(u)} + [(bu - a)\gamma - \rho]f(u) + f'(u)u[r - (bu - a)] + \frac{1 - \gamma}{\gamma} [f'(u)]^{\frac{\gamma}{\gamma-1}} = 0. \quad (\text{G-5})$$

which is the equation (39). Thus, we can have

$$\rho \hat{J} - \mathcal{L}^{\hat{\alpha}} \hat{J} - \frac{\hat{C}^\gamma}{\gamma} = 0 \quad (\text{G-6})$$

By repeating the above arguments, from equation (G-6), we can have

$$\mathbb{E}[e^{-\rho T} \hat{J}(W_T, M_T)] = \hat{J}(W, M) - \mathbb{E} \left[\int_0^T e^{-\rho u} \frac{\hat{C}^\gamma(u)}{\gamma} du \right] \quad (\text{G-7})$$

By sending T to infinity and applying the transversality condition, we can obtain

$$\hat{J}(W, M) = \hat{J}^{\hat{\alpha}}(W, M) \leq J(W, M) \quad (\text{G-8})$$

Therefore, $\hat{J}(W, M) = J(W, M) = \hat{J}^{\hat{\alpha}}(W, M)$. This completes the verification proof.

To finish the proof we then characterize the boundary conditions at $u = 1$, that is $W(t) = M(t), \forall t$.

Consider a small time period $[t, t + h]$, we have

$$\begin{aligned} M(t+h) &= M_0 e^{-a(t+h)} + b \int_0^t e^{-a(t+h-s)} W(s) ds + b \int_t^{t+h} e^{-a(t+h-s)} W(s) ds \\ &= M_t e^{-ah} + b \int_t^{t+h} e^{-a(t+h-s)} W(s) ds. \end{aligned} \quad (\text{G-9})$$

By using the integration by parts, we have

$$\int_t^{t+h} e^{as} W(s) ds = \frac{1}{a} \int_t^{t+h} W(s) de^{as} = \frac{1}{a} \left[e^{a(t+h)} W(t+h) - e^{at} W(t) - \int_t^{t+h} e^{as} dW(s) \right].$$

Therefore, we have

$$M(t+h) = M(t) e^{-ah} + \frac{b}{a} W(t+h) - \frac{b}{a} e^{-ah} W(t) - \frac{b}{a} e^{-a(t+h)} \int_t^{t+h} e^{as} dW(s).$$

The boundary condition $W(t) = M(t)$ holds for all t , by equation (54), thus we plug $W(t+h) = M(t+h)$ in the last equation and obtain

$$\frac{(a-b)}{a} [W(t+h) - e^{-ah} W(t)] = -\frac{b}{a} e^{-a(t+h)} \int_t^{t+h} e^{as} dW(s)$$

which leads to

$$\frac{b-a}{b} [e^{a(t+h)} W(t+h) - e^{at} W(t)] = \int_t^{t+h} e^{as} dW(s).$$

Therefore, we have

$$\frac{b-a}{\alpha b} \left(\int_t^{t+h} a e^{as} W(s) ds + \int_t^{t+h} e^{as} dW(s) \right) = \int_t^{t+h} e^{as} dW(s),$$

and then

$$\frac{b-a}{b} \int_t^{t+h} a e^{as} W(s) ds = \frac{a}{b} \int_t^{t+h} e^{as} dW(s).$$

By using the process of $W(t)$ in the last equation, we obtain

$$(b-a) \int_t^{t+h} e^{as} W(s) ds = \int_t^{t+h} e^{as} ([(\mu-r)\omega(s) + r]W(s) - C(s)) ds + \int_t^{t+h} e^{as} \sigma\omega(s)W(s) dz(s)$$

and then

$$\int_t^{t+h} e^{as} ([(b-a) - (\mu-r)\omega(s) - r]W(s) + C(s)) ds = \int_t^{t+h} e^{as} \sigma\omega(s)W(s) dz(s). \quad (\text{G-10})$$

The left side of equation (G-10) has a finite quadratic variation while the right side is a local martingale, then both sides have to be zero. Hence,

$$[(b-a) - (\mu-r)\omega(s) - r]W(s) + C(s) = 0. \quad (\text{G-11})$$

Therefore,

$$\omega(s) = \frac{1}{\mu-r} \left[(b-a) - r + \frac{C(s)}{W(s)} \right]. \quad (\text{G-12})$$

Plug in $\omega(s)$ into equation (30), we have

$$dW(t) = (b-a)W(t)dt + \sigma\omega(t)W(t)dz(t). \quad (\text{G-13})$$

From equation (31), we have

$$dM(t) = (bW(t) - aM(t))dt.$$

Plug in $W(t) = M(t)$, we have

$$dW(t) = (bW(t) - aW(t))dt.$$

Thus, we obtain

$$dW(t) = (b-a)W(t)dt \quad (\text{G-14})$$

Compare equation (G-13) with equation (G-14), the diffusion term in equation (G-13) should be zero, that is, $\omega(t) = 0$. From equation (G-14), the wealth process is $W(t) = W(0)e^{(b-a)t}$.

By equation (G-12), the consumption process is as follows

$$C(t) = (a + r - b)W(t) = (a + r - b)W(0)e^{(b-a)t}. \quad (\text{G-15})$$

As $C(t) \geq 0$, then $b \leq b^*$. Then we have shown that b must be bounded by $r + a$ to guarantee the existence of optimal policy. Also, note that there is no randomness in the consumption process, thus the objective function is deterministic as

$$\begin{aligned} J(W(0)) &= \int_0^\infty e^{-\rho t} \frac{C^\gamma}{\gamma} dt = \frac{(W(0)(a + r - b))^\gamma}{\gamma} \int_0^\infty e^{((b-a)\gamma - \rho)t} dt \\ &= \frac{(W(0)(a + r - b))^\gamma}{\gamma(\rho - (b - a)\gamma)} \end{aligned}$$

in which the integral exists as $(b - a)\gamma - \rho < 0$.

By $J(W(0)) = M(0)^\gamma f(u)$ and $W(0) = M(0)$, we obtain the boundary condition as $u = 1$,

$$f(1) = \frac{W_0^\gamma}{M_0^\gamma} \frac{(a + r - b)^\gamma}{\gamma(\rho - (b - a)\gamma)} = \frac{[a + r - b]^\gamma}{\gamma(\rho - (b - a)\gamma)}.$$

Recall $J(W, M) = M^\gamma f(\frac{W}{M})$, we can also represent the value function as $J(M, u) = M^\gamma f(u)$. Then we can have $J_u = M^\gamma f'(u)$ and $J_W = \frac{\partial J}{\partial u} \frac{du}{dW} = M^\gamma f'(u) \frac{1}{M} = C^{\gamma-1}(t)$.

Therefore, we can obtain

$$f'(u) = M^{1-\gamma} C^{\gamma-1}(t).$$

As $u = 1$, we have $W(t) = W(0)e^{(b-a)t}$ and the consumption equation at the boundary, we finally derive the first order derivative at the boundary as

$$\begin{aligned} f'(1) &= M^{1-\gamma}(t)(a+r-b)^{\gamma-1}W^{\gamma-1}(t) \\ &= \left(\frac{W(t)}{M(t)}\right)^{\gamma-1} (a+r-b)^{\gamma-1} \\ &= (a+r-b)^{\gamma-1}. \end{aligned}$$

This completes the proof. □

Proof of Proposition 3.

Plugging the optimal policy into equation (30), we could obtain the wealth process $W(t)$ as

$$dW(t) = \left[-\left(\frac{\mu-r}{\sigma}\right)^2 \frac{f'(u_t)}{u_t f''(u_t)} W(t) + rW(t) - M f'(u_t)^{1/(\gamma-1)} \right] dt - \frac{\mu-r}{\sigma} W(t) \frac{f'(u_t)}{u_t f''(u_t)} dz(t). \quad (\text{G-16})$$

where $u_t = \frac{W(t)}{M(t)}$.

From equation (G-16), we could derive

$$\frac{dW(t)}{W(t)} = \left[-\left(\frac{\mu-r}{\sigma}\right)^2 \frac{f'(u_t)}{u_t f''(u_t)} + r - \frac{1}{u_t} f'(u_t)^{1/(\gamma-1)} \right] dt - \frac{\mu-r}{\sigma} \frac{f'(u_t)}{u_t f''(u_t)} dz(t) \quad (\text{G-17})$$

Therefore,

$$\mathbb{E} \left[\frac{dW(t)}{W(t)} \right] = \left[-\left(\frac{\mu-r}{\sigma}\right)^2 \frac{f'(u_t)}{u_t f''(u_t)} + r - \frac{1}{u_t} f'(u_t)^{1/(\gamma-1)} \right].$$

By using the boundary conditions and equation (39), we have $\lim_{u \downarrow 1} f''(u) = \infty$. As $u_t \rightarrow 1$, we can obtain

$$\lim_{u_t \rightarrow 1} \frac{\mathbb{E} \left[\frac{dW(t)}{W(t)} \right]}{dt} = r - f'(1)^{\frac{1}{\gamma-1}}$$

Then by the first derivative boundary condition in Proposition 1, we have

$$\lim_{u_t \rightarrow 1} \frac{\mathbb{E} \left[\frac{dW(t)}{W(t)} \right]}{dt} = b - a.$$

This completes the proof. \square

Proof of Proposition 4:

The proof employs a duality technique developed in Schroder and Skiadas (2002),

Proposition 1. Define

$$\hat{W}(t) = W(t) - bM'_t(W), \quad (\text{G-18})$$

where

$$M'_t(W) = \frac{M_0}{b} e^{-at} + \int_0^t e^{-a(t-s)} W_s ds. \quad (\text{G-19})$$

with $M'_0(W) = \frac{M_0}{b}$. Introduce a dual parameter system as

$$\begin{pmatrix} \hat{a} \\ \hat{b} \end{pmatrix} = \begin{pmatrix} a - b \\ b \end{pmatrix} \Leftrightarrow \begin{pmatrix} a \\ b \end{pmatrix} = \begin{pmatrix} \hat{a} - \hat{b} \\ \hat{b} \end{pmatrix} \quad (\text{G-20})$$

From equation (G-19), we can have $dM'_t(W) = [W_t - aM'_t(W)]dt$, from the dual parameter system (G-20), by plugging equation (G-18), we can obtain

$$dM'_t(W) = [\hat{W}_t - \hat{a}M'_t(W)]dt \quad (\text{G-21})$$

Define

$$\hat{M}'_t(\hat{W}) = \frac{M_0}{\hat{b}} e^{-\hat{a}t} + \int_0^t e^{-\hat{a}(t-s)} \hat{W}_s ds \quad (\text{G-22})$$

with $\hat{M}'_0(\hat{W}) = \frac{M_0}{\hat{b}}$. From equation (G-22), we could find that

$$d\hat{M}'_t(\hat{W}) = [\hat{W}_t - \hat{a}\hat{M}'_t(\hat{W})]dt \quad (\text{G-23})$$

Since $\hat{M}'_0(\hat{W}) = \frac{M_0}{\hat{b}} = \frac{M_0}{b} = M'_0(W)$, $\hat{M}'_t(\hat{W}) = M'_t(W)$ is the unique solution to the ordinary differential equation $dx = [\hat{W}(t) - \hat{a}x]dt$, with $x_0 = \frac{M_0}{\hat{b}}$. Therefore from equation (G-18), we can obtain

$$\begin{aligned} W(t) &= \hat{W}(t) + bM'_t(W) = \hat{W}(t) + \hat{b}\hat{M}'_t(\hat{W}) \\ &= \hat{W}(t) + M_0 e^{-\hat{a}t} + \hat{b} \int_0^t e^{-\hat{a}(t-s)} \hat{W}_s ds \\ &= \hat{W}(t) + M_0 e^{-(a-b)t} + b \int_0^t e^{-(a-b)(t-s)} \hat{W}_s ds \end{aligned}$$

By Proposition 3 and its proof, $\hat{W}(t) = Y(t)$ is a geometrical Brownian motion and $W(t) = W^*(t)$ (the optimal wealth), then we obtain the optimal wealth process in equation (51) and the corresponding consistent performance benchmark process in equation (52). This completes the proof. \square

Proof of Proposition 5:

Let $\varphi(t) = \frac{W(t)}{Y(t)} = \frac{W(t)}{W(t)-M(t)} \in [1, \infty)$, then by

$$\frac{dY(t)}{Y(t)} = ndt + m\sigma dz(t)$$

and Proposition 4, we have

$$\frac{dW(t)}{Y(t)} = \left(a + n + r \frac{W(t)}{Y(t)} \right) dt + m\sigma dz(t).$$

Then we derive the diffusion equation for $\varphi(t)$ as

$$d\varphi(t) = [\varphi(t)(m^2\sigma^2 - n + r) - m^2\sigma^2 + a + n]dt + m\sigma(1 - \varphi(t))dz(t). \quad (\text{G-24})$$

The forward equation for the density p_φ is

$$\frac{1}{2} \frac{\partial}{\partial \varphi^2} ((1 - \varphi)^2 m^2 \sigma^2 p_\varphi) - \frac{\partial}{\partial \varphi} \{ [\varphi(m^2 \sigma^2 - n + r) - m^2 \sigma^2 + a + n] p_\varphi \} = \frac{\partial p_\varphi}{\partial t}. \quad (\text{G-25})$$

Since this forward equation belongs to the class of forward equations (Wong(1964)), for $\varphi \in [1, \infty)$, the stationary distribution of $p_\varphi(\varphi)$ exists and is the solution of the Pearson equation

$$\frac{1}{2} \frac{\partial}{\partial \varphi^2} ((1 - \varphi)^2 m^2 \sigma^2 p_\varphi) - [\varphi(m^2 \sigma^2 - n + r) - m^2 \sigma^2 + a + n] p_\varphi = 0 \quad (\text{G-26})$$

which can be reduced to the first-order ordinary differential equation (ODE) as

$$\frac{dp_\varphi}{d\varphi} = \left[\frac{2(r - n)}{m^2 \sigma^2} \frac{\varphi}{(1 - \varphi)^2} + \frac{2(a + n)}{m^2 \sigma^2} \frac{1}{(1 - \sigma)^2} \right] p_\varphi.$$

The solution to this first-order ODE is equation (56) with the constant k which is subject to the normalization

$$\int_1^\infty p_\varphi d\varphi = 1 \quad (\text{G-27})$$

and the constant k can be expressed in terms of a gamma function in equation (57).

Then the density function of p_ψ can be obtained correspondingly by transforming variable. Since we have

$$\frac{1}{2} \frac{\partial}{\partial \varphi^2} ((1 - \varphi)^2 m^2 \sigma^2 p_\varphi) = -(1 - \varphi) p_\varphi m^2 \sigma^2 + \frac{1}{2} (1 - \varphi)^2 m^2 \sigma^2 \frac{dp_\varphi}{d\varphi}.$$

Then the Pearson equation (G-26) can be reduced to

$$\frac{1}{2}(1-\varphi)^2 m^2 \sigma^2 \frac{dp_\varphi}{d\varphi} - [\varphi(r-n) + a + n]p_\varphi = 0. \quad (\text{G-28})$$

Integrating equation (G-28) over $[1, \infty)$, we can have

$$\frac{1}{2}m^2\sigma^2[(1-\varphi)^2 p_\varphi]_1^\infty + \int_1^\infty m^2\sigma^2 p_\varphi(1-\varphi)d\varphi - (r-n)E[\varphi] = a+n. \quad (\text{G-29})$$

Inspecting first term of equation (G-29), $(\varphi-1)^2 p_\varphi \rightarrow 0$ as $\varphi \rightarrow \infty$ under condition (55). Also, we can write

$$(\varphi-1)^2 p_\varphi = \kappa e^{-\frac{2}{m^2\sigma^2}[(n-r-m^2\sigma^2)\ln(\varphi-1) + \frac{a+r}{\varphi-1}]}.$$

As $\varphi \rightarrow 1$, $\frac{1}{\varphi-1}$ converges to ∞ quicker than $\ln(\varphi-1)$ approaches to $-\infty$, hence equation (G-29) can be reduced to

$$m^2\sigma^2 - m^2\sigma^2 E[\varphi] - (r-n)E[\varphi] = a+n.$$

That is,

$$\mathbb{E}[\varphi] = \frac{a+n-m^2\sigma^2}{n-m^2\sigma^2-r}.$$

This completes the proof. □

APPENDIX H: MODEL DESCRIPTION

The complete model and derivation of the solution are given in Chapter 2 in which a general optimal policy is characterized and an analytical solution is presented. A brief introduction of the model and economic setting is sketched as follows. An investor with initial wealth w_0 confronts with the investment opportunities: constant return $r dt$ in risk-free asset and varying return (of a risky asset) $\mu dt + \sigma dz(t)$ over time period $[t, t + dt]$, where $z(t)$ is a one-dimensional standard Brownian motion. Assume that $\mu > r$, the agent's wealth w_t is governed by

$$dw_t = rw_t dt + \alpha_t w_t [(\mu - r)dt + \sigma dz(t)] - c_t dt. \quad (\text{H-1})$$

where c_t is the consumption rate at time t and α_t is the fraction of the wealth invested in the risky asset.

The agent wants to choose the optimal consumption and risky asset investment policy $\{c_t, \alpha_t\}$ in order to maximize his long-horizon utility as $\sup_{c_t, \alpha_t} \mathbb{E}_0 \int_0^\infty e^{-\rho t} u(c_t) dt$ subject to: (i) the consumption and investment decisions are adapted; (ii) $c_t \geq 0, a.s.$ and the cumulative consumption is finite over any finite horizon, i.e., $\int_0^t c_s ds < \infty, a.s.$; (iii) $w_t \geq 0, a.e.$; and (iv) $w_t \geq m_t, a.e.$, for all time t , where m_t is defined as the weighted average of the whole past wealth path $\{w_s : 0 \leq s \leq t\}$ as follows.

$$m_t = m_0 e^{-at} + b \int_0^t e^{-a(t-s)} w_s ds \quad (\text{H-2})$$

where $a > 0, b \geq 0$. To ensure the existence of available policies we assume that $b \leq r + a$.

Numbers a and b are the tuning parameters in implementing the consistent performance strategy. Recent performance has a higher impact on current time's strategy than remote performance does. Parameter a captures the time sensitiveness regarding to historical performance. Parameter b denotes the effect of the entire historical performance on the benchmark m_t .

Based on our knowledge, the condition (iv) is the consistent performance constraint which is new to the literature; but to develop trading strategy relies on some moving average quantities has a long history in technical analysis. In essence, the consistent performance constraint states that the current wealth always stay at or above its historical weighted average values up to a multiplier. The subsistent level m_t highlights the cumulative investment performance over time instead of a particular extreme performance incurred at a particular time, i.e., the maximum drawdown constraint in Grossman and Zhou (1993). This consistent performance constraint also resembles the ratcheting constraint of consumption studied in Dybvig (1999) and habit consumption in Constantinides (1990); however, this presented consistent performance constraint focus on the wealth and the subsistent wealth level is a weighted average of past wealth.

A discrete-version of the consistent performance contract is

$$m_t = m_0 e^{-at} + b w_1 e^{-a(t-1)} + \dots + b w_{t-1} e^{-a}. \quad (\text{H-3})$$

Hence, the consistent performance constraint ensures that $w_t/w_{t-1} \geq c \equiv b e^{-a}$, a *stable return consistently*. We should notice that $w_t \geq m_t$ is much stronger than the stable return consistently, because it focus on wealth - dollar amount, in addition to

return.

For simplicity, we now assume $b = r + a$ and $\rho + a\gamma - \frac{\gamma(\mu-r)^2}{2(1-\gamma)\sigma^2} \geq 0$. Then, a is the tuning parameter in this strategy. The optimal consistent performance strategy is given by (Proposition 2 in Chapter 2)

$$c_t = h(w_t - m_t), \quad (\text{H-4})$$

and

$$\alpha_t w_t = k(w_t - m_t) \quad (\text{H-5})$$

where $k \equiv \frac{\mu-r}{(1-\gamma)\sigma^2} > 0$ and $h \equiv \frac{1}{1-\gamma} \left(\rho + a\gamma - \frac{\gamma(\mu-r)^2}{2(1-\gamma)\sigma^2} \right) \geq 0$. This optimal policy suggests that in order to meet the consistent performance requirement, the agent first saves a capital buffer, $w_t - m_t$, invests m fraction of this buffer in a risky asset, consumes a constant percentage h of the buffer, and then puts the remaining amount $w_t - (h + m)(w_t - m_t)$ into a risk-free asset. This strategy is similar to the one in constant proportional portfolio insurance studied in Black and Perold (1992), the drawdown constraint in Grossman and Zhou (1993), and the ratcheting constraint in Dybvig (1995).

It can be shown that (see Proposition 4), for all t and s ,

$$\frac{1}{s} \log \frac{m_{t+s}}{m_t} > r, \quad (\text{H-6})$$

which, in turn, yields, $m_t/m_{t-1} > r$ for all t . Hence, the growth rate of the benchmark m_t beats the risk-free interest rate.

A traditional intertemporal asset allocation policy refers to the optimal strategy without the consistent performance constraint. As shown in Merton (1971), the con-

stant portion of the wealth to be consumed is $\frac{1}{1-\gamma} \left(\rho - r\gamma - \frac{\gamma(\mu-r)^2}{2(1-\gamma)\sigma^2} \right)$, and the constant portion of the wealth to be invested in the risky asset is still k .

APPENDIX I: PARAMETER CALIBRATION

We use the past 30 years data in our study. The daily data set of S&P 500 from 1983 to 2012 is used to estimate the market average return and volatility. We can obtain the average daily return of 0.04%, which is equivalent to monthly return of 0.78% (assume 21 trading days per month) or annual return of 9.40%, and the average daily volatility of 1.16%, which is equivalent to monthly volatility of 5.30% or yearly volatility of 18.35%. These estimates are similar with most empirical results. The CPI data set is obtained from the Federal Reserve Bank of Minneapolis and estimated to be 2.94% from 1983 to 2012. The 1-year constant maturity T-bill data set is obtained from the Board of Governors of the Federal Reserve System and estimated to be 4.757% from 1983 to 2012. Hence the inflation adjusted annual market return is 6.46% and the inflation adjusted 1-year T-bill rate is 1.817%. The per capital real consumption data is collected from Federal Reserve Bank of St. Louis and we could obtain the annual consumption growth $\frac{E(dc/c)}{dt} = 0.0208$ and the variance of consumption growth $\frac{var(dc/c)}{dt} = (0.0357)^2$. Referring to Chapter 2, we could have $n = 0.0208$ and $m\sigma = 0.0357$ and the condition $n - r - m^2\sigma^2 = 0.001355 > 0$ is satisfied.

To estimate the pure rate of time discount ρ and the risk-aversion coefficient γ , we refer to Dybvig (1999) and proceed as follows. The procedure to obtain the risk-aversion coefficient is equivalent to ask the question: What percentage increase in consumption would be as attractive as a 70% chance of no increase and a 30% chance of 100% increase? It is to solve the equation $u[(1+x)c] = 0.7u(c) + 0.3u(2c)$, where

$u(c)$ is the felicity function. Suppose this year's budget is \$10 million and there is a 30% chance of increasing to \$20 million and a 70% chance of having the same budget, the agent feels this option is as attractive as having a budget of \$12.5 million for sure. Then we could solve the equation as follows.

$$\frac{12.5^\gamma}{\gamma} = 0.7 \frac{10^\gamma}{\gamma} + 0.3 \frac{20^\gamma}{\gamma} \quad (\text{H-1})$$

By using some numerical methods to solve the nonlinear equation such as Newton and secant methods, we can find the risk-aversion coefficient $\gamma = 0.2927$.

Next, to estimate the pure rate of time preference ρ , we can ask the question: What percentage of increase in consumption both this and next year would be as attractive as a 10% increase in next year only? This parameter implies the extent to postpone your increasing consumption for exchanging a smooth consumption over time. Suppose you are indifference between the case of consuming \$10.48 million during this and next year and the case of consuming \$10 million this year and \$11 million next year. We could solve for ρ from the following equation.

$$\frac{10.48^\gamma}{\gamma} + e^{-\rho} \frac{10.48^\gamma}{\gamma} = \frac{10^\gamma}{\gamma} + e^{-\rho} \frac{11^\gamma}{\gamma} \quad (\text{H-2})$$

By using the previous calculated γ value of 0.2927, we can obtain $\rho = 0.0459$ which belongs to the reasonable estimate range from 0.01 and 0.05. The strategy is updated monthly by using above estimated values.